

UNIVERSITA' DEGLI STUDI DI MILANO

GRADUATE SCHOOL IN ENVIRONMENTAL SCIENCES  
SCUOLA DI DOTTORATO IN SCIENZE AMBIENTALI

Facoltà di Scienze del Farmaco  
Dipartimento di Scienze Farmacologiche e Biomolecolari

CORSO DI DOTTORATO IN SCIENZE AMBIENTALI

XXX Ciclo

Settore Scientifico Disciplinare: BIO/14

UNDERSTANDING CHEMICAL ALLERGEN POTENCY:  
CONTRIBUTION OF KERATINOCYTES

Angela Papale  
Matr. N. R11004

TUTOR: Chiar.ma Prof.ssa Emanuela CORSINI  
CORRELATORE: Chiar.mo Prof. Nicola SAINO

ANNO ACCADEMICO 2016/2017

# TABLE OF CONTENTS

Abstract, *pag.4*

**Chapter 1**                    **Introduction, *pag.8***

Human skin, *pag.9*

Allergic contact dermatitis, *pag.15*

Adverse outcome pathway, *pag.23*

NCTC 2544 and IL-18, *pag.24*

Signal transduction pathway involved in Inflammasome activation,  
*pag. 27*

**Chapter 2**                    **Assessment of chemical-induced contact hypersensitivity: *in vivo***  
**and *in vitro* model, *pag. 34***

**Chapter 3**                    **Objective of the thesis, *pag. 47***

**Chapter 4**                    **Materials and methods: briefly, *pag.49***

Chemicals, *pag. 50*

Cell culture, *pag. 51*

Reconstituted human Epidermis and chemical exposure, *pag. 51*

Viability, *pag. 54*

Alternative IL-18 ELISA, *pag. 54*

Determination of interference of chemical with MTT and IL-18 ELISA,  
*pag. 55*

IL-18 ELISA, *pag. 56*

RNA isolation, *pag. 56*

Microarray and quantitative PCR or Real Time-PCR, *pag. 57*

Small interference RNA, *pag. 57*

Western Blot, *pag. 58*

Co-Immunoprecipitation, *pag. 60*

Data Analysis, *pag. 60*

## **Chapter 5**

**Materials and methods: detail, *pag. 63***

Chemicals, *pag. 64*

Cell counting method, *pag. 67*

EpiDerm™, *pag. 68*

Cell viability, *pag. 70*

ELISA test, *pag. 72*

Total protein determination, *pag. 73*

RNA extraction, *pag. 74*

Agarose gel, *pag. 75*

Retro-Transcription PCR, *pag. 76*

PCR, *pag. 77*

PCR arrays, *pag. 81*

Quantitative PCR o Real-Time PCR, *pag. 82*

Transfection and silencing, *pag. 86*

Protein quantification, *pag. 88*

Western Blot, *pag. 89*

Immuno-precipitation and co-immunoprecipitation, *pag. 90*

## **Chapter 6**

**Results and discussion, *pag. 93***

Results of “Understanding chemical allergen potency: role of NLRP12 and Blimp-1 in the induction of IL-18 in human keratinocytes”, *pag. 94*

Discussion of “Understanding chemical allergen potency: role of NLRP12 and Blimp-1 in the induction of IL-18 in human keratinocytes”, *pag. 102*

Results of “NLRP12 protein and the NLRP3 inflammasome complex in the induction of IL-18 in human keratinocytes: further developments”, *pag. 105*

Discussion of “NLRP12 protein and the NLRP3 inflammasome complex in the induction of IL-18 in human keratinocytes: further developments”, *pag. 110*

Results of “Develop of an *in vitro* method to estimate the sensitization level of contact allergens”, *pag. 111*

Discussion of “Develop of an *in vitro* method to estimate the sensitization level of contact allergens”, *pag. 120*

**Chapter 7**                      **Future perspectives, pag. 125**

**Annex**                        Equivalent Epidermis at VU medical centre of Amsterdam, *pag. 127*

**List of publications, pag. 135**

**Activities, pag. 137**

**References, pag. 138**

---

## **ABSTRACT**

---

Repeated exposure to chemical allergens increases the risk of becoming sensitized. Once an individual has become sensitized, any following exposure to the same chemical may result in allergic contact dermatitis (ACD).

The risk to develop ACD is considered a serious health issue and the identification of potential sensitizing agents within consumer products is therefore crucial. With the enforcement of the 7<sup>th</sup> Amendment to the EU Cosmetics Directive (76/768/EEC) in March 2013, currently known as the Cosmetics Regulation (EU 1223/2009), a ban on the use of animals was introduced for identifying repeated dose toxicity endpoints of chemicals used in cosmetic ingredients and products. This ban results in an urgent need for the development of suitable non-animal methods for safety testing. The development of animal alternatives has become even more urgent due to the Registration, Evaluation, Authorisation and Restriction of Chemicals (REACH) regulation, which may demand toxicity tests for chemicals produced in quantities of over 1 ton per year. Over the last years, many *in vitro* models have been proposed to identify the potential of chemicals to induce skin sensitization to meet current animal welfare, public opinions and legislation constrains. The development of *in vitro*, *in chemico* or *in silico* models for predicting the sensitizing potential of new chemicals is receiving widespread interest.

Keratinocytes (KCs) play a key role in skin sensitization, as they provide the essential danger signals, they are involved in the protein haptentation process, and supply enzymes that are necessary for the metabolic activation of prohaptent.

Human KCs constitutively express several cytokines, including pro-interleukin (IL)-1 $\alpha$ , pro-IL-1 $\beta$  and pro-IL-18. Evidences provided from our group has shown that IL-18 production in human KCs can be used as a sensitive method to identify contact allergens, discriminating them from respiratory allergens and irritants with a sensitivity of 87%, specificity of 95% and

an accuracy of 90%. IL-18 is synthesized as preform, which require proteolytic maturation by cysteine protease caspase-1, which must first be activated by the inflammasome.

More recently, we demonstrated the possibility of combining the Reconstituted human Epidermis (RhE) potency assay with the assessment of IL-18 release to provide a single test for identification and classification of skin sensitizing chemicals, including chemicals of low water solubility or stability (Gibbs et al., 2013). In addition to being able to determine whether or not a chemical is a sensitizer (labelling) it is also equally important to determine the potency of a sensitizer (classification) in order to identify a maximum safe concentration for human exposure (risk assessment).

The purpose of this thesis was to understand the role of several genes and proteins involved in contact allergen-induced NLRP3 inflammasome activation and IL-18 production, and their possible correlation with allergenic potency.

Another objective of this thesis was to extend the list of chemicals tested in the RhE IL-18 potency assay, and to provide a simple method for the *in vitro* estimation of the expected sensitization induction level.

Results obtained during these three years of research activity have shown that several proteins involved in NLRP3 inflammasome activation/regulation were modulated by contact allergens. In particular I focused my attention on the role of NLRP12 and B lymphocyte induced maturation protein-1 (Blimp-1) in IL-18 production. The expression of NLRP3, ASC and caspase-1 activation were investigated by Western blot analysis and the NLRP12 localization characterized by immunoprecipitation.

Regarding potency classification the results obtained using RhE IL-18 potency assay are very promising, and further compounds should be tested to better define the applicability and limitation of RhE IL-18 potency test.



---

**CHAPTER ONE**  
INTRODUCTION

---

During the last few decades, the prevalence of allergic diseases has increased dramatically. The industrialized countries have faced a significant increase, although the rate of increase has recently slowed, of allergic diseases like atopic rhinitis, bronchial asthma, urticaria and allergic contact dermatitis. Within the North American and Western European populations, the prevalence of skin sensitization is approximately 20% (Peiser et al., 2012). This increased prevalence has been attributed to complex interactions between environmental factors and genetic factors (Kim et al., 2014).

Hypersensitivity reactions are often considered a major health problem in relation to environmental chemical exposure. Chemicals that are frequently reported to induce sensitization include products of plants and trees, such as abietic acid and balsam of Peru, metal ions, such as nickel, fragrances and cosmetic ingredients, such as cinammic aldehyde, geraniol, eugenol, p-phenylenediamine (PPD), etc.

ACD is an inflammatory skin disease. **Human skin** is the largest organ of the body, making up 16% of body weight, with several functions, the most important being to form a physical barrier to the environment, allowing and limiting the inward and outward passage of water, electrolytes and various substances while providing protection against microorganisms, ultraviolet radiation, toxic agents and mechanical insults. The regulation of skin defense mechanisms is crucial, as inappropriate or misdirected immune activities are implicated in the pathogenesis of a large variety of acquired inflammatory skin disorders, including psoriasis, atopic and allergic contact dermatitis, lichen planus, alopecia areata and vitiligo (Kadunce et al., 1995).

There are three structural layers in the skin: the epidermis, the dermis and the hypodermis (subcutis). Hair, nails, sebaceous, sweat and apocrine glands are regarded as derivatives of skin (Fig. 1).

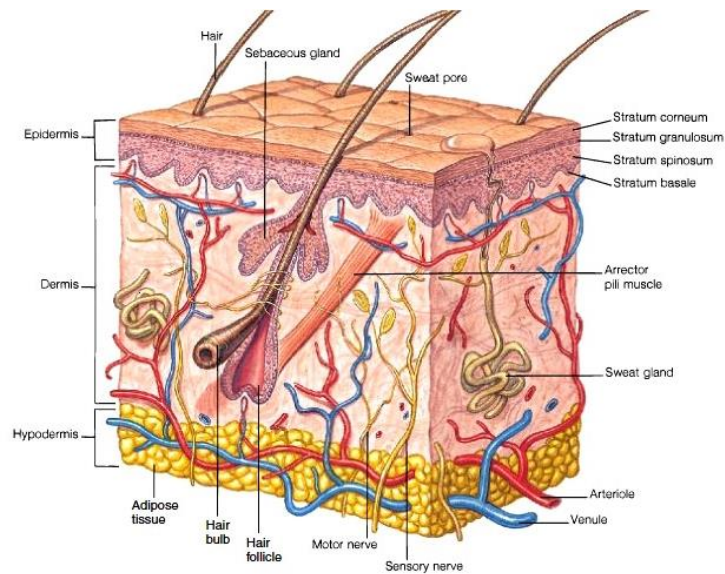


**Fig. 1 Cross-section of the skin [1]**

Skin is a dynamic organ in a constant state of change, as cells of the outer layers are continuously shed and replaced by inner cells moving up to the surface. Although structurally consistent throughout the body, skin varies in thickness according to anatomical site and age of the individual. The epidermis is the outer layer, serving as the physical and chemical barrier between the interior body and exterior environment; the dermis is the deeper layer providing the structural support of the skin, below which is a loose connective tissue layer, the subcutis or hypodermis which is an important depot of fat.

The **epidermis** is a stratified squamous epithelium. The main cells of the epidermis are the KCs. Protein bridges called desmosomes connect the KCs, which are in a constant state of transition from the deeper layers to the superficial (Fig. 2). The four separate layers of the epidermis are formed by the differing stages of keratin maturation. The epidermis varies in thickness from 0.05 mm on the eyelids to  $0.8 \pm 1.5$  mm on the soles of the feet and palms of the hand.

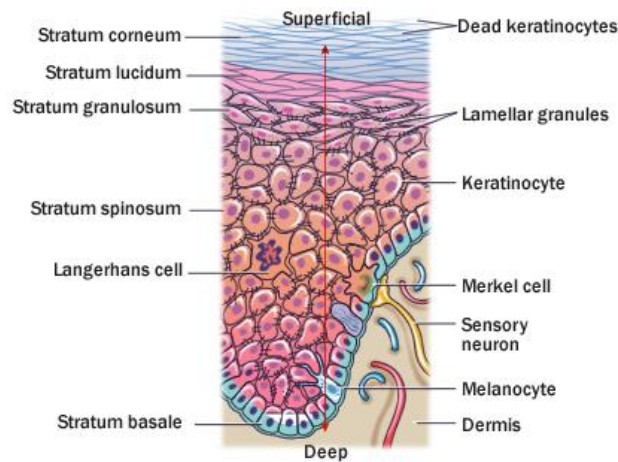


**Fig. 2 Layers of the epidermis [2]**

Moving from the lower layers upwards to the surface, the four layers of the epidermis are:

- *Stratum basale* (basal or germinativum cell layer);
- *Stratum spinosum* (spinous or prickle cell layer);
- *Stratum granulosum* (granular cell layer);
- *Stratum corneum* (horny layer).

In addition, the stratum lucidum is a thin layer of translucent cells seen in thick epidermis. It represents a transition from the stratum granulosum and stratum corneum and is not usually seen in thin epidermis. Together, the stratum spinosum and stratum granulosum are sometimes referred to as the Malpighian layer.

*Stratum basale.* The innermost layer of the epidermis which lies adjacent to the dermis comprises mainly dividing and non-dividing KCs, which are attached to the basement membrane by hemidesmosomes. As KCs divide and differentiate, they move from this deeper layer to the surface. Making up a small proportion of the basal cell population is the pigment (melanin) producing melanocytes. These cells are characterized by dendritic processes, which

stretch between relatively large numbers of neighbouring KCs. Melanin accumulates in melanosomes that are transferred to the adjacent KCs where they remain as granules. Melanin pigment provides protection against ultraviolet (UV) radiation; chronic exposure to light increases the ratio of melanocytes to KCs, so more are found in facial skin compared to the lower back and a greater number on the outer arm compared to the inner arm. The number of melanocytes is the same in equivalent body sites in white and black skin but the distribution and rate of production of melanin is different. Intrinsic ageing diminishes the melanocyte population. Merkel cells are also found in the basal layer with large numbers in touch-sensitive sites such as the fingertips and lips. They are closely associated with cutaneous nerves and seem to be involved in light touch sensation.

*Stratum spinosum.* As basal cells reproduce and mature, they move towards the outer layer of skin, initially forming the stratum spinosum. Intercellular bridges, the desmosomes, which appear as 'prickles' at a microscopic level, connect the cells. Langerhans cells (LC) are dendritic, immunologically active cells derived from the bone marrow, and are found on all epidermal surfaces but are mainly located in the middle of this layer. They play a significant role in immune reactions of the skin, acting as antigen-presenting cells (APC).

In addition, T cells, mainly CD8+ T cells, can be found in the stratum basale and stratum spinosum (Krueger et al., 1989).

*Stratum granulosum.* Continuing their transition to the surface the cells continue to flatten, lose their nuclei and their cytoplasm appears granular at this level.

*Stratum corneum.* The final outcome of keratinocyte maturation is found in the stratum corneum, which is made up of layers of hexagonal-shaped, non-viable cornified cells known

as corneocytes. In most areas of the skin, there are  $10 \pm 30$  layers of stacked corneocytes with the palms and soles having the most. Each corneocyte is surrounded by a protein envelope and is filled with water-retaining keratin proteins. The cellular shape and orientation of the keratin proteins add strength to the stratum corneum. Surrounding the cells in the extracellular space are stacked layers of lipid bilayers. The resulting structure provides the natural physical and water-retaining barrier of the skin. The corneocyte layer can absorb three times its weight in water but if its water content drops below 10% it no longer remains pliable and cracks. The movement of epidermal cells to this layer usually takes about 28 days and is known as the epidermal transit time.

**Dermoepidermal junction/basement membrane** is a complex structure composed of two layers. The structure is highly irregular, with dermal papillae from the papillary dermis projecting perpendicular to the skin surface. It is via diffusion at this junction that the epidermis obtains nutrients and disposes of waste. The dermoepidermal junction flattens during ageing which accounts in part for some of the visual signs of ageing.

The **dermis** varies in thickness, ranging from 0.6 mm on the eyelids to 3 mm on the back, palms and soles. It is found below the epidermis and is composed of a tough, supportive cell matrix. Two layers comprise the dermis:

- *a thin papillary layer;*
- *a thicker reticular layer.*

The papillary dermis lies below and connects with the epidermis. It contains thin loosely arranged collagen fibres. Thicker bundles of collagen run parallel to the skin surface in the deeper reticular layer, which extends from the base of the papillary layer to the subcutis

tissue. The dermis is made up of fibroblasts, which produce collagen, elastin and structural proteoglycans, together with immunocompetent mast cells and macrophages. Collagen fibres make up 70% of the dermis, giving it strength and toughness. Elastin maintains normal elasticity and exhibility while proteoglycans provide viscosity and hydration. Embedded within the fibrous tissue of the dermis are the dermal vasculature, lymphatics, nervous cells and fibres, sweat glands, hair roots and small quantities of striated muscle.

**Subcutis** is made up of loose connective tissue and fat, which can be up to 3 cm thick on the abdomen.

**Blood and lymphatic vessels.** The dermis receives a rich blood supply. A superficial artery plexus is formed at the papillary and reticular dermal boundary by branches of the subcutis artery. Branches from this plexus form capillary loops in the papillae of the dermis, each with a single loop of capillary vessels, one arterial and one venous. The veins drain into mid-dermal and subcutaneous venous networks. Dilatation or constriction of these capillary loops plays a direct role in thermoregulation of the skin. Lymphatic drainage of the skin occurs through abundant lymphatic meshes that originate in the papillae and feed into larger lymphatic vessels that drain into regional lymph nodes.

**Nerve supply.** The skin has a rich innervation with the hands, face and genitalia having the highest density of nerves. All cutaneous nerves have their cell bodies in the dorsal root ganglia and both myelinated and non-myelinated fibres are found. Free sensory nerve endings lie in the dermis where they detect pain, itch and temperature. Specialized corpuscular receptors also lie in the dermis allowing sensations of touch to be received by Meissner's corpuscles and pressure and vibration by Pacinian corpuscles. The autonomic nervous system supplies the motor innervation of the skin: adrenergic fibres innervate blood vessels, hair erector

muscles and apocrine glands while cholinergic fibres innervate eccrine sweat glands. The endocrine system regulates the sebaceous glands, which are not innervated by autonomic fibres.

As well acting as a physical barrier, skin also plays an important **immunological role** (Kupper et al., 2004). It is possible to explain it when the skin is stressed by several stimuli.

**Allergic contact dermatitis (ACD)** is a type of inflammation of the skin and it is the most prevalent form of immunotoxicity in humans in industrialized countries. It can be induced after skin contact with chemical haptens, and develops through a series of immunological events caused by repeated contact with compounds that have skin sensitizing potential (Kimber et al., 2002). It is characterized by clinical manifestations such as red rashes, itchy and blisters. Haptens have two important characteristics: proinflammatory properties and immunogenicity (Vocanson et al., 2009). Their proinflammatory properties provide the first signal that is necessary for innate immunity activation resulting in Dendritic Cells (DCs) activation, migration and maturation. Their immunogenicity depends on hapten-protein complex presentation in the groove of the Major Histocompatibility Complex (MHC) class I/II molecules on DC.

All contact allergens share some common features: they have low molecular weight (<1000 Da), they need to bind to epidermal proteins to form hapten-protein complex, which is actually immunogenic (Krasteva et al., 1999). These small molecules establish stable covalent links with endogenous proteins (Divkovic et al., 2005). Prehaptens to prohaptens transformation occurs upon chemical reactions (oxidation) or due to enzyme activity. Some prehaptens are transformed by UV radiation (Basketter et al., 1995).



ACD is a typical type IV (delayed-type) hypersensitivity response that develops in two phases, the initiation phase in which the immune system is sensitized and the elicitation phase in which the clinical symptoms develop. The third phase, resolution phase, during which the recostitution of skin occurs. The **sensitization phase** (also referred to as afferent phase) of ACD occurs after the contact between haptens and skin, and lasts for 8-15 days in humans (Smith Pease et al., 2003). The first phase of ACD usually has no clinical consequences, but in some cases may present as primary acute ACD. In Fig. 3 the pathogenesis of ACD is shown.

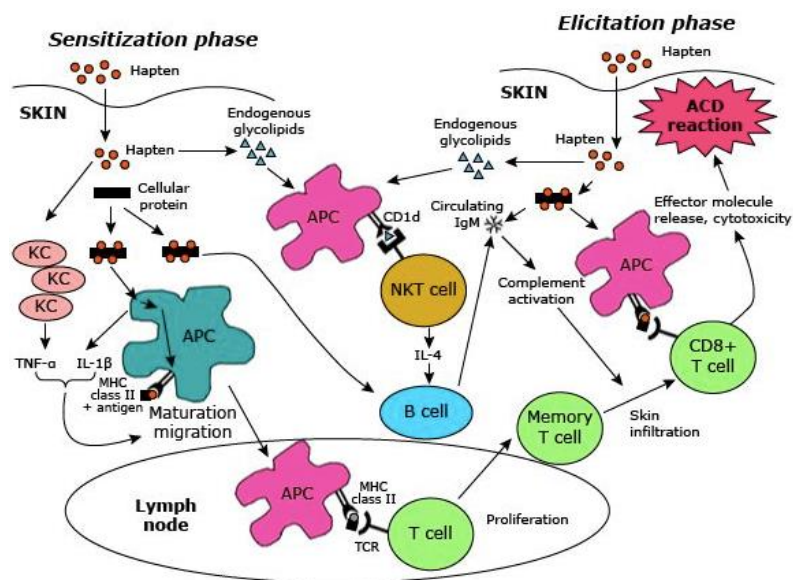


**Fig. 3 Pathogenesis of ACD [3]**

Following absorption through the stratum corneum haptens reach the viable part of the epidermis. KCs are key players in sensitization phase, as they contain enzymes that are required for the conversion of prohaptens into biologically active haptens (Naisbitt et al., 2004). KCs also provide sets of alarmins and cytokines that generate a proinflammatory microenvironment, which is necessary for innate immune system activation.

Among alarmins, the Damage-Associated Molecular Patterns (DAMPs) are sensed by so-called Pattern Recognition Receptors (PRRs) such as the **Toll-Like Receptors (TLRs)** (Faulkner L. et al., 2014). These receptors are involved in the first line of defense against pathogens. To date, ten different TLRs have been identified in humans (Boehme et al., 2004). The primary function of TLRs is the initial recognition of pathogenic microorganisms and subsequent activation of the innate immune response. Activated TLRs promote the phagocytosis of pathogens in innate immune cells such as macrophages and induce the production of reactive oxygen species (ROS), to neutralize pathogens.

TLR2 and TLR4 play an important role in mounting a full immune response to skin sensitizers. Evidence for an involvement of the signaling pathway p38 Mitogen Activated Protein Kinase (p38 MAPK) in skin sensitization further underpin the relevance for TLR. P38 MAPK are enzymes that play an important role in the signal transduction of TLR (Mehrotra et al., 2007). In the keratinocyte cell line NCTC2544 IL-18 production induced by skin sensitizers was greatly decreased after addition of the specific p38 MAPK inhibitor, SB203580 (Galbiati et al., 2011). Similar results were obtained in an experiment using the monocytes THP-1 cell line (Mitjans et al., 2010), indicating that sensitizers activated p38 MAPK in both KCs and DCs.

There is evidence that TLR4 has a role in the induction of ACD, which occurs in IL-12-independent pathway (Martin et al., 2008). The exact role of TLR4 is not fully understood, but it seems that TLR4 may be required for the induction of cytokines in DC with impaired IL-12 function. A possible candidate cytokine induced by TLR4 activation is IL-23 (a member of IL-12 family). IL-23 (like IL-12) participates in DCs activation and enhances hypersensitivity reaction (Martin et al., 2008). IL-23 stimulates (while IL-12 inhibits) IL-17-producing CD8+ cells. TLR2 is important for T-helper 1 response to cutaneous antigens. Skin is colonized with bacteria, which can be the source of TLR2 ligands. TLR2 promotes the Interferon (IFN)- $\gamma$

response to cutaneously introduced antigens (He et al., 2006). There are evidences that heat shock proteins (HSP27 and HSP70) form a link between adaptive and innate immunity during early stages of contact sensitivity. Their interaction with TLR4 increases the production of cytokines known to enhance antigen (Ag) presentation by T cells (Yusuf et al., 2009). TLR2 and TLR4 activation induces the production of Nuclear Factor- $\kappa$ B-dependent (NF $\kappa$ B) pro-inflammatory cytokines and chemokines such as IL-6, IL-12, and tumor necrosis factor (TNF)- $\alpha$ , and of pro-IL-1 $\beta$  and pro-IL-18. The inflammasomes are required to activate and secrete several cytokines that are expressed as nonfunctional proteins after NF $\kappa$ B activation (Nestle et al., 2009).

Another important family of PRRs are the **Nucleotide-binding Oligomerization Domain (NOD)-Like Receptors (NLRs)**. These intracellular receptors recognize pathogens-Associated Molecular Patterns (PAMPs) with the same leucine-rich repeat domains that can be found in TLRs. NLRs are activated by PAMPs such as bacterial RNA, flagellin and breakdown products of peptidoglycan (Feldmeyer et al., 2010). In addition, the NLRs are able to recognize DAMPs such as ATP and uric acid (Kawai & Akira, 2009). Upon activation, NOD receptors can activate NF $\kappa$ B and the inflammasomes (Stutz et al., 2009; Feldmeyer et al., 2010; Latz, 2010).

In skin, haptens are detected by KCs that react by the NLRP3 inflammasome activation. Secreted IL-1 $\beta$  and IL-18 induce KCs to release IL-1 $\alpha$ , TNF- $\alpha$  and Granulocyte-Macrophage Colony-Stimulating Factor (GM-CSF), promoting the activation of DC, including epidermal LCs (Wang, 2002). As APC, LCs migrate towards lymph nodes from the dermis and activate a specific immune response (Fig. 3). Primary function of APC is to capture, process and present Ags to unprimed T cells (Zaba et al., 2009). DC has monocyte origin. Immature DCs reside in non-lymphoid tissues. They form a dense network in the skin and capture haptens

penetrating skin barrier. There are three kinds of DC populations in non-inflamed skin: epidermal LCs, dermal myeloid DCs (dDCs) and dermal plasmacytoid DCs (pDCs). During inflammation, another population of dermal DC occurs, “inflammatory” DCs (Zaba et al., 2009). LCs are epidermal MHC class II DCs specialized in Ag presentation and reside in the suprabasal layers of the epidermis, close to KCs (Ryan et al., 2005). Zaba et al., 2009 have assumed that LCs processed antigens locally and migrated to lymph node for Ag presentation, and they believed that LCs have the role in inducing and maintaining tolerance to cutaneous antigens. It has also been shown that ACD response was not completely abrogated despite full abrogation of LCs, indicating that several types of DCs are involved in T-cell priming (Grabbe et al., 1995). Dermal myeloid DCs are a population of DCs residing in the dermis; they are able to take up Ags, mature and migrate to draining local lymph nodes and present them to B and T cells (Zaba et al., 2009). pDCs are a unique group of resident cutaneous DCs. While both mDCs and pDCs express high levels of HLA-DR and have Ag-presenting capacity, pDCs are characterized by their ability to produce large amounts of IFN-1 (Zaba et al., 2009). DCs respond differently to haptens and irritants with their production of cytokines and expression of co-stimulatory molecules (Aiba et al., 1997). Fully mature DC shows high expression of MHC class II and co-stimulatory molecules (Cluster of Differentiation (CD) 40, CD80, CD86) and also a decreased capacity to internalize antigens (Aiba et al., 1997). MHC II is constitutively expressed on LC, and expression of these molecules is strongly up-regulated by haptens and not irritants (Aiba et al., 1997). DC maturation can be induced by cytokines such as IL-1 $\beta$ , TNF- $\alpha$ , CD40 ligation, expression of IL-12, viral RNA, lipopolysaccharides and contact sensitizers (Arrighi et al., 2001). Protein haptization triggers maturation of DC, probably due to reactive cysteine residues and p38 activation. This process is primarily mediated by the activation of p38 MAPK and is caused by intracellular redox imbalance induced by contact

allergens (Megherbi et al., 2009). Although MAPK may play a crucial role in the activation of DCs, the upstream signals of p38 MAPK remain undetermined (Mizuashi 2005). IL-1 $\beta$  and TNF- $\alpha$  both have a role in LC migration to lymph nodes (Nakae et al., 2001). IL-1 $\alpha$ , IL-1 $\beta$  and TNF- $\alpha$  levels are increased in contact-allergen sensitized skin. IL-1 $\alpha$  is mainly produced by KCs, whereas IL-1 $\beta$  is mainly produced by LC, and both IL-1 $\alpha$  and IL-1 $\beta$  can promote LC migration (Nakae et al., 2001). IL-1 $\alpha$  is mainly involved in contact allergen-specific-priming, while IL-1 $\beta$  is involved in contact allergen-specific antibody production (Nakae et al., 2001).

IL-12 is considered to be important in the generation of allergen-specific T cell response. Other surface molecules that are also expressed after the haptens intake are ICAM-1 (CD54) and B7-2 (CD86) (Aiba et al., 1997).

Generated short-lived effector T cells and long-lived memory T cells migrate to peripheral tissue in order to participate in immune responses and immune surveillance. Relocation of effector and memory T cells is non-random, the process involves adhesion molecules, including selectins, integrins, and corresponding vascular ligands as well as the large family of chemokines and their receptors (Ebert et al., 2005). A fraction of primed T lymphocytes persists as circulating memory cells and can confer protection and give, upon secondary challenge, a qualitatively different and quantitatively enhanced response (Sallusto et al., 1999).

In the dermis, endothelial and lymphatic cells produce Chemokine ligand 19 (CCL19) and CCL21. These chemokines are recognized by the up-regulated CCR7 chemokine receptor of sensitizer-activated DCs, which migrate to afferent lymphatic vessels (Kaplan et al., 2012; Rustenmayer et al., 2011). The activation of sensitizer-specific naive T cells by activated DCs in the skin-draining lymph nodes is the crucial step and concludes the sensitization phase (Kaplan et al., 2012; Rustenmayer et al., 2011). Upon activation, T cells produce IL-2, which is

a T cell growth factor, resulting in abundant T cell expansion (Rustenmayer et al., 2011). Moreover, they receive instructive signals from the skin DCs, resulting in the expression of a combination of homing receptors, that is, chemokine receptors and adhesion molecules, that directs them to the skin. The immunological microenvironment (comprising the amount of sensitizer, danger signals, and other soluble mediators) determines the final phenotype of effector T cells. In the skin-draining lymph nodes, sensitizer-activated DCs produce IL-12 and IFN- $\gamma$ , promoting the differentiation of Th1 cells, which release IFN- $\gamma$  and TNF- $\alpha$  (Peiser et al., 2012). The microenvironment containing IL-6, transforming growth factor (TGF)- $\beta$ , IL-21, IL-23 and IL-1 $\beta$  leads to Th17/22 polarization and the production of IL-17 and IL-22. The presence of IL-4 leads to Th2 polarization and subsequent IL-4, IL-5 and IL-13 production. IL-2 and TGF- $\beta$  in the microenvironment promote the differentiation of regulatory T cells (Tregs), which secrete immunosuppressive IL-10, an important cytokine that limits the extent and duration of ACD and promotes tolerance (Berg et al., 1995).

It has been speculated that the strength of the innate inflammation caused by the contact sensitizer is responsible for the immunogenic or tolerogenic state of DCs and the subsequent effector/memory T cell/Treg ratio (Martin, 2012). Both sensitizing and tolerizing pathways are induced during sensitization, and the balance of these pathways determines the final outcome (Vocanson et al., 2010).

**Elicitation phase** is also known as efferent or challenge phase (Fig. 3). A subsequent exposure to the haptens leads to a rapid activation of the specific lymphocyte(s) clone(s) and to activate and trigger inflammatory process responsible for cutaneous lesions (Rustemeyer et al., 2006). One of the important characteristics of memory CD8<sup>+</sup> cell is their capacity to display immediate effector functions following Ag re-exposure (Walzer et al., 2003). This process lasts for several days and progressively decreases upon physiological down-regulating mechanisms

(Krasteva et al., 1999). A memory response to Ag is much faster than the primary response (Vocanson et al., 2009). Infiltration of hapten-specific effector and memory T cells causes local inflammatory response 24-72 h later (Krasteva et al., 1999; Martin et al., 2008). Recruitment of lymphocytes into inflamed skin is a multistep process and involves recognition of vascular endothelial cells and extravasations; there is a sequential infiltration of the skin, CD8+ cells enter first, and then CD4+ cells due to differential expression of homing-receptors and sequential expression of chemokines (Cavani et al., 2000). CD8+ cells infiltrate skin 9 h after hapten re-exposure, whereas CD4+ cells are recruited after 24 h and this fact is associated with diminishing the reaction severity (Akiba et al., 2002). IFN- $\gamma$  is a key cytokine in local expression of inflammation during the first 24 h, and this inflammation is mediated by the production of KC-derived chemokines (such as IP-10, MIG, I-Tac acting on CXCR3 leukocyte chemokine receptors). MCP-1 and RANTES are the dominant monocyte/macrophage chemo-attractants expressed during the elicitation phase (Goebel et al., 2001). Both subsets of T cells, CD4+ and CD8+, mediate skin inflammatory reaction, however, more studies have shown that hapten-specific CD8+ cells can mediate reaction without CD4+ cells (Krasteva et al., 1999). CD8+ cells have the main effector role during elicitation phase, whereas CD4+ can have pathogenic and regulatory role. There are three steps in the development of elicitation phase of ACD: first step includes early recruitment of CD8+ cells and this is initiated via endothelial activation due to hapten-induced skin inflammation (Vocanson et al., 2009). Second step is activation of hapten-specific cells, and activation of skin-resident cells and cytokine and chemokine production. Third step is arrival of leukocytes to the skin, especially macrophages and neutrophils, and development of clinically observed reaction (Vocanson et al., 2009).

KCs are also important in the elicitation phase of ACD, because, upon re-exposure, they up-regulate co-stimulatory molecules such as CD80, and are able to function as antigen-presenting cells, facilitating activation of hapten-specific effector T cells (Ouwehand et al., 2010). The identification of specific combinations of cytokines and chemokines as biomarkers that are unique to ACD is challenging. These mediators are commonly also found in other inflammatory conditions. However, it is tempting to hypothesize that the distinction between irritant contact dermatitis (ICD) and ACD could be made on the basis of T cell-related factors, as ICD does not involve antigen-specific T cells (Meller et al., 2007). Interestingly, CXCL9, CXCL10 and CXCL11 were recently found to be selectively up-regulated in human skin in nickel-induced ACD as compared with atopic dermatitis (AD) (Quaranta et al., 2014).

To facilitate the use of *in vitro* methods an **adverse outcome pathway (AOP)** for skin sensitization was established (OECD, 2012). AOP is the sequence of events from the molecular initiating event to an *in vivo* outcome of interest. Each AOP represents the existing knowledge concerning the linkage between a molecular initiating event, intermediate events and an adverse outcome at the individual or population level.

Knowledge of the AOP for skin sensitization has evolved rapidly over the past decade and four events that are recognized as key ones, have been identified (Fig. 4):



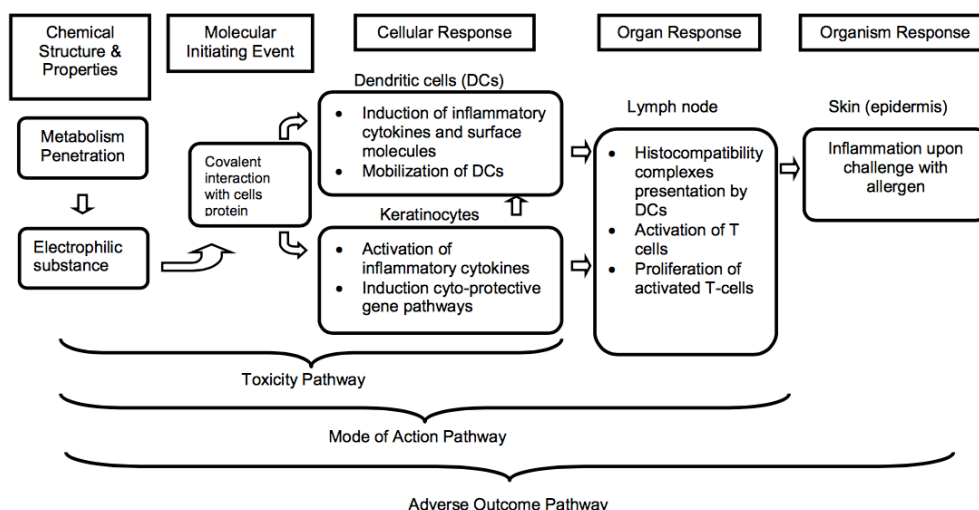


**Fig. 4 Flow diagram of the pathways associated with skin sensitization [4]**

Following a brief description of each key events (KEs) is reported:

1. The first key event is the interaction of the chemical with skin protein. Specifically, the target chemical or its metabolite or abiotic transformation product of the target chemical covalently binds to cysteine and/or lysine residues of skin proteins;
2. The second key event takes place in the keratinocytes. It includes inflammatory responses as well as gene expression associated with specific cell signaling pathways;
3. The third key event is the activation of dendritic cells, which is typically assessed by expression of specific cell surface markers and release of chemokines and cytokines.
4. The final key event is the specific T cell clonal expansion, which is measured in the murine LLNA.

In the last ten years the laboratory of toxicology has been interested in the development of alternative methods to identify contact allergens. In particular, attention focused on KEs 2 and 3. Regarding KE 2, to investigate the role of KCs in allergic contact dermatitis, my experiments were conducted using human KCs cell line, **NCTC 2544**. NCTC 2544 is a commercially available skin epithelial-like cell line originating from normal human skin, which

posses a good expression of cytochrome P450-dependent enzymatic activities. NCTC 2544 is an immortalized, non-tumorigenic cell line, which grows in a monolayer.

In previous studies, we showed that exposure to contact allergens, but not to respiratory allergens or irritants, resulted in a dose-related induction of intracellular IL-18. The assay proved to be useful in the identification and discrimination of contact allergens from respiratory sensitizers and irritants (Corsini et al., 2009, 2013; Galbiati et al., 2011). In the context of the sensitization process, the NCTC 2544 assay was designed to cover the initial phase 'local trauma-proinflammatory cytokine production (danger signals)', necessary for maturation and migration of dendritic cells, and T cells activation.

**IL-18**, formerly known as IFN- $\gamma$ -inducing factor (IGIF), which belongs to the IL-1 cytokine family, has been shown to play a key proximal role in the induction of allergic contact sensitization and to favor Th-1 type immune responses by enhancing the secretion of proinflammatory mediators such as TNF- $\alpha$ , IL-8 and IFN- $\gamma$  (Okamura et al., 1995; Cumberbatch et al., 2001; Antonopoulos et al., 2008). IL-18 does not stimulate Th-2 cells (Robinson et al., 1997 and Kohno et al., 1997). This was shown using an assay in which IL-18 induced translocation of NF $\kappa$ B in Th-1 clones but not Th-2 cells. In these Th-2 clones, nuclear translocation of NF $\kappa$ B was not observed following incubation with IL-18, whereas in the same cells IL-1 $\alpha$  induced NF $\kappa$ B activation and cellular proliferation (Robinson et al., 1997). In another study, Th-2 clones did not express mRNA for IL-18 Receptor  $\alpha$  (IL-18R $\alpha$ ) (Xu et al., 1998 and Yoshimoto et al., 1998), which may be the best explanation for the lack of IFN $\gamma$  production by Th-2 cytokines.

IL-18 has no apparent role in ICD (Antonopoulos et al., 2008), indicating that the role of IL-18 in contact hypersensitivity is not simply part of a general requirement for IL-18 in skin inflammation. Furthermore, Hartwig et al., 2008 demonstrated using IL-18-deficient mice that

the absence of IL-18 does not affect any of the asthma-specific parameters, including allergen-specific immunoglobulin E (IgE), histological changes of the lungs, infiltrating leukocytes, serum cytokine levels and airway hyperresponsiveness. Human keratinocytes constitutively express IL-18 mRNA and protein (Naik et al., 1999), and works published by Naik et al., 1999 and Van Och et al., 2005 showed the induction of IL-18 following exposure to contact sensitizers. IL-18 and IL-1 $\beta$  have some common features: in terms of structure, IL-18 and IL-1 $\beta$  share primary amino acid sequences of the so-called "signature sequence" motif and are similarly folded as all- $\beta$  pleated sheet molecules. IL-1 $\beta$ , IL-18 are synthesized as a biologically inactive precursor molecule lacking a signal peptide which requires cleavage into an active, mature molecule by the intracellular cysteine protease called IL-1 $\beta$  converting enzyme (ICE) or caspase-1. The activity of mature IL-18 is closely related to that of IL-1. IL-18 induces gene expression and synthesis of TNF, IL-1, Fas ligand, and several chemokines. The activity of IL-18 is via the IL-18R complex. The Fig. 5 is a working model of the proposed IL-18 signaling resulting in translocation of NF $\kappa$ B to the nucleus. IL-18R complex is made up of a binding chain termed IL-18R $\alpha$ , a member of the IL-1 receptor family previously identified as the IL-1 receptor related protein (IL-1Rrp), and a signaling chain, also a member of the IL-1R family. IL-18 binds to the IL-18R $\alpha$  chain (Torigoe et al., 1997) (also known as IL-1Rrp) and recruits the IL-18R $\beta$  chain. This heterodimeric complex recruits MyD88 and IL-1R Activating Kinase (IRAK). Phosphorylated IRAK activates TNFR-associated factor-6 (TRAF-6), and in turn, NF $\kappa$ B-Inducing Kinase (NIK) is phosphorylated. This results in activation of IKK and then phosphorylation of I $\kappa$ B. Phosphorylated I $\kappa$ B degrades and releases the p50 and p65 components of NF $\kappa$ B. Free NF $\kappa$ B migrates through nuclear pores and translocate to nuclear DNA for gene transcription.

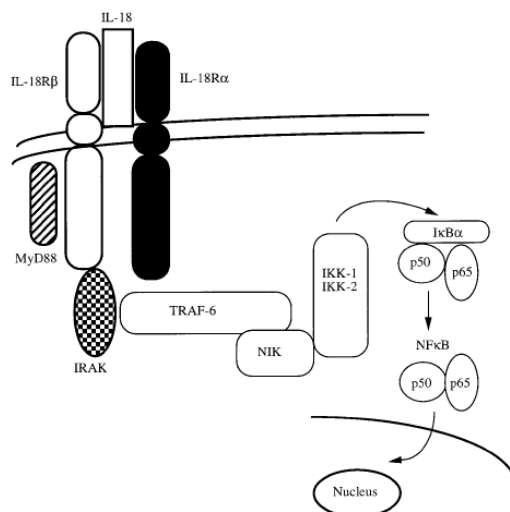


**Fig. 5 Model for IL-18 signal transduction [5]**

Thus on the basis of primary structure, three-dimensional structure, receptor family, signal transduction pathways and biological effects, IL-18 is classified as a member of the IL-1 family. Similar to IL-1, IL-18 participates in both innate and acquired immunity.

**Signal transduction pathways involved in inflammasome activation.**

On the known basis of ACD mechanistic understanding, the relationship between reactivity of molecules toward proteins and their sensitization potential has increased interest and was used to develop experimental assay to predict the skin sensitization potential of chemicals to replace *in vivo* animal tests (Gerberick et al., 2008).

As described, the innate immune system is composed of receptors that collectively serve as a sensor for monitoring the extracellular and intracellular compartments for signs of infection or tissue damage. A key component of cytosolic surveillance is the **inflammasome**, a large multimolecular complex that controls activation of the proteolytic enzyme caspase-1 (Martinon et al., 2002). Caspase-1 in turn regulates maturation of the proinflammatory cytokines IL-1 $\beta$  and IL-18 or the rapid inflammatory form of cell death called “pyroptosis”

(Rathinam et al., 2012). The inflammasome was described a decade ago and contains a cytosolic PRR, typically a **NLR** or a non-NLR AIM2 [absent in melanoma 2 (AIM2)], the apoptosis-associated speck-like protein containing a CARD (**ASC**, also known as PYCARD) which harbours an N-terminal pyrin (PYD) domain and a CARD at C-terminus (Srinivasula et al., 2002) and the **pro-caspase-1**. The ASC configuration facilitates homotypic associations with other PYR and CARD containing proteins required for inflammasome assembly by linking the NLR with pro-caspase-1. The stimuli, the supposed mechanisms, the structure of the known inflammasomes and the key proteins are illustrated in Fig. 6:

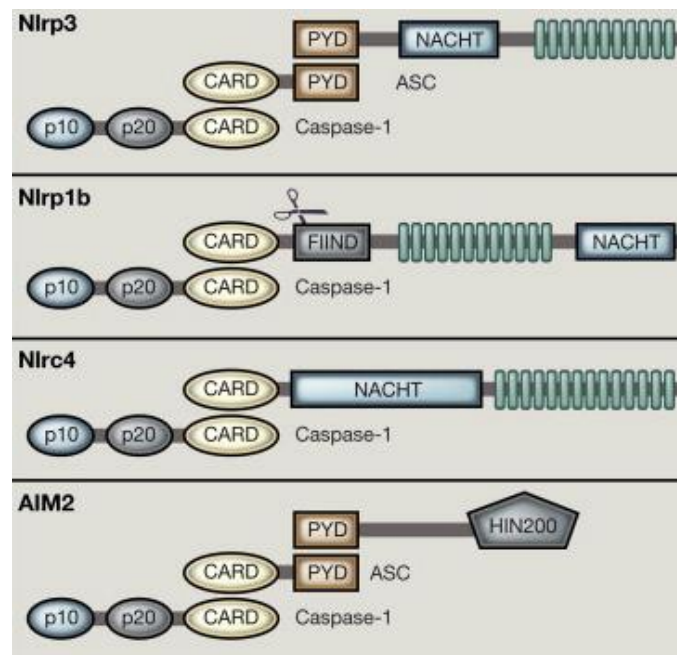


**Fig. 6 Inflammasome subtypes and organization [6]**

The NLRP3 (CIAS, NALP3, cryopyrin) inflammasome is unique amongst inflammasomes in being responsive not only to microbial cues but also a plethora of chemically diverse non-microbial signals arising from, for example, monosodium urate (Martinon et al., 2006), glucose (Zhou et al., 2010) extracellular ATP (Mariathasan et al., 2006) as well as PAMPs

(Mariathasan et al., 2006; Craven et al., 2009). The NLRP3 couples directly to the PYD of ASC via its PYD domain to execute function.

Among the NLRs, NLRP1 (NALP1) inflammasome is the original oligomeric complex discovered consisting of caspase-1, caspase-5, NLRP1 and ASC (Martinon et al., 2002). It is presently the only known inflammasome containing a FIIND (function to find) domain, which undergoes autocleavage to confer functionality (Finger et al., 2012). Both anthrax lethal factor from *Bacillus anthracis* (Boyden and Dietrich, 2006) and muramyl dipeptide (Faustin et al., 2007) initiate its activation.

The NLRC4 (IPAF) inflammasome is characterized by the presence of an intrinsic CARD domain that interacts directly with procaspase-1 (Mariathasan et al., 2004). The main triggers for this inflammasome are bacterial flagellins of gram-negative bacteria with type III or IV secretion systems exemplified by *Salmonella typhimurium* and *Shigella flexneri* (Mariathasan et al., 2004; Amer et al., 2006; Miao et al., 2006; Franchi et al., 2006). Activation has also been shown to be flagellin-independent (Suzuki et al., 2007) indicating that other, as yet unknown, bacterial ligands are also sensed by NLRC4.

The non-NLR AIM2 inflammasome belongs to the haematopoietic expression, IFN-inducible, nuclear localization and length of 200 amino acid domain (HIN200) family (Burckstummer et al., 2009; Fernandes-Alnemri et al., 2009). It is distinct from the NLR inflammasomes in having a HIN group containing a PYD domain that associates with the PYD of ASC to effect function. AIM2 detects double-stranded DNA within the cytosol (Fernandes-Alnemri et al., 2009; Rathinam et al., 2010) for which direct binding has been demonstrated (Hornung et al., 2009).

Among NLR inflammasome complexes, the **NLR3 inflammasome** has been the most widely characterized and is a crucial signaling node that controls the maturation of IL-1 $\beta$  and IL-18 (De Nardo et al., 2011).

Activation of the NLR3 inflammasome is thought to be regulated at both the transcriptional and post-translational levels (Vanaja et al., 2015). The general mechanisms by which NLR3 inflammasome is activated are summarized in Fig. 7.

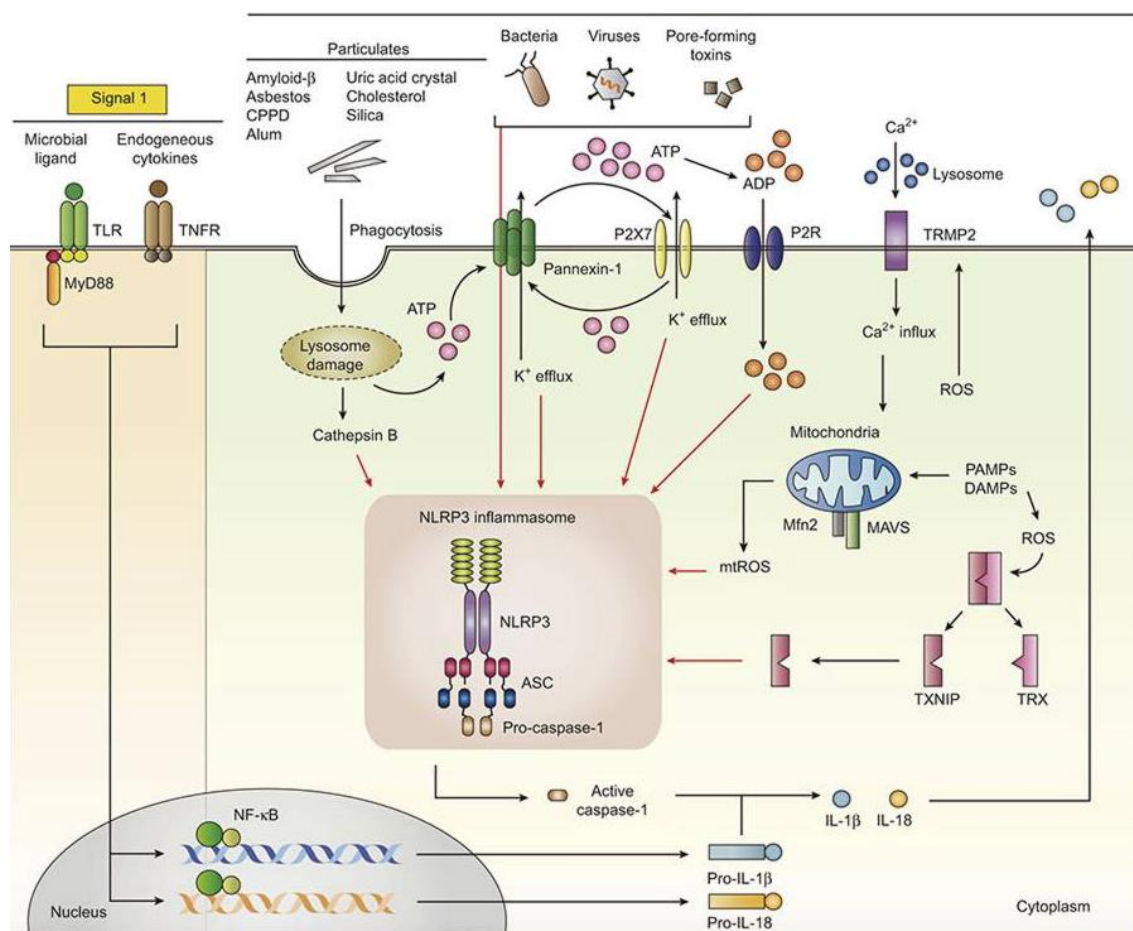


**Fig. 7 NLR3 activation [7]**

The first signal in inflammasome activation involves the priming signal, mediated by microbial ligands recognized by TLRs or cytokines such as TNF- $\alpha$ . Signal 1 activates the NF $\kappa$ B pathway, leading to up-regulation of pro-IL-1 $\beta$ /pro-IL-18 and NLR3 protein levels. The signal 2 is

mediated by numerous PAMP or DAMP stimulation, and promotes the assembly of ASC and pro-caspase-1, leading to activation of the NLRP3 inflammasome complex (Franchi et al., 2010).

Briefly, molecular mechanisms suggested for NLRP3 activation to induce caspase-1 activation and IL-1 $\beta$ /IL-18 maturation are: pore formation and potassium (K<sup>+</sup>) efflux, mitochondrial ROS generation and lysosomal destabilization and rupture. Evidence supports that the aberrant activation of the NLRP3 inflammasome is associated with the pathogenesis of various autoinflammatory, autoimmune, and chronic inflammatory and metabolic diseases. Thus, activation of the NLRP3 inflammasome should be tightly regulated to prevent unwanted host damage and excessive inflammation.

The three molecular mechanisms suggested are following described: physiologically, cytosolic K<sup>+</sup> levels in all cells at rest are high with a substantial exit of intracellular K<sup>+</sup> ions warning the cell of danger. A change in K<sup>+</sup> ion concentration induces cleavage of immature IL-1 $\beta$  and IL-18 into their corresponding processed entities (Perregaux and Gabel, 1994) through the purinergic P2X7 receptor (Falzoni et al., 1995; Ferrari et al., 1997). Abundant in haematopoietic cells (Collo et al., 1997; Ferrari et al., 2006), the P2X7 receptor is an ion channel gated by extracellular Adenosine Triphosphate (ATP) which generates an initial cation current on binding of the nucleotide (Surprenant et al., 1996) and has since been shown to link with the NLRP3 inflammasome (Mariathasan et al., 2004; Duncan et al., 2007). Low cytosolic K<sup>+</sup> concentrations also initiate activation of NLRP1 (Petrilli et al., 2007), NLRC4 (Arlehamn et al., 2010) and AIM2 (Petrilli et al., 2007; Fink et al., 2008; Muruve et al., 2008). Intriguingly, activation of caspase-1 by intracellular bacteria does not require ATP or intracellular K<sup>+</sup> depletion (Franchi et al., 2007). A distinct second phase of the P2X7 ion current, indicative of large pore formation, is also observed in the presence of ATP (Di Virgilio,



1995; Falzoni et al., 1995; Surprenant et al., 1996) and in macrophages this pore activity has since been attributed to the pannexin-1 hemichannel associating with P2X7 (Pelegri and Surprenant, 2006); the pannexin pore is the gateway exploited by microbes for the intracellular delivery of toxins and consequent inflammasome activation (Kanneganti et al., 2007). Molecules involved in sterile inflammation are associated with transient ROS generation (Fubini and Hubbard, 2003). It is not clear how ROS trigger such activation but one proposed mechanism suggests that dissociation of constitutively-expressed thioredoxin-interacting protein from thioredoxin allows the former to bind to the LRR domain of the inflammasome (Zhou et al., 2010). Another route of inflammasome activation by ROS is postulated as being due to Nicotinamide Adenine Dinucleotide Phosphate (NADPH) oxidase (Nox) activity (Dostert et al., 2008). However, contradictory effects were reported in patients with chronic granulomatous disease who carry a mutation in the p22phox gene and in whom IL-1 $\beta$  secretion as a measure of inflammasome activity was Nox-independent (van Bruggen et al., 2010). A role for ROS signals emanating from damaged mitochondria has also been cited as a source of NLRP3 activation (Zhou et al., 2011) as well as NLRP3 oligomerization induced by the Mitochondrial Antiviral Signaling protein, MAVS (Park et al., 2013) and de-ubiquitination of the inflammasome (Juliana et al., 2012). Sterile inflammation may also evoke inflammasome activation following damage by crystalline or particulate matter. Such compounds including alum, silica, asbestos, adjuvants and cholesterol (Duewell et al., 2010; Rajamaki et al., 2010) cause lysosomal disruption following their phagocytosis by macrophages. Consequently, lysosomal proteases such as cathepsin D are released into the cytosol and are then sensed by as yet unknown substrates triggering NLRP3 activation (Halle et al., 2008; Hornung et al., 2008). Use of a cathepsin B inhibitor partially impaired

inflammasome activation providing some support for the mechanism (Hornung et al., 2008); however, the possibility of off-target effects of these small molecules cannot be excluded.

---

**CHAPTER TWO**  
ASSESSMENT OF CHEMICAL-INDUCED CONTACT  
HYPERSENSITIVITY: *IN VIVO* AND *IN VITRO* MODELS

---

The assessment of the skin sensitization potential of chemicals represents an important component of the safety assessment, relevant in the context of several EU regulations aiming at the protection of human health. Predictive testing to identify and characterize substances causing skin sensitization historically has been based on animal tests. Officially accepted animal test methods for skin sensitization potential assessment include the Buehler occluded patch test in the Guinea pig, the Guinea Pig Maximization Test by Magnusson & Kligman (GPMT) and the Mouse Local Lymph Node Assay (LLNA) with its non radioactive modifications (LLNA: DA and the LLNA: BrdU Elisa). The Organization for Economic Co-operation and Development (OECD) Test Guideline (TG) regulates all of these *in vivo* methods: TG406 for the GPMT and Buehler test; TG429 for the LLNA; TG442A and 442B for the LLNA: DA and the LLNA: BrdU Elisa respectively. Whereas the mouse LLNA measures the response provoked during the induction of sensitization, the two Guinea pig test measure challenge induced elicitation reactions in previously sensitized animals. The LLNA is considered a reduction and refinement method compared to the traditional Guinea pig tests. There has been a continuous effort to find alternative approaches, which avoid testing on animals wherever possible. Whenever replacement is not possible, the development of methods that use fewer animals or cause least harm to the animals is supported. The **'Three Rs Principle'** (replacement, reduction and refinement of animal use) is present in all relevant EU legislations. In early 2003, the 7<sup>th</sup> amendment to the European Union's Cosmetics Directive (76/768/EEC) was adopted, and according to it an immediate end to animal testing in the EU for cosmetic products and a complete ban of animal testing for ingredients by 11 March 2009. The animal testing ban was reinforced by a marketing ban on all cosmetic ingredients or products tested for the purposes of the Directive outside the EU after the same date. Since 11 July 2013 the new EU Regulation 1223/2009 (**Cosmetics Regulation**) is in force, which prohibits the marketing of cosmetic

products, the final formulation, ingredients or combinations of ingredients, which have been tested on animals, and also prohibit each test currently, carried out using animals.

Starting from the *in vivo* observation that in mouse IL-1 $\alpha$  expression by KC was selectively increased after *in vivo* application of contact sensitizers but not tolerogen or irritant (Enk and Katz, 1992), similar results were reproduced *in vitro* using the murine KC cell line HEL30 (Corsini et al., 1998). Same results were also obtained by Van Och et al (2005) and, furthermore, the authors observed that the ranking of potency was similar to the ranking established using the local lymph node assay. Similarly, using human KC it has been demonstrated that allergens but not irritants induced IL-12 (Muller et al., 1994; Corsini et al., 1999). Trinitrobenzene sulphonic acid induced the expression of CD40 on KC, whereas Sodium Lauryl Sulfate (SLS) did not (Coutant et al., 1999). All together these studies indicate the possibility to identify contact sensitizer using murine or human KC.

In the screening of new chemicals for human use, it should be very important both from safety and economic point of view to have biological markers to discriminate allergy and irritation events that have different impact on human health (Corsini and Roggen, 2009; dos Santos et al., 2009; Galbiati et al., 2010).

On the other side, the EU Regulation on chemicals and their safe use, **REACH**, which came into force in 2007, gives greater responsibility to industry to manage the risks from chemicals and to provide safety information on the substances to allow safe handling. The REACH Regulation also calls for the progressive substitution of the most dangerous chemicals where possible.

To achieve a complete replacement of animals in skin sensitization assessment, dose-response information and evaluation of relative skin sensitizing potency to support effective

risk assessment are necessary. In this context, potency is based on the concentration of chemicals needed to induce a positive response. While a number of methods, reflecting the major key events described in the OECD adverse outcome pathway for skin sensitization (OECD GD168), are at various stages of acceptance, validation, development and use, currently it is not possible to rank chemicals for their sensitizing potency, an issue that is important for a full safety assessment (Corsini et al., 2014). It is expected that a predictive method to totally replace animal testing will be in the form of a test battery comprising molecular, cell-based, and/or computational methods, the so-called “Integrated Approaches to Testing and Assessment (IATA)”. Currently available *in vitro* methods support the discrimination between skin sensitizers (i.e., UN GHS Category 1, where UN GHS stands for United Nations Globally Harmonized System of Classification and Labelling of Chemicals) and non-sensitizers in combination with other complementary information (i.e., in the context of an IATA). Depending on the regulatory framework, positive results may be used on their own to classify a chemical to UN GHS Category 1. They cannot, however, be used on their own to sub-categorize skin sensitizers into UN GHS subcategories 1A and 1B or to predict potency for safety assessment decisions, which is necessary to fully replace animal testing.

A number of assays for the *in vitro* identification of contact and respiratory sensitization have been developed within the integrated European Framework Program 6 Project SENS-IT-IV. The aim of the SENS-IT-IV EU Framework Programme 6 funded integrated Project (LSHB-CT-2005-018681) was to develop and optimize an integrated testing strategy consisting of *in vitro* human cell based assays, which will closely mimic sensitization mechanisms *in vivo*. These assays should provide an alternative approach to the LLNA. *In vitro* assays for risk assessment of potentially sensitizing substances can, once formally validated and implemented into European regulations, replace the LLNA (Kimber et al., 1990, 1991). In principle, a test system

comprised of KC alone may not be useful in establishing allergenic potential as these cells lack antigen-presenting capacity. However, in addition to chemical processing LC activation requires the binding of cytokines produced by KC as a result of initial chemical exposure. The irritant capacity of allergens might present an additional risk factor so that irritant allergens may be stronger allergens than non-irritant ones (Grabbe et al., 1996). In that case, the potency of chemicals to induce cutaneous sensitization may be assessed as a function of KC cytokine expression.

Potency assessments is important as: (1) potency data are required for hazard classification and can lead to improvements in risk management; (2) potency data can facilitate risk assessment for skin sensitization. The evidence is that concentration of chemicals vary by up to four or five orders of magnitude with respect to their relative skin sensitizing potency (Jowsey et al., 2006).

Based on the estimation of the concentration of chemical required to induce a stimulation index of three relative to concurrent vehicle-treated controls (EC3 value), the LLNA has proven very useful in assessing the skin sensitizing potency of chemicals: extreme, strong, moderate and weak were the categories proposed. In this scheme extreme sensitizers were defined as those having an EC3 value of less than 0.1%, strong= EC3 values of equal to or greater than 0.1% and less than 1%, moderate= EC3 values of equal to or greater than 1% and less than 10% and weak= EC3 values of equal to or greater than 10%. This scheme is summarized in Table 1. All the other chemicals, that are inactive in the LLNA and for which an EC3 value cannot be derived, should be classified as non-sensitizer.

CATEGORY	EC3 VALUES (%)
Extreme	< 0.1
Strong	≥ 0.1 - <1
Moderate	≥ 1 - < 10
Weak	≥10 - ≤ 100

**Table 1: categorization of contact allergens [8]**

Importantly, determinations of relative potency based on EC3 values appear to correlate closely with what is known of the relative ability of contact allergens to cause skin sensitization among human, by the human repeated insult patch test (HRIPT) (Basketter et al., 2000; Gerberick et al., 2001; Griem et al., 2003).

A decision on collocation to a category was achieved using information from experimental human studies, specifically the HRIPT or the human maximization test (HMT) as published by Kligman (Kligman, 1989). Most data are able to offer a no-effect level (NOEL), and where multiple data exist, the highest value has been taken. For a few substances, a lowest-effect level (LOEL) has been calculated. To understand the potency categorization on the basis of human data, the criteria is provided in Table 2, where the skin sensitizers are distributed into 6 potency categories:

POTENCY CATEGORY	HRIPT/HTM NOEL	DIAGNOSTIC PACTH TEST DATA	USE INFORMATION
Extreme	< 25 µg/cm <sup>2</sup>	< 3% in most dermatology clinics	Probably low exposure concentration
Strong	25-500 µg/cm <sup>2</sup>	< 1% in most dermatology clinics	Lower use concentration may raise
Moderate	500-2500 µg/cm <sup>2</sup>	Up to 1% in major dermatology clinics	By 1 category; higher use concentration may drop a category
Weak	> 2500 µg/cm <sup>2</sup>	Less common/ frequent positive results than category 3	By 1 category; higher use concentration may drop a category
Very weak	> 10000 µg/cm <sup>2</sup>	Rarely positive except in selected patients with eczema	Possibly despite high use
Non sensitizers	negative	An absence of positive despite testing in many clinics	Use could be high or low

**Table 2. Outline of potency categorization guidance [9]**



Here the key point is that larger NOEL values equate to lower skin sensitization potency. Where there are multiple values, the higher value should always be used. The converse argument would always apply to LOEL values, where the smaller value must be adopted. As always, the final decision on a category will have considered all of the available evidence. This includes diagnostic patch test data, where this exists, judged against the use volume information. Diagnostic patch test data can be taken from the clinical literature and from the Scientific Committee on Consumer Safety (SCCS) review.

In the context of alternative methods, four non-animal tests have been recently validated (Table 3):

- **Direct peptide reactivity assay (DPRA)**, which measures depletion of a cysteine- and a lysine-containing peptide in the presence of the test chemical (Gerberick et al., 2007);
- **The KeratinoSens assay™**, which is based on a luciferase reporter gene under the control of an anti-oxidant response element of the human AKR1C2 gene stably inserted into HaCaT keratinocytes (Emter et al. 2010);
- **The human cell line activation test (h-CLAT)**, addressing CD86 and CD54 upregulation in THP-1 cells (Sakaguchi et al., 2009);
- and the **IL-8 Luc assay**, which measures the effects of chemicals on IL-8 promoter activity in the IL-8 reporter cell line THP-G8 cells (Kimura et al., 2015).

The first three methods have been validated by European Union Reference Laboratory for alternatives to animal testing (EURL-ECVAM), while the last by Japanese Center for the Validation of Alternative Methods (JaCVAM).

Placed in the context of the AOP, the DPRA evaluates key event 1: the protein/peptide

reactivity of a substance, the KeratinoSens™ represents key event 2 and gives a measure keratinocytes activation and h-CLAT, Myeloid U937 skin sensitization test (MUSST) and IL-8 Luc assay describe key event 3, the dendritic cell activation.

	Test Guideline (TG)/ Methods	Endpoint	Data interpretation (OECD TG)	Data interpretation for potency assessment
KE 1	TG 442C <b>DPRA</b>	Cys/Lys peptide depletion (0-100%)	Depletion ≤ 6.38%: No Sensitizer Depletion > 6.38%: Sensitizer	0% ≤ depletion ≤ 6.38%: minimal reactivity 6.38% ≤ depletion ≤ 22.62%: low reactivity 22.62% ≤ depletion ≤ 42.47%: moderate reactivity 42.47% ≤ depletion ≤ 100%: high reactivity
KE 2	TG 442D <b>KeratinoSens</b>	Luciferase gene induction (activation of Keap1-Nrf2-ARE pathways)	test chemical is sensitizer if: -Luciferase fold induction is higher than 1.5 -viability ≥ 70%	dose-response data from 12 concentrations used to calculate EC <sub>1.5</sub> and IC <sub>50</sub> values.
	TG 442E <b>h-CLAT</b>	Induction of CD86 and CD54	test chemical is sensitizer if: -RFI <sub>CD86</sub> ≥ 150% and/or -RFI <sub>CD54</sub> ≥ 200% -viability ≥ 50%	dose-response data from 8 concentrations used to calculate EC <sub>150</sub> for CD86 and EC <sub>200</sub> for CD54. - EC <sub>150</sub> or EC <sub>200</sub> ≤ 13 µg/ml: cat. 1A - EC <sub>150</sub> or EC <sub>200</sub> > 13 µg/ml: cat. 1B
KE 3	TG draft* <b>U-SENS™ (MUSST)</b>	Induction of CD86	test chemical is sensitizer if: -S.I. <sub>CD86</sub> ≥ 150% (no interference from cytotoxicity, solubility) -viability ≥ 70%	Minimum of 4 concentrations tested: - EC <sub>150</sub> ≤ 40 µg/ml and CV70 ≤ 100 µg/ml: cat. 1A
	<b>IL-8 Luc Assay</b>	Luciferase gene induction (IL-8 and glyceraldehyde 3-phosphate dehydrogenase (GAPDH) expression)	test chemical is sensitizer if: FInSLO-LA ≥ 1.4 lower limit of the 95% CI of FInSLO ≥ 1.0	11 concentrations tested correlation between EC 1.4 and EC3 values investigated (Takahashi et al., 2011).

\*[http://www.altex.ch/resources/altex\\_2017\\_2\\_187\\_192\\_Editorial2.pdf](http://www.altex.ch/resources/altex_2017_2_187_192_Editorial2.pdf)

**Table 3. OECD adopted *in chemico/in vitro* methods [10]**

## **DPRA**

The majority of skin sensitizers are electrophilic in nature, which underpin their ability to react with the nucleophilic aminoacids of proteins. This haptentation process is reproduced *in vitro* in the DPRA, which quantifies the amount of unbound peptides in the reaction mixture by High Performance Liquid Chromatography (HPLC) following the covalent bond formation between hapten and aminoacid residues in the peptide. When the mean peptide depletion of the cysteine and lysine peptides is greater than 6.38%, the chemical is judged as a sensitizer (Table 3). However, as the chemical reactivity varies markedly between various functional groups, the reaction rate of test chemicals with the DPRA peptide may not be linearly related to their *in vivo* sensitization potency, making the DPRA unsuitable for potency assessment. This is also collected in the OECD guideline, where the different DPRA classes of reactivity (i.e., low, moderate and high) are actually assigned a positive prediction, without any sub classification. In the DPRA non allergens and weak allergens demonstrated minimal to low peptide reactivity, whereas moderate to extremely potent allergens displayed moderate to high peptide reactivity (Gerbeich et al., 2007).

## **The KeratinoSens™**

The KeratinoSens™ assay is based on a luciferase reporter gene under the control of an anti-oxidant response element (Nrf2) of the human AKR1C2 gene stably inserted into HaCaT KCs (Emter et al., 2010). It measures a cellular defense mechanism triggered by chemical allergen-induced oxidative stress.

For each chemical, the assay allows the calculation of the EC1.5, EC2 and EC3 (concentration in  $\mu\text{M}$  for 1.5, 2, and 3 fold induction of the luciferase activity and the IC50 (concentration in  $\mu\text{M}$  resulting in 50% reduction in cellular viability). A substance is considered to be a sensitizer

if an induction equal or exceeding 1.5-fold compared to the vehicle control is observed at a concentration below 1mM and at which cells remain >70% viable (Table 3). The correlation analysis of the individual parameters (logarithmic normalized) for the 244 chemicals against the EC3 in the LLNA gave a R2 (%) of 44.8% for EC2 and 33.5% for IC50, statistically significant but not impressive. Similar values were obtained when comparing *in vitro* results with human data (Natsch et al., 2015). While the assay can be useful for hazard identification and labeling, it cannot provide an estimation of the no induction sensitization level or the point of departure for skin sensitization. One of the limitations of all traditional cell cultures is that cells are grown in aqueous solutions, in which the intrinsic poor solubility of lipophilic substances or the instability of certain chemicals (i.e., anhydride) in water can affect the correct potency classification, resulting in a weak correlation. The other bottleneck of many *in vitro* methods, which may give false negative results, is the limited metabolic capacity of the cell lines used. The possibility to use reconstituted human epidermis to overcome these problems will be later discussed.

### ***h-CLAT***

The h-CLAT assay, developed by KAO and Shiseido, measures the selective induction of the surface markers CD54 and CD86 in the human promyelocytic cell line THP-1, which functions as a DC surrogate (Sakaguchi et al, 2009). A substance is considered a sensitizer if the relative fluorescence intensity (RFI) of CD86 and/or CD54 is greater than 150% or 200% at any tested dose in at least two out of three experiments. From dose response curves of the three experiments, the median concentration inducing 150% of CD86 RFI and/or 200% of CD54 RFI (EC150 or EC200) is calculated like the EC3 value in the LLNA (Table 3). The lower EC value obtained is considered the minimal induction threshold (MIT). Based on the MIT value, the h-

CLAT can be used to score strong sensitizers if MIT < 10 µg/mL and weak if MIT = 10-5000 µg/mL (Jaworska et al., 2015). The same limitations described for the KeratinoSens™ also apply to the h-CLAT. While the assay can be useful for hazard identification and labeling, it cannot provide an estimation of the no induction sensitization level or the point of departure for skin sensitization.

### ***U-SENS™***

The U-SENS™ assay, developed by l’Oreal, known as MUSST (Myeloid U937 Skin Sensitization Test), is based on dendritic cell activation following exposure to sensitizers in the U937 human myeloid cell line by measuring the induction of the expression of CD86 by flow cytometry. A substance inducing an increase in CD86 protein expression of Stimulation Index (SI) 150% is considered to be a sensitizer (Table 3). The predictive performance of U-SENS™ was assessed via a comprehensive comparison analysis with the available human and LLNA data of 175 substances. U-SENS™ showed 79% specificity, 90% sensitivity and 88% accuracy.

### ***IL-8 Luc Assay***

The assay, validated by JaCVAM, evaluates the effect of chemicals on IL-8 promoter activity in the IL-8 reporter cell line THP-G8 (Takahashi et al., 2011). It is a high throughput method for detection of IL-8 mRNA induction by sensitizers. With regards to potency, a rank classification is possible, with an accuracy of 70.9%, an over-prediction rate of 10.7% and an under prediction rate of 18.4% (Kimura et al., 2015). Also, this assay cannot provide an estimation of the no induction sensitization level or the point of departure for skin sensitization (Table 3).

Besides the validated tests, there are several other methods at different stages of development and acceptance. Among them, of my particular interest was the **RhE IL-18 potency test** (Gibbs et al., 2013), based on the use of reconstructed human epidermis.

Currently, methods based on skin models are being explored to resolve sensitizing potency. These methods have several advantages over traditional cell cultures, and are expected to have broader applicability. Topical application in relevant vehicles (e.g., in the vehicle used in animal tests or in a cosmetic/dermatological formulation) is only possible in 3D models which mimic *in vivo* bio-availability of a chemical more closely, and which may therefore lead to improved assessment of sensitizer potency (Natsch et al., 2015).

RhE IL-18 potency assay is based on the possibility of combining the epidermal equivalent potency assay, based on the irritation potential, with the assessment of IL-18 release to provide a single test for identification and classification of skin sensitizing chemicals, including chemicals of low water solubility or stability (Gibbs et al., 2013). A protocol was developed using different 3D-epidermal models including in house VUMC model, epiCS® (previously EST1000™, Cell Systems, Troisdorf, Germany), MatTek EpiDerm™ (MatTek In Vitro Life Science Laboratories, Bratislava, Slovak Republic) and SkinEthic™ (Episkin, Lyon, France) RhE. Following topical exposure for 24 h to contact allergens a robust increase in IL-18 release was observed only after exposure to contact allergens. Correlating the *in vitro* RhE sensitizer potency data, which assesses the chemical concentration which results in 50% cytotoxicity (EE-EC50) with human and animal data showed a superior correlation with human DSA05 (induction dose per skin area, in  $\mu\text{g}/\text{cm}^2$ , in a human repeat-insult patch test or human maximization test that produces a positive response in 5% of the tested population) data compared to LLNA data. Also, a good correlation was observed for release of IL-18 (SI-2) into culture supernatants with human DSA05 data.

Given the complexity of the biological mechanisms underlying the acquisition of skin sensitization it is proposed that, in the near future, no single non-animal test method will be able to replace the currently used regulatory animal tests, instead a combination of methods addressing key mechanisms of the sensitization AOP will be needed to achieve full replacement.

In conclusion, the alternative methods able to discriminate between sensitizers and non-sensitizers are already available. Therefore, it is clear that at the moment the more realistic way forward to fully replace animal testing seems to have as more as possible validated alternative methods (*in vitro*, *in silico*) covering the different biological key events of skin sensitization, and use them in an integrated testing strategy.

---

**CHAPTER THREE**  
**OBJECTIVE OF THE THESIS**

---



The aims of my PhD project were:

1. To understand at the molecular level the mechanism of action underlying contact allergen-induced IL-18 production for a better understanding of the mechanisms defining potency.

**Understanding chemical allergen potency: role of NLRP12 and Blimp-1 in the induction of IL-18 in human keratinocytes**

A. Papale, E. Kummer, V. Galbiati, M. Marinovich, C.L. Galli, E. Corsini

**NLRP12 protein and the NLRP3 inflammasome complex in the induction of IL-18 in human keratinocytes: further developments (manuscript in preparation)**

A. Papale, V. Viscardi, C. Lossani, N. Marchetti, V. Galbiati, E. Corsini

2. To expand the list of chemicals tested to prove the validity of the RhE IL-18 assay not only for hazard identification but also for the estimation of the allergenic potency required for a full replacement of animals.

**Development of an *in vitro* method to estimate the sensitization induction level of contact allergens**

V. Galbiati, A. Papale, M. Marinovich, S. Gibbs, E. Roggen, E. Corsini

---

**CHAPTER FOUR**  
MATERIALS AND METHODS: BRIEFLY

---

**Chemicals** used for:

- *Understanding chemical allergen potency: role of NLRP12 and Blimp-1 in the induction of IL-18 in human keratinocytes;*
- *NLRP12 protein and the NLRP3 inflammasome complex in the induction of IL-18 in human keratinocytes: further developments (manuscript in preparation).*

The extreme skin sensitizer 2,4-Dinitrochlorobenzene (DNCB) (CAS #97-00-7) and the strong sensitizer PPD (CAS#106-50-3) were used. The use of both sensitizers is reported in materials and methods detail/chemicals section. For experiments using submerged keratinocytes NCTC 2544 cell culture, DNCB and PPD were dissolved in dimethyl sulfoxide (DMSO), 0.2% final concentration in culture medium., while acetone/olive oil (AOO, 4:1) was used for experiments using RhE. Cell culture media and all supplements were from Sigma-Aldrich Co. (St. Louis, Mo, USA) at the highest purity available, while RhE and RhE medium (EPI-100-MM- 60) were from MatTek corporation (MatTek *In Vitro* Life Science Laboratories, Bratislava, Slovakia).

**Chemicals** used for:

- *Development of an in vitro method to estimate the sensitization induction level of contact allergens.*

A total of 10 contact sensitizers and 4 non-sensitizers were studied. Chemicals were selected from the Interagency Coordinating Committee on the Validation of Alternative Methods (ICCVAM) database and the LLNA database of 341 chemicals (Gerberick et al., 2005; Kern et al., 2010), and not previously tested in the RhE assay, namely benzoquinone, chlorpromazine, chloramine T, benzyl salicylate, diethyl maleate, dihydroeugenol, benzyl cinnamate, 2,4-dichloronitrobenzene, imidazolidinyl urea, and limonene as contact sensitizers while benzyl alcohol, isopropanol, dimethyl isophthalate and 4-aminobenzoic acid as non-sensitizers in the LLNA. The use of all sensitizers is reported in materials and methods detail/chemicals section.

**Cell culture** used for:

- *Understanding chemical allergen potency: role of NLRP12 and Blimp-1 in the induction of IL-18 in human keratinocytes;*
- *NLRP12 protein and the NLRP3 inflammasome complex in the induction of IL-18 in human keratinocytes: further developments (manuscript in preparation).*

For experiments the human KC cell line NCTC 2544 was used (Istituto Zooprofilattico, Brescia, Italia). Cells were seeded at a density of  $2.5 \times 10^5$  cells/ml (for more information, see materials and methods detail/cell counting section) in RPMI 1640 containing 2 mM l-glutamine, 0.1 mg/ml streptomycin, 100 IU/ml penicillin and 0.1% gentamycin, supplemented with 10% heated-inactivated fetal calf serum (media) and cultured at 37°C in 5% CO<sub>2</sub>. For IL-18 production, cells were seeded in 24-well plates (0.5 ml/well). For NLRP12 and Blimp-1 mRNA expression and Western blot analysis, cells were seeded in 100 mm Petri dishes (10 ml/Petri). After o.n. adherence, cells were treated for different times 3, 6 and 24 h with DNCB (1.0, 1.5 and 2 µg/ml), PPD (7.5, 15 and 30 µg/ml) or DMSO as vehicle control (0.2% final concentration in culture medium). Only for DNCB, additional time points were analyzed: 30 min, 1 and 2 h. For NLRP12 co-immunoprecipitation, cells were seeded in 100 mm Petri dishes (10 ml/Petri). After 24 h for PPD (30 µg/ml) and 3 h for DNCB (2 µg/ml) or DMSO as vehicle, the cellular pellets were lysed for co-immunoprecipitation experiments.

**Reconstituted human epidermis (RhE)** used for:

- *Understanding chemical allergen potency: role of NLRP12 and Blimp-1 in the induction of IL-18 in human keratinocytes.*

EpiDerm™ Skin Model (EPI-200) was used (the technology and the applications are described in materials and methods detail/EpiDerm™). RhE was maintained according to the supplier's instructions at 37°C, 5% CO<sub>2</sub> and 95% relative humidity.

### **Chemical exposure**

After 24 h of equilibration time, RhE was transfected with siNLRP12 and siBlimp-1 for 48 h (see small interference RNA section). RhE was then exposed to DNCB (1.5 mg/ml) or AOO as vehicle control. Finn Chamber filter paper disks were impregnated with DNCB and AOO and applied topically to the RhE stratum corneum for 24 h (Gibbs et al. 2013). Culture supernatants were harvested for IL-18 analysis by enzyme-linked immunosorbent assay (ELISA).

### **Reconstituted human epidermis (RhE)** used for:

*- Development of an in vitro method to estimate the sensitization induction level of contact allergens.*

RhE were exposed to described chemicals (Table 4).

### **Chemical exposure**

The assay was performed in order to determine the EC50 value of the chemical (EC50 = effective chemical concentration required to reduce RhE metabolic activity corresponding to cell viability to 50% of the maximum value compared to vehicle exposed cultures) and the release of IL-18 associated with its treatment. According to the SOP (Gibbs et al., 2013; Teunis et al., 2013, 2014), the maximum solubility of chemical was first identified by dissolving the compound in different vehicles. Dilutions were made in the following order: 200, 100, 50, 25, 12.5, 6.25, 3.12, 1.56, 0.78, 0.39, 0.20 and 0.10 mg/ml until a clear solution was reached. The vehicle with the highest dissolving capacity was chosen. Vehicles used are reported in the Table 4.

<b>Chemical name</b>	<b><i>In vitro</i> vehicle</b>
Benzoquinone	AOO
Chlorpromazine	Medium
Chloramine T	Medium
Benzyl salicylate	AOO
Diethyl maleate	AOO
Dihydroeugenol	AOO
Benzyl cinnamate	AOO
2,4-Dichloronitrobenzene	AOO
Imidazolidinyl urea	medium
limonene	AOO
Benzyl alcohol	AOO
Isopropanol	AOO
Dimethyl isophthalate	AOO
4-aminobenzoic acid	AOO

**Table 4. Chemicals and vehicles for RhE exposure [11]**

Chemicals were then tested in dose-response experiments starting with the highest soluble concentration and decreasing with 2-fold serial dilutions for a total of five concentrations. Test chemicals stock solutions were freshly prepared in acetone:olive oil (4:1) or in medium. For exposure, Finn Chamber filter paper discs 8 mm (Epitest LTD Oy, Finland) were impregnated with chemicals or vehicle controls and applied topically to the RhE stratum corneum. Cultures were incubated with chemicals for 24 h. After chemical exposure, filter paper discs were removed and metabolic activity was determined immediately by the MTT assay, while culture supernatants were harvested and stored at 80°C for IL-18 quantification

by ELISA as described below. Chemicals were tested in single in two independent RhE batches. Control conditions (unexposed, vehicle(s) and positive control (DNCB 3 mg/ml in AOO)) were tested in double in each experiment.

**Viability** used for:

*- Development of an in vitro method to estimate the sensitization induction level of contact allergens.*

The MTT and other assays used in the experiments are described in materials and methods detail/cell viability section. After 24 h exposure, filter paper discs were removed from RhE. The MTT analysis was performed in 24-well plates. Thiazolyl blue tetrazolium bromide (MTT) (Sigma-Aldrich) solution in PBS (0.5 ml/well of a 5 mg/ml solution) was added to the 24-well plate, RhE cultures were placed on top and further incubated for 2 h under standard culture conditions. Cultures were then transferred to a new 24-well plate containing 0.3 ml isopropanol to dissolve the formazan crystals. Plates were incubated overnight, sealed with parafilm and protected from the light at room temperature. The absorbance was measured at 595 nm and cell viability is expressed as a % relative to the absorbance value of vehicle control treated RhE. The RhE-EC50 values were obtained by linear regression analysis based on changes in metabolic activity (MTT).

**“Alternative” IL-18 ELISA** used for:

*- Development of an in vitro method to estimate the sensitization induction level of contact allergens.*

We had developed an alternative IL-18 ELISA using antibodies not derived from ascites. In this case, ELISA plates were coated with capture antibody (Mouse anti-human IL-18-UNLB,

Southern Biotech, AL, USA) 0.1 mg/ml in PBS (dilution 1:5000, 100 ml/well) and incubated on at 4°C. After blocking for 1 h in 1% BSA in PBS, samples and standard curve (recombinant human IL-18, MBL International, MA, USA) were plated (100 ml/well) for 2 h at RT. After washing, rabbit anti IL-18 (MyBioSource, CA, USA) was added (dilution 1:1000 in blocking buffer – 100 ml/well) for 1 h at RT. After 1 h, a goat anti rabbit IgG-horseradish peroxidase conjugate (BIO-RAD, Segrate, Italy) was added (dilution 1:15.000 in blocking buffer, 100 ml/well). After washing, the substrate solution (tetramethylbenzidine (TMB) liquid substrate, Sigma-Aldrich, MO, USA) was added (100 ml/well). Plates were read at 595 nm. Results were calculated in pg/ml from a standard curve and then converted to a SI, calculated as:

$$IL-18 SI = IL-18 \text{ in chemical treated RhE} / IL-18 \text{ in vehicle treated RhE}$$

IL-18 SI<sub>2</sub> values were obtained by linear regression analysis based on the chemical concentration resulting in a 2-fold increase in IL-18 release.

#### **Determination of interference of chemical with MTT assay and IL-18 ELISA**

If chemicals interfere with the readouts, they need to be excluded from the RhE IL-18 assay, following outside of the applicability domain of the assay. In order to determine whether a chemical interferes with the MTT assay, the highest soluble chemical concentration is incubated with the MTT solution in the absence of RhE. If a color change is observed, then the chemical must be excluded. To determine if a chemical interferes with the ELISA, a known amount of recombinant human IL-18 (e.g. 250 pg/ml) is spiked directly into conditioned media of RhE treated with the chemical suspected for interference. If the calculated concentration differs from the nominal concentration of IL-18, the chemical must be excluded from the RhE potency assay as it interferes with the ELISA.



**IL-18 ELISA** used for:

- *Understanding chemical allergen potency: role of NLRP12 and Blimp-1 in the induction of IL-18 in human keratinocytes.*

For the assessment of IL-18 production in NCTC 2544 cells, monolayers were gently washed twice with 0.5 ml of phosphate-buffered saline (PBS) and lysed in 0.25 ml of 0.5% Triton X-100 in PBS. Cell lysates were stored at -80°C until measurement. Intracellular IL-18 content was assessed by specific sandwich ELISA as described in materials and methods detail/IL-18 ELISA (Galbiati and Corsini, 2012). Results were normalized by cellular protein content. The protein content of the cell lysate was measured using a commercially available kit (Bicinchoninic acid solution and Copper (II) sulfate solution, Sigma-Aldrich Co.) as described in materials and methods detail/total protein determination. Results are expressed as a stimulation index (SI), as described below. For the assessment of IL-18 release, culture supernatants were harvested and stored at -80 °C for IL-18 analysis by ELISA. For the assessment of IL-18 release in RhE, after chemical exposure, culture supernatants were harvested and stored at -80°C for IL-18 analysis by ELISA.

Results were calculated in pg/ml from a standard curve and then converted to a SI, calculated as:

$$IL-18 SI = IL-18 \text{ in chemical treated cells or RhE} / IL-18 \text{ in vehicle treated cells or RhE}$$

**RNA isolation** used for:

- *Understanding chemical allergen potency: role of NLRP12 and Blimp-1 in the induction of IL-18 in human keratinocytes.*

For total Ribonucleic Acid (RNA) extraction, after treatment culture media was discarded, NCTC 2544 cells washed with PBS, and scraped in 5 ml of cold PBS, transferred in 14 ml

polypropylene tubes and centrifuged for 5 min at 1200 rpm at 5 °C. The supernatant was discarded, and cell pellets lysed with 1 ml of Tri-reagent (Sigma-Aldrich). For total RNA extraction on RhE, inserts were washed with PBS, lysed with 1 ml of Tri-reagent (Sigma-Aldrich Co.), homogenized for 20 sec at room temperature, snap-frozen twice, sonicated for 15 sec (50 Hz), and finally, centrifuged for 5 min at 15,000 rpm. Total RNA was extracted following as described in materials and methods detail/RNA extraction.

**Microarray and quantitative Polymerase Chain Reaction (qPCR) o Real-Time PCR** used for:

- *Understanding chemical allergen potency: role of NLRP12 and Blimp-1 in the induction of IL-18 in human keratinocytes.*

To identify genes involved in inflammasome activation, cells were treated for 6 h with PPD 30 µg/ml or DMSO as vehicle control and total RNA extracted. After Retro Transcription (RT) (described in materials and methods detail/Retro Transcription PCR), the inflammasome RT<sup>2</sup> Profiler PCR Array from Qiagen (Hilden, Germany) was used following the supplier's instructions (see materials and methods detail/PCR arrays).

For the synthesis of cDNA, 2.0 µg of total RNA were retrotranscribed using a high-capacity cDNA reverse transcription kit from Applied Biosystems (Foster City, CA, USA), following the supplier's instructions. For real-time PCR analysis, TaqMan-PCR technology was used. For each PCR, 10 ng of total RNA was used. The 18S ribosomal RNA was used as endogenous reference. Quantification of the transcripts was performed by the  $2^{-\Delta\Delta CT}$  method (Livak and Schmittgen 2001), as described in methods detail/ quantitative PCR or Real-Time PCR.

**Small Interference RNA (siRNA)** used for:

- *Understanding chemical allergen potency: role of NLRP12 and Blimp-1 in the induction of IL-18 in human keratinocytes.*

The effect of inducing RNA interference on NLRP12 and Blimp-1 was performed using commercially available reagents (Qiagen) following manufacturer's instructions (see methods detail/transfection and silencing). Briefly, cells were seeded  $1.6 \times 10^5$  cells/ml in 24-wells plates and after overnight adherence, transfection reagent, siNLRP12 (20 nM final concentration) and siBlimp-1 (40 nM final concentration) were added in RPMI 1640 containing 2 mM l-glutamine, 0.1 mg/ml streptomycin, 100 IU/ml penicillin and 0.1% gentamycin to promote the silencing (48 h). After 4 h of incubation, fetal calf serum was added (10% final concentration). As control siRNA, a siRNA sequence that will not cause the specific degradation of any cellular message was used (Qiagen). RhE was transfected directly in Assay Medium (EPI- 100-ASY), supplied by MatTek corporation, with transfection reagent, siNLRP12 (60 nM final concentration) and siBlimp-1 (80 nM final concentration) to promote silencing. As control siRNA, a siRNA sequence that will not cause the specific degradation of any cellular message was used (from Qiagen). Silencing was conducted following manufacturer's instructions. 48 hrs after siRNA transfection, NLRP12 and Blimp-1 contents in whole-cell lysate were assessed by WB using specific antibodies, to confirm the silencing of proteins. Cells were then treated with DNCB (2  $\mu$ g/ml) and PPD (15  $\mu$ g/ml), or DMSO as vehicle control, while RhE was treated with DNCB (1.5 mg/ml), or AOO as vehicle control for 24 h to assess IL-18 production.

**Western Blot (WB)** used for:

- *Understanding chemical allergen potency: role of NLRP12 and Blimp-1 in the induction of IL-18 in human keratinocytes;*

- *NLRP12 protein and the NLRP3 inflammasome complex in the induction of IL-18 in human keratinocytes: further developments (manuscript in preparation).*

For WB analysis, after established time of incubation, culture media was discarded, cells washed with PBS, scraped in 5 ml of cold PBS, transferred in 14 ml polypropylene tubes and centrifuged for 5 min at 1200 rpm at 5°C. The supernatant was discarded, and cells lysed in 100 µl of homogenization buffer (50 mM TRIS, 150 mM NaCl, 5 mM EDTA pH 7.5, 0.5% Triton X-100, 50 µM PMSF, 2 µg/mL aprotinin, 1 µg/mL pepstatin and 1 µg/mL leupeptin). Hundred microliters of sample buffer 2X (125 Mm Tris HCl pH 6.8, 4% SDS, 20% glycerol, bromophenol blue, 6% β-mercaptoethanol) were added and denatured for 10 min at 100°C. The protein content was assessed using a commercial kit (Bio-Rad, Hercules, CA, USA), as described in materials and methods detail/protein quantification. Forty micrograms of proteins were electrophoresed into a 10% sodium dodecyl sulfate (SDS)–polyacrylamide gel under reducing condition. The proteins were then transferred to polyvinylidene difluoride (PVDF) membrane (Amersham, Little Chalfont, UK). Proteins were visualized using mouse monoclonal anti-β-actin Ab (clone AC-15, 42 kDa; 1:5000) from Sigma-Aldrich, rabbit polyclonal anti-NLRP12 Ab (95–100 kDa; 1:1000) from Tocris Bioscience (Avonmouth, Bristol, UK), rabbit monoclonal anti-Blimp-1/PRDF1 Ab (clone C14A4, 95–100 kDa; 1:500), rabbit monoclonal anti-NLRP3 antibody (110 kDa; 1:500), rabbit monoclonal anti-TMS1 (ASC) antibody (22 kDa; 1:1000), rabbit monoclonal anti-caspase-1 antibody (the pro-caspase-1: 48 kDa and the activated subunit: 20 kDa) from Cell Signaling Technology (Danvers, MA, USA) as primary antibodies and developed using enhanced chemiluminescence (Bio-Rad). The image of the blots was acquired with the Molecular Imager Gel Doc XR (Bio-Rad). The optical density (OD) of the bands was calculated and analyzed by means of the Image Lab version 4.0.1. For more information about WB, see materials and methods detail/Western Blot.

### **Co-immunoprecipitation (Co-IP)** used for:

- *NLRP12 protein and the NLRP3 inflammasome complex in the induction of IL-18 in human keratinocytes: further developments (manuscript in preparation).*

Two hundred microliters of proteins were incubated in RIA buffer 2X (pH 7.2) (400 mM NaCl, 20 mM EDTA, 20 mM Na<sub>2</sub>HPO<sub>4</sub>, 1% Nonidet P-40 and 0.1% sodium dodecyl sulfate (SDS) with a polyclonal anti-NLRP12 antibody (95-100 kDa; 1:200) from Tocris Bioscience (Avonmouth, Bristol, UK) overnight at 4°C on a wheel. Protein A/G plus agarose beads (Santa Cruz Biotechnology) were added and incubation was continued for 2 h at 4 °C on the wheel. Beads were collected by gravity and washed in RIA buffer 1X containing 0.1% SDS four times. Sample buffer 1X was then added to the samples and the mixture was boiled for 10 min. Beads were collected by centrifugation and the supernatant was loaded onto an acrylamide gel for SDS-PAGE. The proteins were then transferred to PVDF membrane and the immunoprecipitated protein NLRP12 was visualized using rabbit polyclonal anti-NLRP12 antibody (100 kDa; 1:500) from LS Bio LifeSpan Bioscience, Inc (Seattle, Washington); NLRP3, ASC and Caspase-1 are used with the same dilution described in WB. For more information about the technique, see materials and methods detail/immunoprecipitation and co-immunoprecipitation.

### **Data analysis of cell culture**

All experiments were repeated at least three times. Data are expressed as mean ± SEM. Statistical analysis was performed using InStat software version 3.0a (GraphPad Software, La Jolla, CA, USA). Statistical significance was determined by ANOVA followed by a multiple comparison test as indicated in the legends. Effects were designated significant at  $p < 0.05$ .

## Data analysis of RhE

According to SOP (Gibbs et al., 2013; Teunis et al., 2013, 2014), all chemicals were tested in at least two independent experiments using different RhE batches. Data obtained in two independent experiments is presented. As results are incorporated into a prediction model, it is not feasible and not necessary to run stats on each independent experiment. The following readouts were used: (1) For the assessment of allergenicity (YES/NO): if the fold increase in intracellular IL-18 is 2.0 in at least one of the concentrations tested the chemical is classified as contact sensitizer (H317). In case the two experiments gave inconsistent results (e.g. one positive and one negative), a third experiment was done, and the majority was used for classification (e.g. if two positives and one negative, the classification will be contact allergen). (2) For potency assessment: the arithmetic means of the values obtained in the two experiments for both cytotoxicity (MTT assay) expressed as of EC50 and IL-18 SI2 (chemical concentration resulting in 2 fold increases in IL-18 release) were considered. Statistical analysis was performed using GraphPad InStat version 3.0a for Macintosh (GraphPad Software, San Diego, CA, USA).

*EE potency assay*: the EE EC50 value is the effective chemical concentration required to reduce metabolic activity (corresponding to cell viability) to 50% of the maximum value. The 100% value for cell viability corresponds to the vehicle control (1% DMSO culture medium or AOO 4:1). EE EC50 values were obtained by linear regression analysis based on changes in metabolic activity (MTT). Statistical significances were determined by Kruskal–Wallis (nonparametric, one way ANOVA) using GraphPad Prism version 4.00 for Windows (GraphPad Software, San Diego, CA, USA). Differences were considered significant for  $p < 0.05$ .

*IL-18 potency assessment:* IL-18 SI-2 and SI-5 values were obtained by linear regression analysis based on the chemical concentration resulting in a 2 fold or 5 fold release in IL-18. Statistical significances were determined by Kruskal–Wallis (nonparametric, one way anova) using GraphPad Prism version 4.00 for Windows (GraphPad Software, San Diego, CA, USA). Differences were considered significant for  $p < 0.05$ . Correlations were determined by nonparametric two-tailed correlation Spearman Analyses using GraphPad Software, San Diego, CA, USA.

---

**CHAPTER FIVE**  
MATERIALS AND METHODS: DETAIL

---



## Chemicals

Several chemicals were used to perform the experiments, classified as weak, moderate, strong and extreme sensitizers, based on their potency. By Toxinet databases, PubChem and European Chemical Agency (EChA) here are reported some information about them:

***2,4-Dinitrochlorobenzene or 1-chloro-2,4-dinitrobenzene (DNCB)*** is an extreme sensitizer. It has been used as an immunostimulant in several conditions including some forms of cancer, and in the treatment of alopecia and warts. It has also been investigated in HIV infection and leprosy. Moreover it is used as a reagent for the detection and determination of nicotinic acid, nicotinamide and other pyridine compounds. It is used in the manufacture of intermediates for the production of dyes and pesticides and explosives, as a reagent, and as an algicide.

***1,4-benzenediamine or para-Phenylenediamine (PPD)*** is a strong sensitizer that is an aniline derivate used as a hair and fur dye, photographic developer, in photochemical measurements, chemical intermediate in the manufacturing of dyes, antioxidants, rubber accelerators, and component of some temporary tattoos (“black henna”).

***1,4-benzoquinone*** is an extreme sensitizer used in topical skin lightening preparations. 1,4-benzoquinone metabolites are used as photographic reducers and developers, antioxidants, stabilizers in paints, oils, and motor fuels, an antioxidant in fats and oils, and as a chemical intermediate and reagents.

***Chlorpromazine*** is a strong sensitizer and it is used to treat a wide range of conditions including anxiety, behavioral problems, nausea and vomiting, and schizophrenia. These medications are neuroleptic agents that affect adrenergic and/or dopaminergic receptor sites, metabolic inhibition of oxidative phosphorylation, and the excitability of neuronal membranes.

**Chloramine T** is a strong sensitizer. Hypochlorite is produced by hydrolysis. Most household bleach solution contains 3% to 5% hypochlorite, while swimming pool disinfectants and industrial strength cleaners may contain up to 20% hypochlorite. It is used as a biocide and mild disinfectant.

**Benzyl salicylate** is a moderate sensitizer. It is a salicylic acid benzyl ester, a chemical compound most frequently used in cosmetics as a fragrance additive or UV light absorber. It appears as an almost colorless liquid with a mild odor described as very faint, sweet-floral, slightly balsamic by those who can smell it, but many people either can't smell it at all or, describe its smell as "musky". Trace impurities may have a significant influence on the odor. It occurs naturally in a variety of plants and plant extracts and is widely used in blends of fragrance materials. It is also used as a solvent for crystalline synthetic musk's and as a component and fixative in floral perfumes such as carnation, jasmine, lilac, and wallflower.

**Diethyl maleate** is a moderate sensitizer. It is used in many organic syntheses as a dienophile for diene synthesis. It is used as an additive and intermediate for plastics, pigments, pharmaceuticals, and agricultural products. It is also an intermediate for the production of paints, adhesives, and copolymers.

**Dihydroeugenol or 2-methoxy-4-propylphenol** is a moderate sensitizer. It is a colorless to pale yellow liquid with a spicy odor and earthy taste. This substance is used in the following products: washing and cleaning products, biocides (e.g. disinfectants, pest control products), air care products, polishes and waxes, perfumes and fragrances and cosmetics and personal care products. Other release to the environment of this substance is likely to occur from: indoor use as processing aid and outdoors use as processing aid.

**Benzyl cinnamate** is a weak sensitizer. It is a component of heavy oriental perfumes and as fixative. It's used as a flavoring agent.

**Imidazolidinyl urea** is a weak allergen. It is an antimicrobial preservative used in cosmetics. It is chemically related to diazolidinyl urea which is used in the same way. Imidazolidinyl urea acts as a formaldehyde releaser.

**Limonene** is a weak allergen and it is a monoterpene and volatile hydrocarbon which occurs naturally in some trees and bushes. It is the predominant monoterpene in citrus oil and widely used as a flavor and fragrance additives for food and household cleaning products and solvents.

**Benzyl alcohol** is not classified as sensitizer in LLNA test. It is common preservative in parenteral medication. It is also used in perfumes and flavors, as a bacteriostatic or viricidal agent in cosmetic, ointments, emulsions, and lotions, as a photographic developer for films and lithography, and as a dye for textiles, nylon carpets and sheet plastics.

**Isopropanol** is not classified as sensitizer in LLNA test. Primarily used as a topical antiseptic. Typical household preparation contains 70% isopropanol. It is also used as a solvent in many household, cosmetic, and topical pharmaceutical products. Isopropanol baths are occasionally used in some cultural practices to relieve fevers.

**Dimethyl isophthalate** is not classified as sensitizer in LLNA test. It is a plasticizer, it is a component of polyester resins, and perfume fixative.

**4-aminobenzoic acid or para-aminobenzoic acid (PABA)** is not classified as sensitizer in LLNA test. PABA and its esters are ingredients in sunscreens. PABA is available in some health food stores, but it is not considered an essential nutrient. PABA has been used in the treatment of peyronie's disease and various rickettsial diseases. The aminoalkyl esters of PABA are local anesthetics such as benzocaine and butesin.

## Cell counting methods

A key step in experimental studies involves the counting of cells or their density. Counting cells can be done in a number of ways, but in our experiments we used the manual cell counting, the hemocytometer (or hemacytometer/haemocytometer), Hemo, for blood; cyto, for cell; meter, for measuring: measuring blood cells (Fig. 8). When the hemocytometer was invented, Louis-Charles Malassez was trying to count blood cells.



**Fig. 8 The house Neubauer chamber or hemocytometer [12]**

The cover glass, which is placed on the sample, does not simply float on the suspension, but is held in place at a specified height (usually 0.1mm). Additionally, a grid is etched into the glass of the hemocytometer. This grid, an arrangement of squares of different sizes, allows for an easy counting of cells. This way it is possible to determine the number of cells in a specified volume.

10  $\mu$ L of count solution are introduced by capillarity in the space between the slide and the hemocytometer. It is possible to count the cells by the microscope. The Fig. 9 represents what it is possible to see under the microscope: the first small square of the top, a big square in the middle of your field of view:

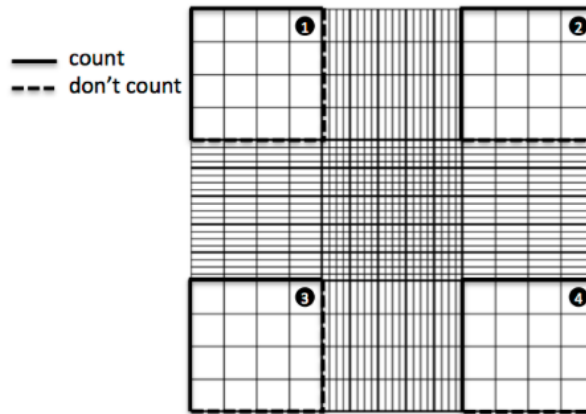


**Fig. 9 hemacytometer squares [13]**

Once get the cell numbers in the first square as in Fig. 9, it is possible to count the cells in the second. If the cells are counted on the top and right sides but not on the bottom and left sides of the first square, it needs to do the same thing with the second one. It is possible to take the average, as reported below:

Take the average of cells per big square  $1+2+3+4$  (Fig.9) and divided by the total number of squares, multiply it by the dilution factor ( $\times 10^5$ ). With the measured cell density obtained, it is possible to calculate how much more medium it is necessary to reach the recommended cell density, for NCTC 2544 cell line is  $2.5 \times 10^5$ .

Final Volume= recommended cell density x initial volume/ measured cell density.

### **EpiDerm™**

EpiDerm™, patented by MatTek corporation, is a proven *in vitro* model system for chemical, pharmaceutical and skin care product testing, used in multiple ECVAM validations and OECD accepted test guidelines.

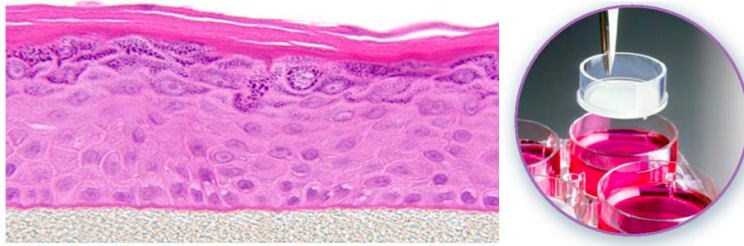


**Fig. 10 RhE on left, tissue culture insert on right [14]**

Also known generically as a Reconstructed human Epidermis (RhE), EpiDerm™ is a ready-to-use, highly differentiated 3D tissue model consisting of normal, human-derived epidermal keratinocytes (NHEK) cultured on specially prepared tissue culture inserts (Fig. 10).

Cultured at the air-liquid interface (ALI), EpiDerm™ allows for the evaluation of topically applied compounds, chemicals, cosmetic/personal care product ingredients and final formulations. EpiDerm™ is the gold standard for a broad range of highly predictive *in vitro* applications. EpiDerm™ exhibits human epidermal tissue structure and cellular morphology with greater uniformity and reproducibility. It is 3D structure consisting of organized and proliferative basal cells, spinous and granular layers, and cornified epidermal layers are mitotically and metabolically active.

The EpiDerm™ 3D human tissue model is used across a diverse range of applications including safety and risk assessment, and biological efficacy. With ALI culture technology, EpiDerm™ can be used to evaluate biological responses to topical applications of formulations or ingredients. It is possible to use EpiDerm™ to determine the skin irritation potential of liquids, solids, gels, lotions, ointments or creams; to determine the skin corrosion potential of test materials; to measure the electrical impedance of EpiDerm™ to assess the efficacy of topically applied moisturizers including creams, gels and lotions; to utilize existing transdermal permeation equipment or MatTek's simple single insert permeation devices to assess API

permeation and flux to determine relative safety with the EpiDerm™ MTT ET-50 assay; to identify phototoxic effects of topical or systemic test substances using the EpiDerm™ Phototoxicity Assay (pre-validated); to identify genotoxic effects of topical or systemic test substances using EpiDerm™ Genotoxicity Assays (pre-validated); to evaluate active compounds for effects on epidermal differentiation using the under-developed EpiDerm™ tissue model.

### **Cell viability**

Cell viability and cytotoxicity assays are used for drug screening and cytotoxicity tests of chemicals. They are based on various cell functions such as enzyme activity, cell membrane permeability, cell adherence, ATP production, co-enzyme production, and nucleotide uptake activity. Many have established methods such as Colony Formation method, Crystal Violet method, Tritium-Labeled Thymidine Uptake method, MTT, and WST methods, which are used for counting the number of live cells. Here are described the used tests during my studies:

**Trypan Blue** is a widely used assay for staining dead cells. Trypan blue is a vital stain used to selectively color dead tissues or cells blue. It is a diazo dye. Live cells or tissues with intact cell membranes are not colored. Since cells are very selective in the compounds that pass through the membrane, in a viable cell trypan blue is not absorbed; however, it traverses the membrane in a dead cell. Hence, dead cells are shown as a distinctive blue color under a microscope. In this method, cell viability must be determined by counting the unstained cells with a microscope. However, Trypan Blue staining cannot be used to distinguish between the healthy cells and the cells that are alive but losing cell functions.

Cellular enzymes such as **lactate dehydrogenase (LDH)** are used to evaluate cytotoxicity. When the cell membranes are compromised or damaged in any way, LDH, a soluble yet stable

enzyme found inside every living cell, is released into the surrounding extracellular space. Since this only happens when cell membrane integrity is compromised, the presence of this enzyme in the culture medium can be used as a cell death marker. The relative amounts of live and dead cells within the medium can then be quantified by measuring the amount of released LDH, using a LDH cytotoxicity assay. When using an LDH colorimetric assay, the amount of LDH released in the surrounding environment is measured with an enzymatic reaction, which converts iodonitrotetrazolium or INT (a tetrazolium salt) into a red color formazan. When LDH is present in the cell culture, it reduces  $\text{NAD}^+$  to NADH and  $\text{H}^+$  through the oxidation of lactate to pyruvate. Afterward, the catalyst (diaphorase) then transfers  $\text{H}/\text{H}^+$  from  $\text{NADH} + \text{H}^+$  to the tetrazolium salt INT to form the red colored formazan salt. The amount of color produced is measured at 490 nm by standard spectroscopy and is proportional to the amount of damaged cells in the culture.

The colorimetric LDH cytotoxicity assay can also be used with different cell types for chemical-mediated cytotoxicity and is ideal for supernatants from cells in culture. I performed LDH test on RhE medium to prove the cytotoxicity of a specific chemicals.

Among the enzyme-based assays, the **MTT assay** is the best known method for determining mitochondrial dehydrogenase activities in the living cells. In the method, MTT, a yellow tetrazole, is reduced to a purple formazan by NADH. However, MTT formazan is insoluble in water, and it forms purple needle-shaped crystals in the cells. Therefore prior to measuring the absorbance, an organic solvent is required to solubilize the crystals. The absorbance of this colored solution can be quantified by measuring at a certain wavelength (usually between 500 and 600 nm) by a spectrophotometer.



## ELISA Test

ELISA is a biochemical technique used mainly in immunology to detect the presence of an antibody or an antigen in a sample.

This method is based upon consecutive incubation steps with different antibodies and the samples of interest, resulting in the visualization via a substrate reaction of the amount of proteins present in the cell lysates (in this case, IL-18). In Fig. 11 each step is described: initially, the ELISA plate is coated with a coating antibody directed against IL-18 epitope(s). To avoid non-specific binding of the antibodies, a blocking step is performed. The samples (antigens) are subsequently added to the plate for incubation, along with a IL-18 standard curve, elsewhere on the plate. During this incubation step the IL-18 protein, present in supernatant, binds to the coating antibody. Unbound protein is washed away and the IL-18 protein is detected with an IL-18 specific biotinylated detection antibody. Incubation with streptavidin-horseradish peroxidase (HRP) will allow binding to the biotiny and a subsequent last step is the incubation with the TMB (3,3',5,5'-Tetramethylbenzidine) substrate. TMB produces a deep blue color during the enzymatic degradation of  $H_2O_2$  by HRP. OD can be read at 595 or 655 nm, the substrate reaction should be stopped through addition of sulphuric acid (stop solution), changing the deep blue color into a clear yellow color. The absorbance is then read at 450 nm.

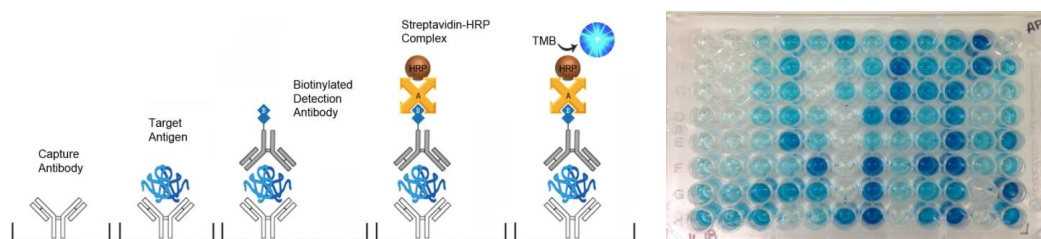


**Fig. 11 Sandwich ELISA platform overview [15], on the right house 96-well plate [16]**

### **Total protein determination**

The protein determination of the samples must be performed parallel to ELISA IL-18, because the results of ELISA IL-18 describe the production of IL-18 in cell lysates samples and the protein quantity in each sample must be subtract. Total protein content of the cell lysates is determined by the bicinchoninic acid (BCA) methods. The BCA assay, is a biochemical assay for determining the total concentration of protein in a solution, similar to Lowry protein assay, Bradford protein assay or biuret reagent. The total protein concentration is exhibited by a color change of the sample solution from green to purple in proportion to protein concentration, which can then be measured using colorimetric techniques. The BCA assay primarily relies on two reactions.

First, the peptide bonds in protein reduce  $\text{Cu}^{2+}$  ions from the copper(II) sulfate to  $\text{Cu}^+$  (a temperature dependent reaction). The amount of  $\text{Cu}^{2+}$  reduced is proportional to the amount of protein present in the solution. Next, two molecules of bicinchoninic acid chelate with each  $\text{Cu}^+$  ion, forming a purple-colored complex that strongly absorbs light at a wavelength of 562 nm.

The amount of protein present in a solution can be quantified by measuring the absorption spectra and comparing these data with protein solutions of known concentration. During my experiments a standard curve was used, considering the lowest point (white) and the highest point of the curve (1 mg/ml of BSA) with other intermediate concentrations: 0.04, 0.1, 0.2, 0.4, 0.6, 0.8 mg/ml.

## RNA extraction

RNA extraction was performed by trizol (also known as Tri reagent) for the isolation of total RNA. This procedure is complicated by the ubiquitous presence of ribonuclease enzymes in cells and tissues, which can rapidly degrade RNA (Peirson et al., 2007). Trizol is a mixture of guanidine thioacyanate and phenol, which effectively dissolves DNA, RNA and protein on homogenization or lysis of tissue sample. After adding chloroform and centrifuging, the mixture separates into 3 phases with the upper clear aqueous phase containing the RNA, as in Fig. 12.

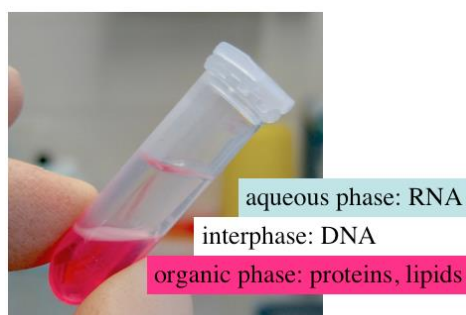


**Fig. 12 Phases of RNA extraction [17]**

The next steps in the extraction are washes and precipitation of the RNA. Moreover, there are commercial kits that enable simple RNA extractions, usually using a column that binds the RNA. At the end of extraction, RNA concentration of each samples is revealed by NanoDrop™ spectrophotometer. It is common for nucleic acid samples to be contaminated with other molecules (i.e. proteins, organic compounds, other). In table 5 are reported the potential contamination factors: they are described by two values, the 260 nm and 280 nm ratio ( $A_{260}/A_{280}$ ), and 260nm and 230 nm ratio ( $A_{260}/A_{230}$ ). Pure RNA has an  $A_{260}/A_{280}$  ratio of 2.0;

the A260/230 ratio is used as a secondary measure of nucleic acid purity. The A260/A230 ratio values for pure samples are often higher than the respective A260/A280 ratio values. As a guideline, the A260/A230 ratio should be greater than 1.5, ideally close to 1.8.

	Low Reading	High Reading
A260/A230 Ratio	<ul style="list-style-type: none"> <li>• Carbohydrate carryover (often a problem with plants).</li> <li>• Residual phenol from nucleic acid extraction.</li> <li>• Residual guanidine (often used in column based kits).</li> <li>• Glycogen used for precipitation.</li> </ul>	<ul style="list-style-type: none"> <li>• Making a Blank measurement on a dirty pedestal.</li> <li>• Using an inappropriate solution for the Blank measurement. The blank solution should be the same pH and of a similar ionic strength as the sample solution. Example: Using water for the Blank measurement for samples dissolved in TE may result in low 260/230 ratios.</li> </ul>
A260/A280 Ratio	<ul style="list-style-type: none"> <li>• Residual phenol or other reagent associated with the extraction protocol.</li> <li>• A very low concentration (&gt; 10 ng/ul) of nucleic acid.</li> </ul>	<ul style="list-style-type: none"> <li>• Residual RNA from nucleic acid extraction.</li> </ul> <p>* High 260/280 purity ratios are not normally indicative of any issues.</p>

**Table 5. Table of potential contamination factors [18]**

### Agarose gel

The overall quality of an RNA preparation may be assessed by electrophoresis on a denaturing agarose gel; this will also give some information about RNA yield. A denaturing gel system is suggested because most RNA forms extensive secondary structure via intramolecular base pairing, and this prevents it from migrating strictly according to its size. Ethidium bromide was added to visualize the gel on a UV transilluminator. In my experiments, it was loaded 1 µg of total RNA. At the end of electrophoresis it was possible to analyze the quality of RNA by Quantity one program and to print the image of RNA separation, as in Fig. 13, to understand if it is intact or degraded.

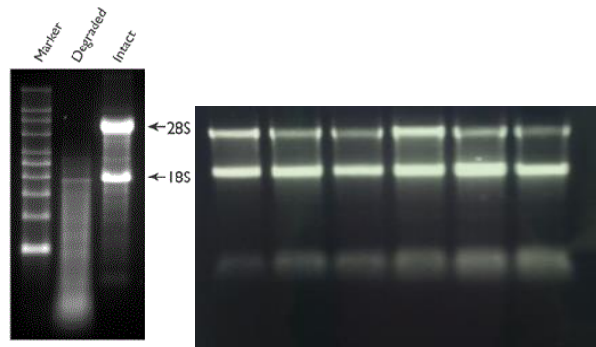


**Fig. 13 Intact vs. Degraded RNA on left side [19]; house RNA on right side [20]**

In Fig. 13 intact total RNA run on a denaturing gel will have sharp 28 Svedberg (28S) and 18S rRNA bands (eukaryotic samples). The 18S and 28S ribosomal RNA bands are clearly visible in the intact RNA sample. The degraded RNA appears as a lower molecular weight smear.

### **Retro Transcription PCR (RT-PCR)**

RT-PCR is the synthesis of complementary DeoxyriboNucleic Acid (cDNA) from RNA templates. This process is catalyzed by the reverse transcriptase enzyme (RTase), which is the replicating enzyme of retroviruses. Reverse transcriptase was discovered in 1970, and since then, it has played an instrumental role in the advancement of molecular biology and biotechnology research. In the presence of all four deoxynucleotide triphosphates (dNTP: dATP, dCTP, dGTP, and dTTP) and under well-defined salt and pH conditions, the reverse transcriptase extends a primer complementary to the RNA to produce a cDNA for the RNA template (Fig. 14). RT-PCR is one of many variants of PCR.

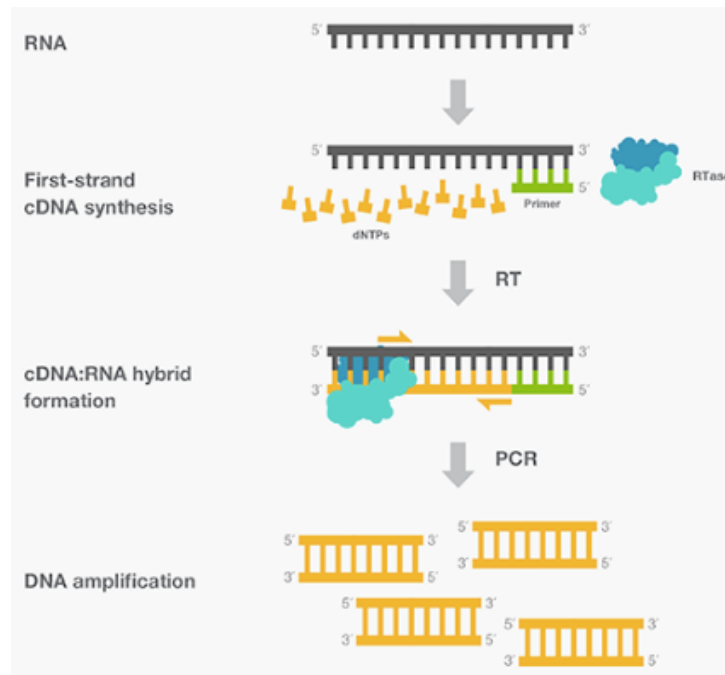


**Fig. 14 RT-PCR. [21]**

### **Polymerase Chain Reaction (PCR)**

PCR is a revolutionary method developed by Kary Mullis in the 1980s. PCR is based on using the ability of DNA polymerase to synthesize new strand of DNA complementary to the offered template strand. Because DNA polymerase can add a nucleotide only onto a preexisting 3'-OH group, it needs a primer to which it can add the first nucleotide. This requirement makes it possible to delineate a specific region of template sequence that the researcher wants to amplify. At the end of the PCR reaction, the specific sequence will be accumulated in billions of copies (amplicons). Components of PCR are:

- DNA template, the sample DNA that contains the target sequence. At the beginning of the reaction, high temperature is applied to the original double-stranded DNA molecule to separate the strands from each other.
- DNA polymerase: a type of enzyme that synthesizes new strands of DNA complementary to the target sequence. The first and most commonly used of these

enzymes is *Taq* DNA polymerase (from *Thermis aquaticus*), whereas *Pfu* DNA polymerase (from *Pyrococcus furiosus*) is used widely because of its higher fidelity when copying DNA. Although these enzymes are subtly different, they both have two capabilities that make them suitable for PCR: 1) they can generate new strands of DNA using a DNA template and primers, and 2) they are heat resistant.

- Primers: short pieces of single-stranded DNA those are complementary to the target sequence. The polymerase begins synthesizing new DNA from the end of the primer.
- Nucleotides (dNTPs or deoxynucleotide triphosphates): single units of the bases A, T, G, and C, which are essentially "building blocks" for new DNA strands.

Typically, PCR consists of a series of 20-40 repeated temperature changes, called cycles, with each cycle commonly consisting of two or three discrete temperature steps (Fig. 15). The cycling is often preceded by a single temperature step at a very high temperature (>90 °C), and followed by one hold at the end for final product extension or brief storage. The temperatures used and the length of time they are applied in each cycle depend on a variety of parameters, including the enzyme used for DNA synthesis, the concentration of bivalent ions and dNTPs in the reaction, and the melting temperature ( $T_m$ ) of the primers (Rychlik W et al., 1990).

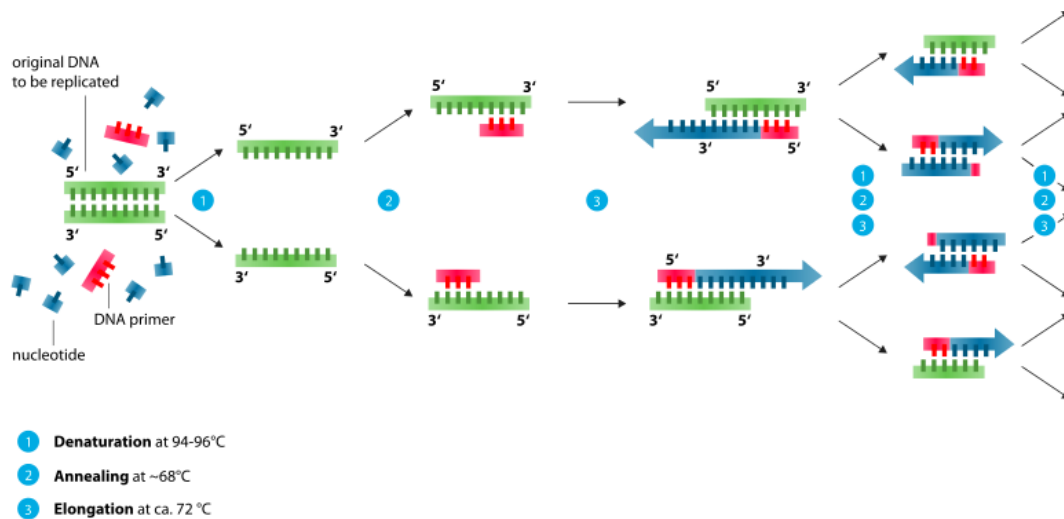


**Fig. 15 PCR steps [22]**

The individual steps common to most PCR methods are as follows:

- Initialization: This step is only required for DNA polymerases that require heat activation by hot-start PCR (Sharkey, 1994). It consists of heating the reaction chamber to a temperature of 94-96°C, or 98°C
- Denaturation: This step is the first regular cycling event and consists of heating the reaction chamber to 94-98°C for 20-30 sec. This causes DNA melting, or denaturation, of the double-stranded DNA template by breaking the hydrogen bonds between complementary bases, yielding two single-stranded DNA molecules.
- Annealing: The reaction temperature is lowered to 50-65°C for 20-40 seconds, allowing annealing of the primers to each of the single-stranded DNA templates. Two different primers are typically included in the reaction mixture: one for each of the two single-stranded complements containing the target region. The primers are single-stranded sequences themselves, but are much shorter than the length of the target region, complementing only very short sequences at the 3' end of each strand.



It is critical to determine a proper temperature for the annealing step because efficiency and specificity are strongly affected by the annealing temperature. This temperature must be low enough to allow for hybridization of the primer to the strand, but high enough for the hybridization to be specific, i.e., the primer should bind *only* to a perfectly complementary part of the strand, and nowhere else. If the temperature is too low, the primer may bind imperfectly. If it is too high, the primer may not bind at all. A typical annealing temperature is about 3-5°C below the  $T_m$  of the primers used. Stable hydrogen bonds between complementary bases are formed only when the primer sequence very closely matches the template sequence. During this step, the polymerase binds to the primer-template hybrid and begins DNA formation.

- Extension/elongation: The temperature at this step depends on the DNA polymerase used; the optimum activity temperature for Taq polymerase is approximately 75-80°C, though a temperature of 72°C is commonly used with this enzyme. In this step, the DNA polymerase synthesizes a new DNA strand complementary to the DNA template strand by adding free dNTPs from the reaction mixture that are complementary to the template in the 5'-to-3' direction, condensing the 5'-phosphate group of the dNTPs with the 3'-hydroxy group at the end of the nascent (elongating) DNA strand. The precise time required for elongation depends both on the DNA polymerase used and on the length of the DNA target region to amplify. As a rule of thumb, at their optimal temperature, most DNA polymerases polymerize a thousand bases per minute. Under optimal conditions (i.e., if there are no limitations due to limiting substrates or reagents), at each extension/elongation step, the number of DNA target sequences is doubled. With each successive cycle, the original template

strands plus all newly generated strands become template strands for the next round of elongation, leading to exponential (geometric) amplification of the specific DNA target region.

The processes of denaturation, annealing and elongation constitute a single cycle. Multiple cycles are required to amplify the DNA target to millions of copies. The formula used to calculate the number of DNA copies formed after a given number of cycles is  $2^n$ , where  $n$  is the number of cycles. Thus, a reaction set for 30 cycles results in  $2^{30}$ , or 1073741824, copies of the original double-stranded DNA target region.

- Final elongation: This single step is optional, but is performed at a temperature of 70-74°C (the temperature range required for optimal activity of most polymerases used in PCR) for 5-15 min after the last PCR cycle to ensure that any remaining single-stranded DNA is fully elongated.
- Final hold: The final step cools the reaction chamber to 4-15°C for an indefinite time, and may be employed for short-term storage of the PCR products.

### **PCR arrays**

RT<sup>2</sup> Profiler™ PCR Arrays are the most reliable and sensitive gene expression profiling real-time PCR technology for analyzing a focused panel of genes involved in a signal transduction, biological process, or disease-related pathway. RT<sup>2</sup> Profiler PCR Arrays have gained popularity in the research of cancer, immunology, stem cells, toxicology, biomarker discovery and validation, and phenotypic analysis of cells and transgenic animals. In my experience, it was used Inflammasome PCR array PAHS-097Z to study down and up regulated genes involved in the inflammasome pathway and it was used a 96-well plate, where in each well lyophilized

primers are present to amplify a specific gene (Fig. 16). Moreover, in some plate, some wells are used to host housekeeping genes, genomic DNA control, Reverse transcription controls and positive PCR controls.

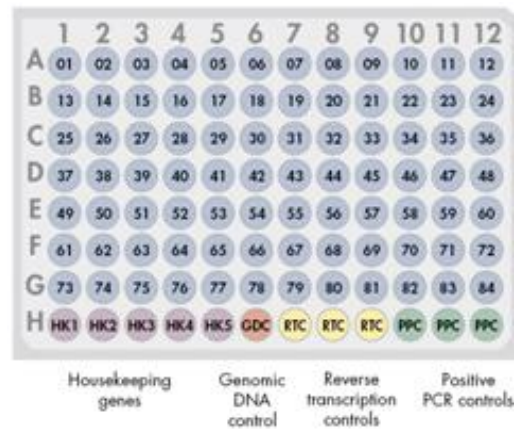


**Fig. 16 Schematic representation of a common 96-well plate RT<sup>2</sup> Profiler PCR array [23]**

The PCR array performs gene expression analysis with real-time PCR sensitivity and the multi-gene profiling capability of a microarray. It was mixed the cDNA template with the appropriate ready-to-use PCR master mix, aliquotated equal volumes to each well and then run the Real-Time PCR program.

### **qPCR or Real-Time PCR**

qPCR or Real-Time PCR method was invented by Heid et al., 1996. The method detects the increasing amount of template while the amplification is still progressing. Real-time qPCR has been used in a growing number of research applications including gene expression quantification. qPCR uses two basic quantification methods which are increasingly used and suitable for different applications: Absolute quantification and relative quantification. Absolute quantification is used to determine the absolute/exact quantity of a genomic DNA or RNA template within an unknown sample by using a standard curve that is prepared from

a dilution series of control template of known concentration. Relative quantification is used to measure the relative concentration of template (or target gene) in unknown samples normalized to a stably expressed reference gene, and compared relatively to a calibrator sample (for example time zero, or untreated sample). Real-time PCR uses several different fluorescence detection technologies (probe) to detect PCR products. One of them is SYBR Green, which is used as a dye for the quantification of double stranded DNA (dsDNA) PCR products. This fluorescent dye must be added in the reaction mixture, which contains template cDNA (or genomic DNA), gene specific primers (forward and reverse), and buffer. After annealing of the primers, a few dye molecules bind to the double stranded DNA, resulting in a significant increase of molecules to emit light upon excitation. With each cycle, more and more dye molecules bind with newly synthesized DNA. If the reaction is monitored continuously, an increase of fluorescence can be viewed by using a computer. Another detection technologies to detect PCR products is Taqman, that is used in my experiment. In Fig. 17 TaqMan hydrolysis principle is showed.

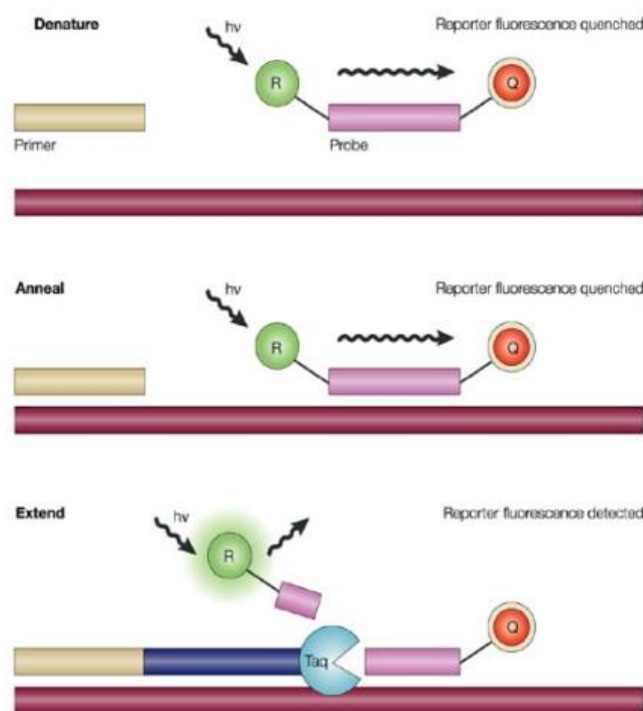


**Fig. 17 TaqMan probe mechanism [24]**

1. At the start of real-time PCR, the temperature is raised to denature the double-stranded cDNA. During this step, the signal from the fluorescent dye on the 5' end of the TaqMan probe is quenched by the nonfluorescent quencher on the 3' end.
2. In the next step, the reaction temperature is lowered to allow the primers and probe to anneal to their specific target sequences.
3. *Taq* DNA polymerase synthesizes new strands using the unlabeled primers and the template. When the polymerase reaches a TaqMan probe, its endogenous 5' nuclease activity cleaves the probe, separating the dye from the quencher. The 5'-nuclease activity of thermostable polymerases used in the polymerase chain reaction (PCR) cleaves hydrolysis probes during the amplicon extension step, which separates the detectable reporter fluorophore (R) from a quencher (Q). Fluorescence emitted when excited by an external light source ( $h\nu$ ) at each PCR cycle is proportional to the amount of product formed.

A PCR has three phases, exponential phase, linear phase and plateau phase as shown in Fig. 18 a, the exponential phase is the earliest segment in the PCR, in which product increases exponentially since the reagents are not limited. The linear phase is characterized by a linear increase in product as PCR reagents become limited. The PCR will eventually reach the plateau phase during later cycles and the amount of product will not change because some reagents become depleted. Real-time PCR exploits the fact that the quantity of PCR products in exponential phase is in proportion to the quantity of initial template under ideal conditions (Heid et al., 1996; Gibson et al., 1996). During the exponential phase PCR product will ideally double during each cycle if efficiency is perfect, i.e. 100%. It is possible to make the PCR amplification efficiency close to 100% in the

exponential phases if the PCR conditions, primer characteristics, template purity, and amplicon lengths are optimal.

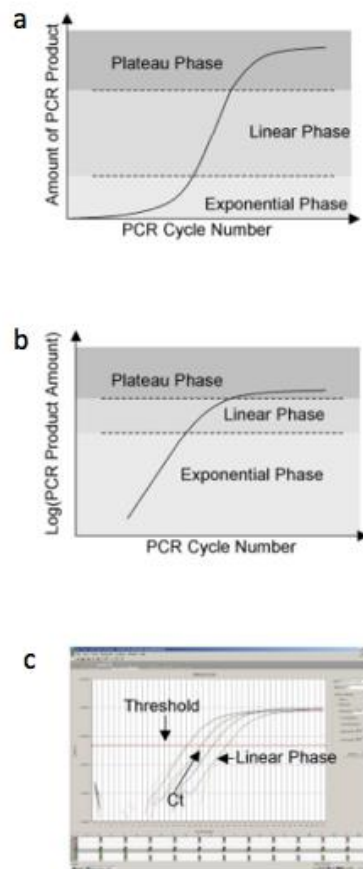


**Fig. 18 Real-Time PCR [25]**

As shown in Fig. 18 b and c, the plot of logarithm 2-based transformed fluorescence signal versus cycle number will yield a linear range at which logarithm of fluorescence signal correlates with the original template amount. A baseline and a threshold can then be set for further analysis. The cycle number at the threshold level of log-based fluorescence is defined as Ct number, which is the observed value in most real-time PCR experiments. Since relative quantification is the goal for most for real-time PCR experiments, several data analysis procedures have been developed. In our experiments we used mathematical model  $\Delta\Delta Ct$  model (Livak et al., 2001). In the following model, the experiment will involve a control sample

and a treatment sample. For each sample, a target gene and a reference gene (18S) for internal control are included for PCR amplification. Typically several replicates (in my experiment, 2) are used for each sample to derive amplification efficiency. The efficiency-calibrated model is a more generalized  $\Delta\Delta Ct$  model. Ct number is first plotted against cDNA input (or logarithm cDNA input), and the slope of the plot is calculated to determine the amplification efficiency (E).  $\Delta Ct$  for each gene (target or reference) is then calculated by subtracting the Ct number of target sample from that of control sample. As shown in Equation 1, the ratio of target gene expression in treatment versus control can be derived from the ratio between target gene efficiency ( $E_{\text{target}}$ ) to the power of target  $\Delta Ct$  ( $\Delta Ct_{\text{target}}$ ) and reference gene efficiency ( $E_{\text{reference}}$ ) to the power of reference  $\Delta Ct$  ( $\Delta Ct_{\text{reference}}$ ). The  $\Delta\Delta Ct$  model can be derived from the efficiency-calibrated model, if both target and reference genes reach their highest PCR amplification efficiency. In this circumstance, both target efficiency ( $E_{\text{target}}$ ) and control efficiency ( $E_{\text{control}}$ ) equals 2, indicating amplicon doubling during each cycle, then there would be the same expression ratio derived from  $2^{-\Delta\Delta Ct}$  (Pfaffl, 2001; Livak et al., 2001).

$$\text{Ratio} = (E_{\text{target}})^{\Delta Ct_{\text{target}}} / (E_{\text{reference}})^{\Delta Ct_{\text{reference}}} \quad \text{Equation 1}$$

$$\text{Whereas } \Delta Ct_{\text{target}} = Ct_{\text{control}} - Ct_{\text{treatment}} \text{ and } \Delta Ct_{\text{reference}} = Ct_{\text{control}} - Ct_{\text{treatment}}$$

$$\text{Ratio} = 2^{-\Delta\Delta Ct} \quad \text{Equation 2}$$

$$\text{Whereas } \Delta\Delta Ct = \Delta Ct_{\text{reference}} - \Delta Ct_{\text{target}}$$

### **Transfection and Silencing**

Transfection is a procedure that introduces foreign nucleic acids into cells to produce genetically modified cells. The transfection methods are broadly classified into three groups;

biological, chemical, and physical. These methods have advanced to make it possible to deliver nucleic acids to specific subcellular regions of cells. Transfection is a powerful analytical tool for study of gene function and regulation and protein function. The introduced genetic materials (DNAs and RNAs) exist in cells either stably or transiently depending on the nature of the genetic materials (Recillas-Targa, 2006). For stable transfection, introduced genetic materials that usually have a marker gene for selection (transgenes) are integrated into the host genome and sustain transgene expression even after host cells replicate (Glover et al., 2005). In contrast with stably transfected genes, transiently transfected genes are only expressed for a limited period of time and are not integrated into the genome (Recillas-Targa, 2006). Transiently transfected genetic materials can be lost by environmental factors and cell division, so the choice of stable or transient transfection depends on the objective of the experiment. The main purpose of transfection is to study the function of genes or gene products, by enhancing or inhibiting specific gene expression in cells, and to produce recombinant proteins in mammalian cells (Wurm, 2004). In my experiments, small interference RNA (siRNA) procedures were used. In the last few years, siRNAs have been used in a number of different experimental settings to silence gene expression. In some, chemically synthesized or *in vitro* transcribed siRNAs have been transfected into cells, injected into mice, or introduced into plants (e.g. by a particle gun). In others, siRNAs have been expressed endogenously from siRNA expression vectors or PCR products in cells or in transgenic animals. RNA interference (RNAi) is a phenomenon in which the introduction of dsRNA into a diverse range of organisms and cell types causes degradation of the complementary mRNA (Fig. 19, step 1). In the cell, long dsRNAs are cleaved into short 21-25 nucleotide small interfering RNAs, or siRNAs, by a ribonuclease known as Dicer (step 2). The siRNAs



subsequently assemble with protein components into an RNA-induced silencing complex (RISC), unwinding in the process (step 3). Activated RISC then binds to complementary transcript by base pairing interactions between the siRNA antisense strand and the mRNA. The bound mRNA is cleaved (step 4) and sequence specific degradation of mRNA (step 5) results in gene silencing (McManus, 2002; Dillin A, 2003; Tuschl, 2002).

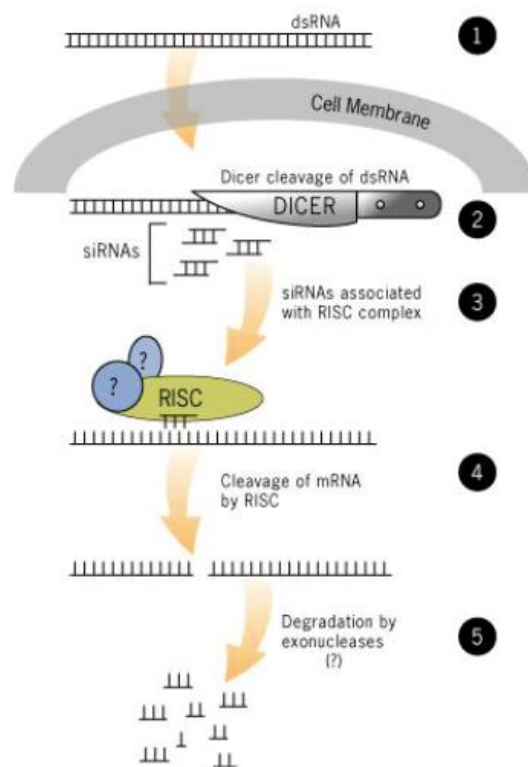


**Fig. 19 RNAi Mechanism [26]**

### Protein quantification

A rapid and accurate method for the estimation of protein concentration is essential for WB analysis. In my experiments it was used an assay described by Bradford (Bradford, 1976): it is a protein determination method that involves the binding of Coomassie Brilliant Blue G-250 dye to proteins (Bradford, 1976). The dye exists in three forms: cationic (red), neutral (green), and anionic (blue). Under acidic conditions, the dye is predominantly in the red cationic form ( $A_{\max}=470 \text{ nm}$ ). However, when the dye binds to protein, it is converted to a stable

unprotonate blue form ( $A_{\max}=595 \text{ nm}$ ) (Reisner et al. 1975, Fazekes de St. Groth et al. 1963, Sedmack and Grossberg 1977). It is this blue protein-dye form that is detected at 595 nm in the assay using a spectrophotometer or microplate reader. In any protein assay, the ideal protein to use as a standard is a purified preparation of the protein being assayed. In the absence of such an absolute reference protein, another protein must be selected as a relative standard. The best relative standard to use is one that gives a color yield similar to that of the protein being assayed. Selecting such a protein standard is generally done empirically. Alternatively, if only relative protein values are desired, any purified protein may be selected as a standard. The two most common protein standards used for protein assays are bovine serum albumin (BSA) and gamma-globulin. In my experiments, to quantify the protein concentration in each sample, a standard curve it was used, considering the lowest point (white) and the highest point of the curve (15 mg/ml of BSA) with other intermediate concentrations: 10, 5, 2, 1 mg/ml.

### **Western Blot (WB)**

WB is an important technique used in cell and molecular biology. WB is often used in research to separate and identify proteins. In this technique a mixture of proteins is separated based on molecular weight through gel electrophoresis. Polyacrylamide gel is generally used for the electrophoretic separation of proteins, and Sodium Dodecyl Sulfate (SDS) is generally used as a buffer (as well as in the gel) in order to give all proteins present a uniform negative charge, since proteins can be positively, negatively, or neutrally charged. This type of electrophoresis is known as SDS-polyacrylamide gel electrophoresis (PAGE). Prior to electrophoresis, protein samples are quantified (as described) and are boiled to denature the proteins present. This

ensures that proteins are separated based on size and prevents proteases (enzymes that break down proteins) from degrading samples. Following electrophoretic separation, the proteins are transferred to a membrane (typically nitrocellulose or PVDF, where they are blocked with milk (or other blocking agents). The membrane is then incubated with labels antibodies specific to the protein of interest. The unbound antibody is washed off leaving only the bound antibody to the protein of interest. As the antibodies only bind to the protein of interest, only one band should be visible. The thickness of the band corresponds to the amount of protein present; thus doing a standard can indicate the amount of protein present (Mahmood et al., 2012).

In my experiments, the proteins were detected by chemiluminescent methods that depend on incubation of the western blot with a substrate that will luminesce when exposed to the reporter on the secondary antibody. The light is then detected by charge-coupled device (CCD) camera, which capture a digital image of the western blot or photographic film. The use of film for western blot detection is slowly disappearing because of non-linearity of the image (non accurate quantification). The image is analyzed by densitometry, which evaluates the relative amount of protein staining and quantifies the results in terms of OD. Newer software allows further data analysis such as molecular weight analysis if appropriate standards are used.

### **Immunoprecipitation (IP) and co-immunoprecipitation (Co-IP)**

Proteins generally act by binding to other molecules, including proteins. When proteins bind to other proteins, it is possible to speak of protein-protein interactions. It has become apparent that protein-protein interactions are critically important to many processes that

take place in the cell, including signal transduction, regulation of gene expression, vesicular transport, nuclear import and export, and cell migration (Pawson and Nash, 2003). This has led to the recognition of protein-protein interactions as targets for drug development and to an increased interest in the identification of novel protein-protein interactions (Fry and Vassilev, 2005; Fry, 2006). Co-IP is a technique that is used to confirm novel protein-protein interactions in the context of a living cell or organism. In addition, Co-IP is also used to study the dynamics of protein-protein interactions in response to intra- or extracellular stimuli. In a Co-IP experiment, a protein of interest is isolated by IP. IP is one of the most widely used methods for antigen detection and purification. The principle of an IP is very straightforward (Fig. 20): an antibody (monoclonal or polyclonal) against a specific target protein forms an immune complex with that target in a sample, such as a cell lysate. The immune complex is then captured, or precipitated, on a beaded support to which an antibody-binding protein is immobilized (such as Protein A or G), and any proteins not precipitated on the beads are washed away. Finally, the antigen (and antibody, if it is not covalently attached to the beads and/or when using denaturing buffers) is eluted from the support and analyzed by SDS-PAGE, often followed by WB detection to verify the identity of the antigen. Co-IP is an extension of IP that is based on the potential of IP reactions to capture and purify the primary target (i.e., the antigen) as well as other macromolecules that are bound to the target by native interactions in the sample solution.

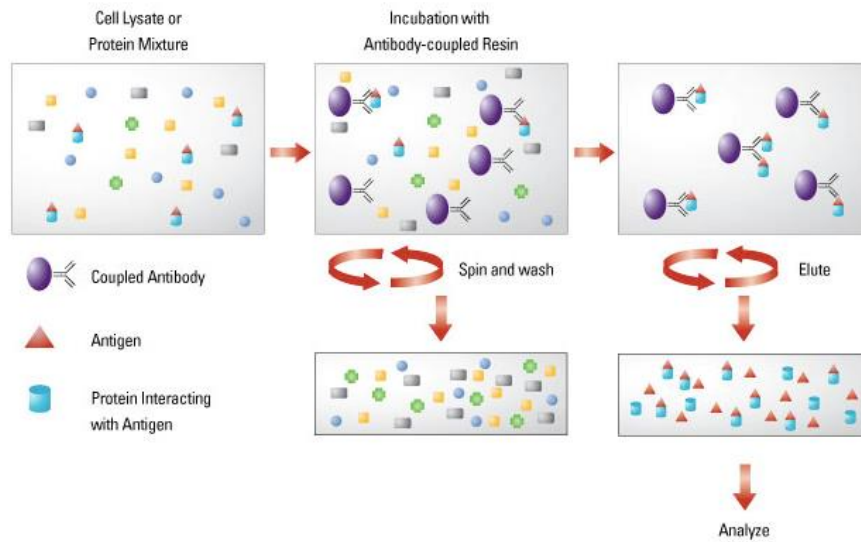


**Fig. 20 Schematic summary of a standard immunoprecipitation assay [27]**

Subsequently, the presence of binding partners can be assessed by immunoblotting. If the proteins are bound, it is possible to visualize on the same membrane them. Anyway, if the proteins are not bound, It is possible to visualize the immunoprecipitated protein.

---

**CHAPTER SIX**  
**RESULTS AND DISCUSSION**

---

**RESULTS of “Understanding chemical allergen potency: role of NLRP12 and Blimp-1 in the induction of IL-18 in human keratinocytes”.**

The first objective of my thesis was to investigate the molecular mechanism underlying contact allergen-induced IL-18 production in human KCs (Papale et al., 2017). To identify genes selectively upregulated by contact allergens and correlated with the activation of the inflammasome a commercially available inflammasome RT<sup>2</sup> Profiler PCR array was used. NCTC 2544 cells were treated for 6 h with PPD (30 µg/ml) or with DMSO as vehicle control. In Table 6, the more activated genes identified in this preliminary screen are reported.

Genes	Fold change $2^{-\Delta(\Delta CT)}$
CARD18	5.31
CCL7	10.57
NLRP12	15.35
NLRX1	23.10
CCL5	30.70

**Table 6. Genes overexpressed by PPD in NCTC 2544 cells following 6 h of treatment [28]**

To confirm these results, cells were treated for 3, 6, 24 h with PPD (30 µg/ml) or DMSO as vehicle control. Even with different kinetics, the expression of CARD18, NLRP12, NLRX1 and CCL5 could be confirmed by real-time PCR (Fig. 21), while the upregulation of CCL7 was not.

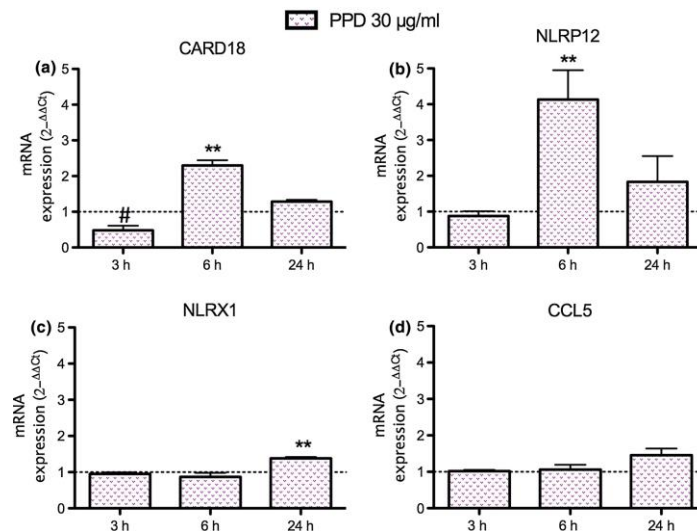


**Fig. 21 Induction of the selected genes by real-time PCR [28].** NCTC 2544 cells were treated for 3, 6, 24 h with PPD 30  $\mu\text{g/ml}$ , or DMSO as vehicle control. To confirm the expression of the identified genes, real-time PCR was used, as described in “Materials and methods” section. Each value represents the mean  $\pm$  SEM of  $n=3$  independent experiments. Statistical analysis was performed with analysis of variance followed by Dunnett’s test, with \*\* $p < 0.01$  and # $p < 0.05$  versus vehicle-treated cells at the different time points.

Among these four genes, NLRP12 was chosen by a bibliographic search on ACD and its role in contact allergen-induced KCs activation was investigated. Its expression and specific role in KCs is currently unknown, which represented an additional challenge. NLRP12/Monarch1 is an intracellular protein consisting of an N-terminal PYD, a central NACHT (NOD domain) and a C-terminal leucine-rich repeat (LRR) region (Tuncer et al., 2014). The full-length human NLRP12 cDNA encodes for 1062-aa protein with an estimated molecular weight of approximately 120 kDa (Ye et al., 2008). Human NLRP12 is expressed predominantly in cells of myeloid lineage, including neutrophils, eosinophils, monocytes, macrophages and immature dendritic cells, and its expression is downregulated in response to pathogens, pathogens products and inflammatory cytokines, indicative of an inhibitory role in innate immune activation (Wu et al., 2013; Shami et al., 2001; Wang et al., 2002; Lich et al., 2007). Moreover, Lord et al. (2009) found that the promoter of NLRP12 contains a Blimp-1/PRDM1 binding site. It has been shown that Blimp-1 reduces NLRP12 activity and expression in myeloid cells during cell differentiation (Martins et al., 2006; Chang et al., 2000).



To investigate the effects of contact allergens on NLRP12 and Blimp-1 expression in KCs, dose-response and time-course experiments were performed. The expression of NLRP12 and Blimp-1 was investigated both at the mRNA and protein level. Cells were treated with the extreme sensitizer DNCB (LLNA EC3= 0.05%) and the strong allergen PPD (LLNA EC3= 0.11%) at concentrations selected from previously published data (Corsini et al., 2009). As NLRP12 and Blimp-1 are reported to be inversely related (Lord et al. 2009), data are presented as ratio Blimp-1/NLRP12. An increased Blimp-1/NLRP12 ratio should be indicative of increased inflammasome activation. As shown in Fig. 22, both allergens modulated NLRP12 and Blimp-1 gene expression with a different kinetic. In the first series of experiments, cells were treated with increasing concentration of DNCB (1-2 µg/ml) and PPD (7.5-30 µg/ml) for 3, 6 and 24 h. No changes were observed with DNCB (Figure 22 a), while PPD showed statistically significant changes in Blimp-1/NLRP12 ratio at 6 h (Fig. 22 b). This prompted us to investigate the effect of DNCB at earlier time points. Cells were, then, treated for 30 min, 1 and 2 h. As shown in the inset of Fig. 22 a, DNCB induced a very early activation of Blimp-1, suggesting that extreme allergens may more rapidly activate the inflammasome.

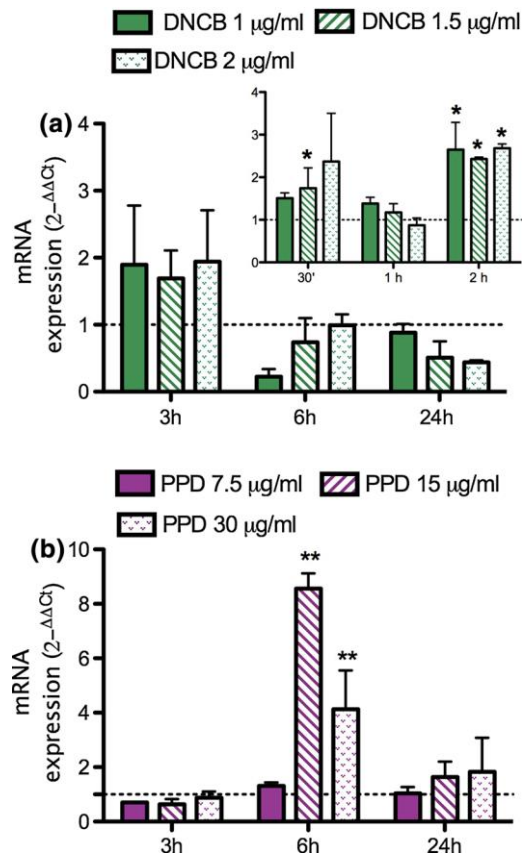


**Fig. 22 Effects of contact allergens on NLRP12 and Blimp-1 gene expression [28].** NCTC 2544 cells were treated for different times with DNCB 1-2  $\mu\text{g/ml}$  (a) and PPD 7.5-30  $\mu\text{g/ml}$  (b) or DMSO as vehicle control. After treatments, NLRP12 and Blimp-1 mRNA expression was evaluated by real-time PCR, as described in “Materials and methods” section. Results are expressed as Blimp-1/NLRP12 ratio. Each value represents the mean  $\pm$  SEM of  $n = 3$  independent experiments. Statistical analysis was performed with analysis of variance followed by Dunnett’s test, with  $*p < 0.05$ ,  $**p < 0.01$  versus vehicle treated cells at the different time points.

In a similar way, as shown in Fig. 23, both allergens modulated NLRP12 and Blimp-1 protein expression. In particular, the extreme allergen DNCB modulated the expression already at 30 min (Fig. 23 a), while the strong allergen PPD modulated protein expression after 24 h of treatment (Fig. 23 b). In both cases, contact allergens induced an increase of Blimp-1 protein expression and a decrease of NLRP12 protein expression, where the extreme allergen more rapidly modulated their expression (Fig. 23 a). As a consequence of an increase of Blimp-1 protein expression and a decrease of NLRP12 protein expression, a different kinetic of IL-18

production was observed, with DNCB inducing a more rapid (3 h) production of IL-18 (Fig. 23 c) compared to PPD (Fig. 23 d).

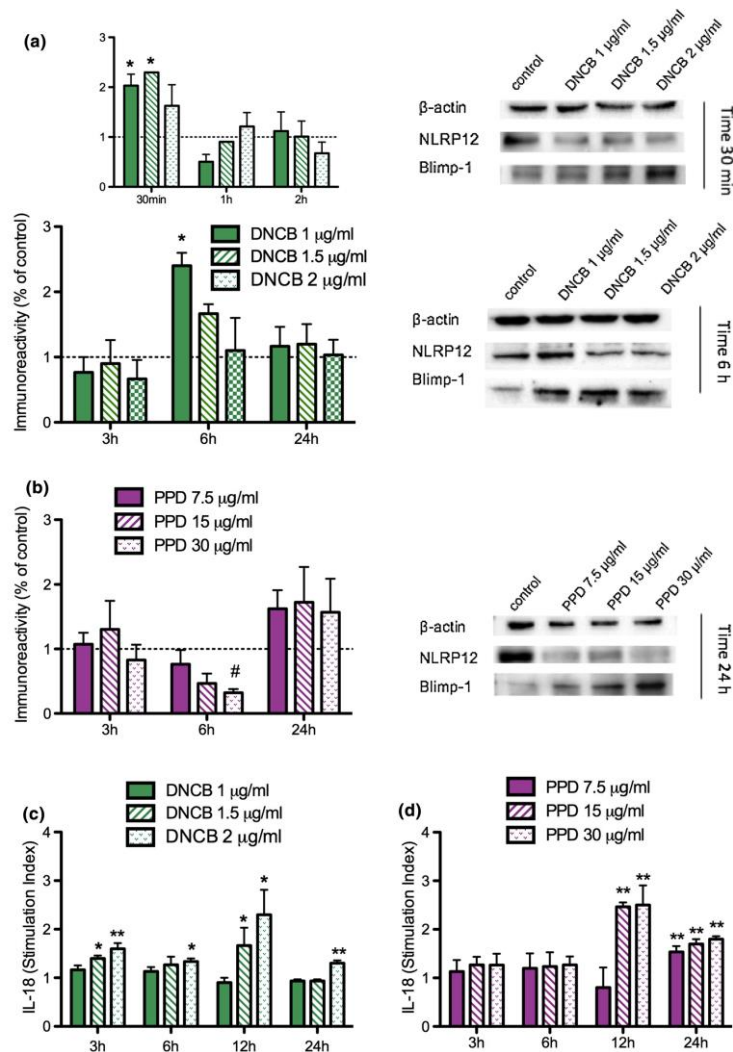


**Fig. 23 Effects of contact allergens on NLRP12 and Blimp-1 protein expression [28].** NCTC 2544 cells were treated for different times with DNCB 1-2 µg/ml (a) and PPD 7.5-30 µg/ml (b) or DMSO as vehicle control. After treatment, NLRP12 and Blimp-1 protein expression was assessed by Western blot analysis. Representative Western blots are reported at 30 min and 6 h for DNCB (a) and 24 h for PPD (b). At 3, 6, 12 and 24 h IL-18 production was assessed by ELISA (c, d). Results are expressed as mean±SEM of n= 3 independent experiments. Statistical analysis was performed with analysis of variance followed by Dunnett's test, with \*p < 0.05, \*\*p < 0.01 and #p < 0.05 versus vehicle-treated cells at the different time points.

NLRP12 is one of the most elusive members of the NLR family. In monocytes/macrophages, its expression is associated with the shutdown of the inflammatory response (Arthur et al., 2010). To investigate its role in IL-18 production, the effects of inducing RNA interference on NLRP12 and Blimp-1 were assessed. NCTC 2544 cells were transfected with NLRP12 and

Blimp-1 siRNA for 48 h. After transfection, cells were treated for 24 h with DNCB 2  $\mu\text{g/ml}$  or PPD 15  $\mu\text{g/ml}$  and intracellular IL-18 production assessed by ELISA. As shown in Fig. 24, NLRP12 silencing, despite its reduced expression both at mRNA and protein level (Fig. 24 a, b), did not result in increased allergen-induced IL-18 production (Fig. 24 e, f), while Blimp-1 silencing was associated with a significant induction of NLRP12 mRNA and protein expression (Fig. 24 c, d), which resulted in a significant reduction in contact allergen-induced IL-18 (Fig. 24 e, f). These data are suggestive of an inhibitory role of NLRP12 in inflammasome activation, consistent with data reported in immune cells (Lord et al., 2009).

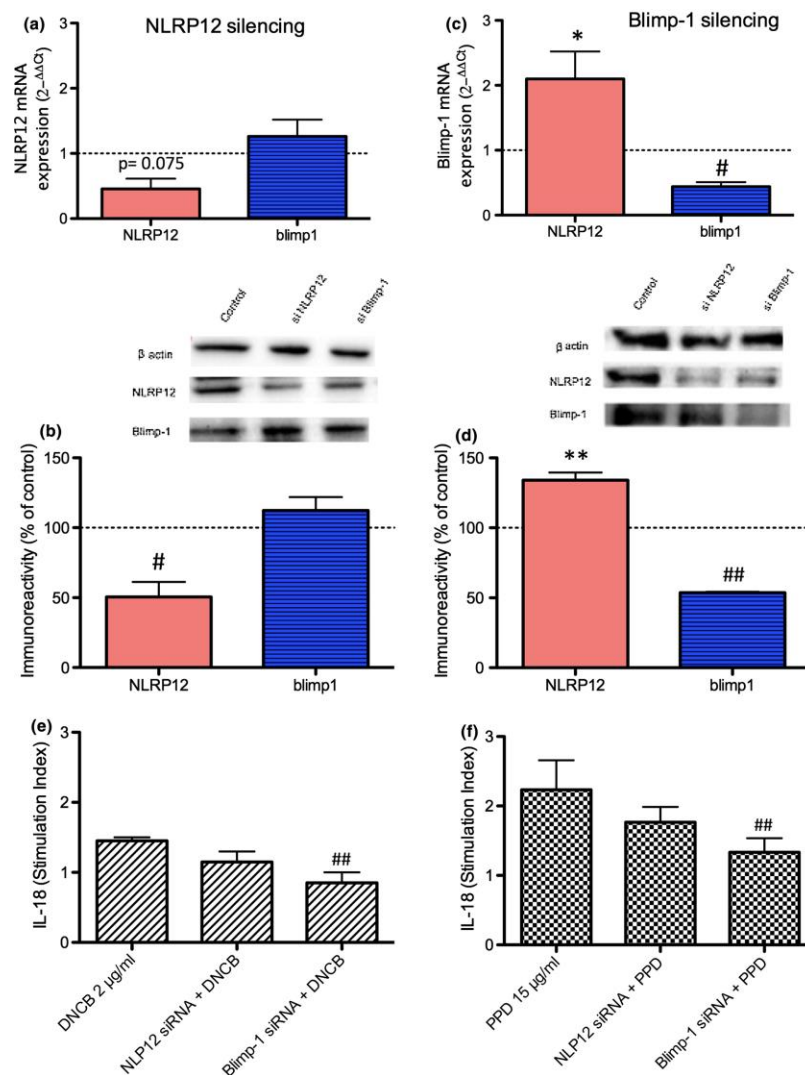


**Fig. 24 Effects of NLRP12 and Blimp-1 silencing on contact allergen induced IL-18 production [28].** NCTC 2544 cells were transfected with NLRP12 and Blimp-1 siRNA for 48 h. After silencing, gene expression was assessed by real-time PCR (a, c), while protein expression was assessed by Western blot analysis (b, d) with representative

Western blots shown. After silencing, cells were treated with DNCB (2 µg/ml) or PPD (15 µg/ml) for 24 h and then IL-18 production was assessed by ELISA (e, f). Results (a, b, c, d) are expressed as mean ± SEM of n= 3 independent experiments. Statistical analysis was performed with analysis of variance followed by Dunnett's test, with \*p < 0.05, \*\*p < 0.01, #p < 0.05 and ##p < 0.01 versus vehicle (transfection reagent)-treated cells. Results (e, f) are expressed as mean ± SEM of n= 3 independent experiments. Statistical analysis was performed with analysis of variance followed by Dunnett's test, with ###p < 0.01 versus DNCB or PPD alone.

To strengthen these results, an experiment was set up upregulating Blimp-1 expression by treating cells with DNCB 1 µg/ml for 6 h (Fig. 25). Cells were then extensively washed with culture media to remove DNCB and then exposed to PPD 30 µg/ml or DMSO as vehicle control for 18 h.

As shown in Fig. 25, a statistically significant increase was observed in cells pulse DNCB compared to cells exposed to DMSO 6 h + PPD 18 h, further supporting our hypothesis.

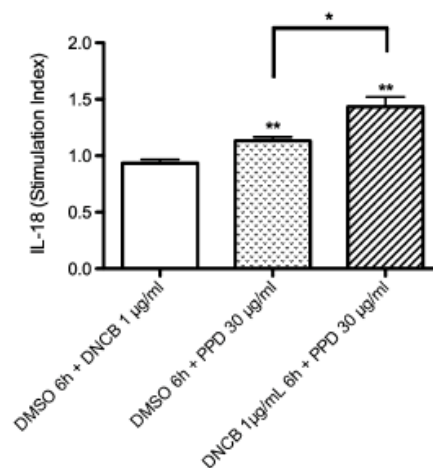


**Fig. 25 Effects of Blimp-1 induction on allergen-induced IL-18 production [28].** NCTC 2544 cells were treated with DNCB 1 µg/ml or DMSO as vehicle control for 6 h and then with DNCB 1 µg/ml or PPD 30 µg/ml for 18 h, and IL-18 production was assessed by ELISA. Results are expressed as mean ± SEM of n= 3 independent experiments. Statistical analysis was performed with analysis of variance followed by Dunnett's test, with \*\*p < 0.01 versus vehicle-treated cells and \*p < 0.05 versus vehicle + PPD 30 µg/ml-treated cells.

Similarly, to confirm the results obtained in the NCTC 2544 cell line, a more realistic model was used. Commercially available RhE was used. RhE was transfected with NLRP12 and Blimp-1 siRNA for 48 h. After transfection, RhE was treated for 24 h with DNCB 1.5 mg/ml or with AOO as vehicle control. The amount of IL-18 present in culture supernatants was quantified

by ELISA. As shown in Fig. 26, Blimp-1 silencing was associated with the induction of NLRP12 (Fig. 26 b), as observed in the NCTC 2544 cells. Under this experimental condition, a statistically significant reduction in DNCB-induced IL-18 release was observed in RHE in which Blimp-1 was silenced (Fig. 26 c), confirming results obtained in the KCs cell line. Also in this case, NLRP12 silencing failed to upregulate DNCB-induced IL-18 production, suggesting that the remaining NLRP12 was sufficient to balance allergen-induced inflammasome activation and IL-18 production. On the contrary its upregulation resulted in a reduction of contact allergen-induced IL-18 production.

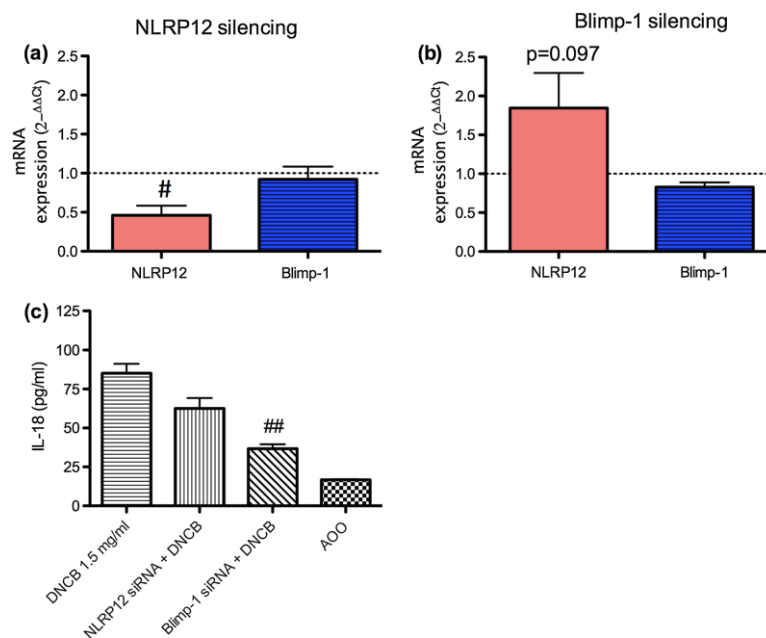


**Fig. 26 Effect of NLRP12 and Blimp-1 silencing in reconstructed human epidermis [28].** RHE was transfected with NLRP12 and Blimp-1 siRNA for 48 h. After silencing, gene expression was assessed by real-time PCR (a, b). After silencing, RHE was exposed to DNCB (1.5 mg/ml) or AOO as vehicle control for 24 h, and IL-18 release was assessed by ELISA (c). Results are expressed as mean  $\pm$  SEM of n= 3 independent experiments. Statistical analysis was performed with analysis of variance followed by Dunnett's test, with # p<0.05 versus vehicle (transfection reagent)-treated cells (a, b). Results are expressed as mean  $\pm$  SEM of n= 3 independent experiments. Statistical analysis was performed with analysis of variance followed by Dunnett's test, with ##p<0.01 versus DNCB alone (c).

**DISCUSSION of “Understanding chemical allergen potency: role of NLRP12 and Blimp-1 in the induction of IL-18 in human keratinocytes”.**

The first objective of my thesis was to better understand the molecular mechanism involved in contact allergen-induced inflammasome activation and IL-18 production. Using the inflammasome RT<sup>2</sup> Profiler PCR array, among the genes selectively upregulated by PPD, NLRP12 was identified. We could then demonstrate that DNCB and PPD differently affected Blimp-1/NLRP12 expression. Interestingly, the extreme allergen DNCB more rapidly downregulated NLRP12 expression and more rapidly induced IL-18 production. As demonstrated in monocytes/macrophages (Williams et al., 2005) also in KCs, NLRP12 and Blimp-1 expression is inversely correlated. IL-18 is a cytokine that plays a key proximal role in the induction of allergic contact sensitization and favors Th-1-type immune response by enhancing the secretion of proinflammatory mediators such TNF- $\alpha$  and interferon- $\gamma$  (Okamura et al., 1995; Cumberbatch et al., 2001; Antonopoulus et al., 2008). Human KCs constitutively express IL-18 mRNA and protein, and it has been shown its induction following exposure to contact sensitizers (Corsini et al., 2009; Galbiati and Corsini, 2012; Naik et al., 1999).

NLRP12, in contrast to other NLR proteins that promote inflammation, acts as an attenuator of inflammatory responses (Ye et al., 2008), and it has been characterized in monocytes/macrophages as a negative regulator of both canonical and non-canonical NF- $\kappa$ B signaling (Lich et al., 2007). NLRP12 was also found to attenuate the development of contact hypersensitivity (Arthur et al., 2010). More recently, mutations that result in a truncated form of NLRP12 were linked to hereditary periodic fevers that manifest with recurrent fevers, joint pain and skin urticaria (Jéru et al., 2008).

Lord et al. (2009) found that reducing NLRP12 expression with small interference RNA in myeloid/monocyte cells, an increase in NF- $\kappa$ B activation and cytokine expression in response to TLR2/TLR4 agonists (TNF- $\alpha$  was observed, suggesting that NLRP12 is a negative regulator of inflammation). The NLRP12 promoter contains a Blimp-1/PRDM1 binding site. It has been shown that Blimp-1 reduces NLRP12 activity and expression (Williams et al., 2005). The expression of NLRP12 and Blimp-1 appears to be inversely correlated. It has been proposed that the transcriptional silencing of NLRP12 is essential for the development of a proper immune response (Struwe and Warren, 2010). NLRP12 gene silencing is mediated by Blimp-1 during both innate immune activation and cellular differentiation (Lord et al., 2009). We speculate that the ability of different allergens to induce IL-18 may be linked to their ability to modulate NLRP12 and Blimp-1 gene and protein expression differently, depending on their potency. Indeed different kinetics were observed, with the extreme allergen DNCB modulating Blimp-1/NLRP12 gene and protein expression more rapidly, compared to the strong allergen PPD.

SiRNA is widely used to silence the expression of specific genes to assess the individual contribution of these genes to an assortment of cellular phenotypes. In order to understand the role of NLRP12 and Blimp-1 in allergen induced IL-18 production, silencing experiments were performed. Silencing Blimp-1, the gene and protein of NLRP12 was significantly increased, supporting the role of Blimp-1 as repressor of NLRP12 expression (Williams et al., 2005). The following scenario can be imagined (Fig. 27): in non - activated situation NLRP12 acts as a negative regulator of inflammation, preventing the inflammasome activation and consequently IL-18 production (Fig. 27 a), on the contrary following exposure to contact allergens, Blimp-1 expression significantly increase to downregulate NLRP12 expression, which in turn facilitates the activation of the inflammasome and IL-18 maturation (Fig. 27 b).



The inhibitory role of NLRP12 in IL-18 production was evident after Blimp-1 silencing, which resulted in NLRP12 overexpression and in an almost complete abrogation of contact allergen-induced IL-18 production. Equally, inducing Blimp-1 by DNCB, a statistical increase in PPD-induced IL-18 was observed, supporting the role of NLRP12 as negative regulator of inflammation. Surprisingly, NLRP12 downregulating did not result in increased contact allergen induced IL-18 production, suggesting that in our experimental conditions, the degree of reduction was not sufficient to significantly affect inflammasome activation and IL-18 production induced the strong allergens used.

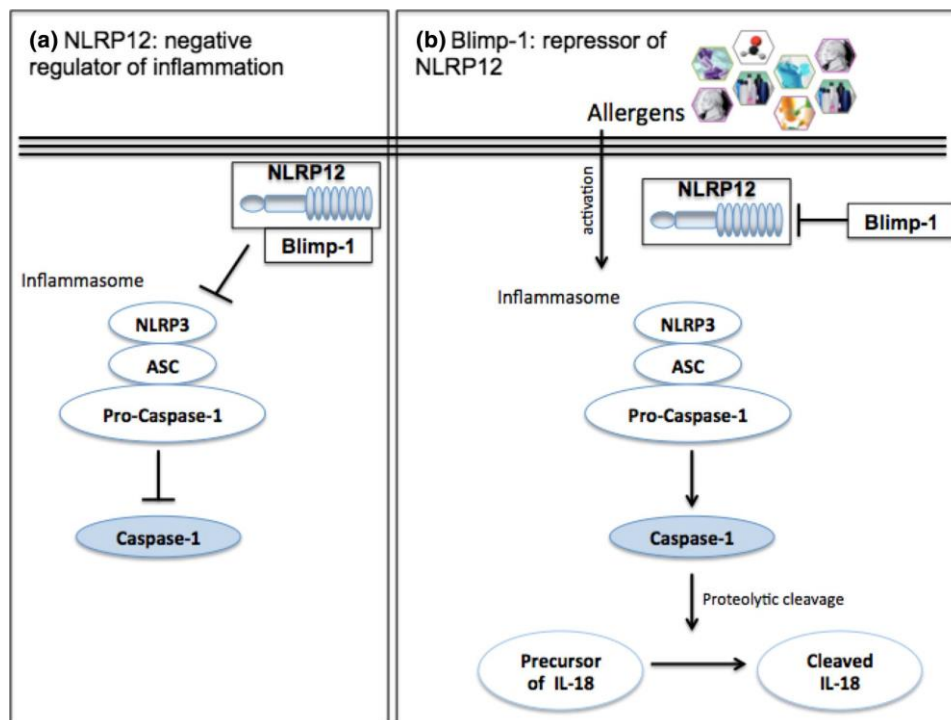


**Fig. 27 NLRP12 and Blimp-1 role in inflammasome activation [28].** NLRP12 is supposed to act as a negative regulator of inflammation before immune stimulation (a), but during infection its expression is reduced to allow for a full inflammatory response. In this context, Blimp-1 plays a pivotal role (b): It is a repressor of NLRP12. NLRP12 inhibition leads to inflammasome activation and the activated caspase-1 drives the proteolytic cleavage of pro-IL-18 in IL-18.

In conclusion, we demonstrated the role of NLRP12 and Blimp-1 in contact allergen-induced IL-18 production in human KCs.

**RESULTS of “NLRP12 protein and the NLRP3 inflammasome complex in the induction of IL-18 in human keratinocytes: further developments”**

I next investigated contact allergen-induced caspase-1 activation and by immunoprecipitation the link of NLRP12 with the inflammasome NLRP3 (manuscript in preparation).

NLRP3 inflammasome consists of three different protein: NLRP3, ASC and Caspase-1, I wanted to investigate if contact allergens could modulate these three proteins and where NLRP12 protein could bind within the inflammasome by immunoprecipitation experiments.

To investigate the effects of contact allergens on NLRP3 protein expression, dose-response and time-course experiments were performed. NCTC 2544 cells were treated for different times with increasing concentration of PPD and DNCB.

As shown in Fig. 28, both allergens upregulated NLRP3 with a similar kinetic but with DNCB inducing an higher up-regulation at 3 h compared to PPD. In the first series of experiments, cells were treated with increasing concentration of PPD (7.5-30 µg/ml) and DNCB (1-2 µg/ml) for 3, 6 and 24 h. PPD showed statistically significant increase at all time investigated, with higher induction observed at 24 h (Fig. 28 a), while a more rapid NLRP3 protein production was observed with DNCB (Fig. 28 c), suggesting that extreme allergen may more rapidly activate the inflammasome. In Fig. 28 b, the results of co-immunoprecipitation experiment with PPD 30 µg/ml at 24h of treatment were shown. NLRP12 was immunoprecipitated and as expected a reduction in NLRP12 in PPD treated cells was observed. Nevertheless, NLRP3 co-precipitated with NLRP12 in both control and treated cells.

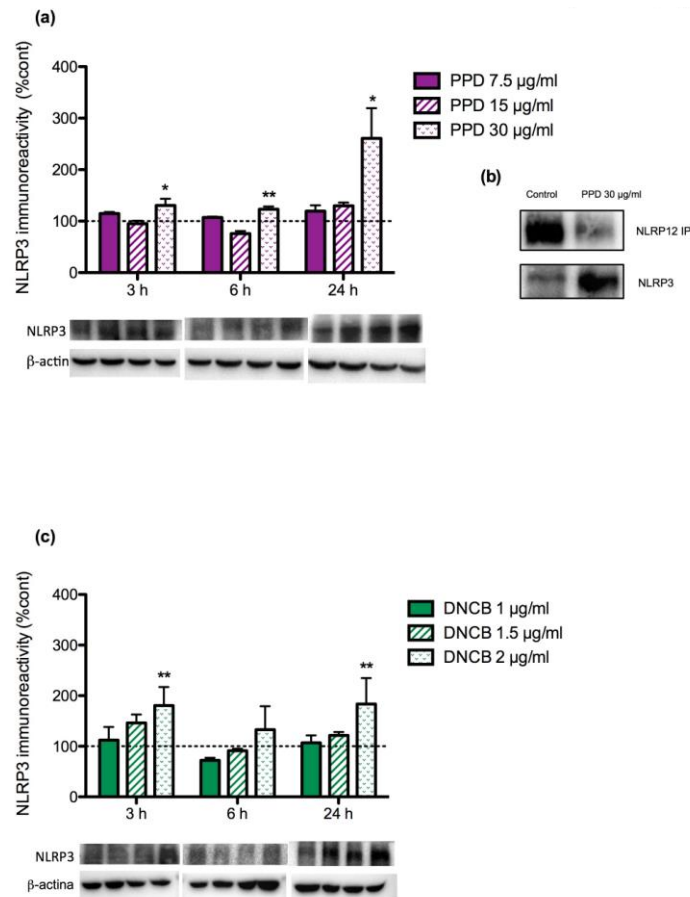


**Fig. 28 Effects of contact allergens on NLRP3 protein expression and analysis of interaction between NLRP12 and NLRP3 by Co-IP experiments [29].**

NCTC 2544 cells were treated for different times with PPD 7.5, 15 and 30 µg/ml (a) and DNCB 1, 1.5 and 2 µg/ml (c) or DMSO as vehicle control. After treatment, NLRP3 expression was assessed by WB analysis. Representative blots are reported at the bottom of each graph. Results are expressed as mean ± SEM of n= 3 independent experiments. Statistical analysis was performed by Dunnett's test, with \*\*p<0,01 and \*p<0,05 versus vehicle-treated cells at different point.

NCTC 2544 cells were treated for 24 h with 30 µg/ml or DMSO as vehicle control and immunoprecipitated by anti-NLRP12 specific antibody, NLRP3 protein was then visualized by WB in NLRP12 immunoprecipitated samples (b).

In a similar way, the effect of contact allergens on ASC protein expression was investigated in dose-response and time-course experiments. NCTC 2544 cells were treated for different times with increasing concentrations of the strong allergen PPD and the extreme sensitizer DNCB. As shown in Fig. 29, both allergens also induced ASC protein with a different kinetic. In the first series of experiments, cells were treated with increasing concentration of PPD (7.5-30 µg/ml) and DNCB (1-2 µg/ml) for 3, 6 and 24 h. PPD showed an up-regulation that reached

statistically significance at 6 and 24h, while a more rapid ASC protein production already at 3 h ( $p < 0.05$ ) were observed with DNCB, (Fig. 29 c), suggesting that extreme allergen may more rapidly activate the inflammasome, confirming previous results (Papale et al., 2017). In Fig. 29 b, the results of co-immunoprecipitation experiment with PPD 30  $\mu\text{g/ml}$  at 24 h of treatment are shown. NLRP12 was immunoprecipitated and as already shown in Fig. 28 c in the control group there is more NLRP12, however, while NLRP12 clearly co-immunoprecipitated in allergen-treated cells, ASC seems to associate to NLRP12 only in control cells. This suggest that following allergen exposure NLRP12 is displaced from ASC, leaving it free to interact with pro-caspase-1 facilitating its activation.

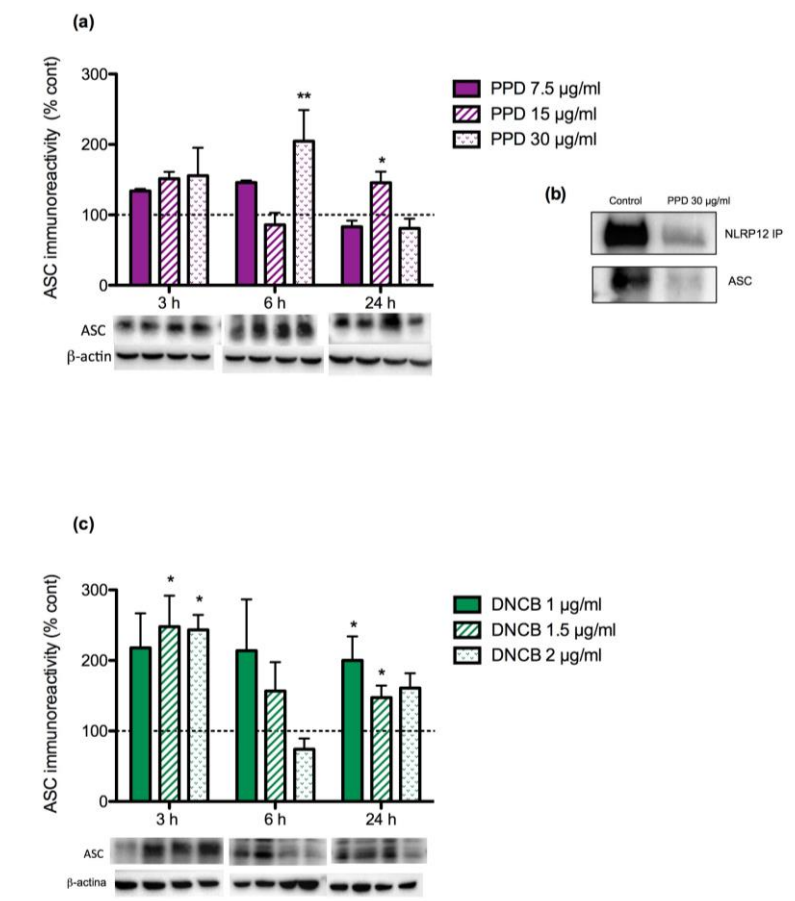


**Fig. 29 Effects of contact allergens on ASC protein expression and analysis of interaction between NLRP12 and ASC by coimmunoprecipitation [29].**

NCTC 2544 cells were treated for different times with PPD 7.5, 15 and 30  $\mu\text{g/ml}$  (a) and DNCB 1, 1.5 and 2  $\mu\text{g/ml}$  (c) or DMSO as vehicle control. After treatment, ASC expression was assessed by WB analysis. Representative blots are reported at the bottom of each graph. Results are expressed as mean  $\pm$  SEM of  $n = 3$  independent

experiments. Statistical analysis was performed by Dunnett's test, with  $**p<0,01$  and  $*p<0,05$  versus vehicle-treated cells at different point.

NCTC 2544 cells were treated for 24 h with 30  $\mu\text{g}/\text{ml}$  or DMSO as vehicle control and immunoprecipitated by anti-NLRP12 specific antibody, ASC protein was then visualized by WB in NLRP12 immunoprecipitated samples (b).

Finally the effect of contact allergens on caspase-1 activation was investigated in dose-response and time-course experiments. NCTC 2544 cells were treated for different times with the strong allergen PPD and the extreme sensitizer DNCB.

As shown in Fig. 30, both allergens induced Caspase-1 activation with a different kinetic, consistent with the previously published IL-18 production (Papale et al., 2017). In the first series of experiments, cells were treated with increasing concentration of PPD (7.5-30  $\mu\text{g}/\text{ml}$ ) and DNCB (1-2  $\mu\text{g}/\text{ml}$ ) for 3, 6 and 24 h. The results are expressed as ratio between caspase-1/pro-caspase-1, to appreciate the activation of caspase-1. PPD showed statistically significant activation at 24 h (Fig. 30 a), while a more rapid caspase-1 activation already at 3 h ( $p< 0,01$ ) was observed with DNCB, (Fig. 30 c), further supporting the idea that extreme allergens more rapidly activate the inflammasome and IL-18 maturation. In Fig. 30 b, the results of co-immunoprecipitation experiment with PPD 30  $\mu\text{g}/\text{ml}$  at 24 h of treatment were shown.

I then wanted to investigate if caspase-1 associated with NLRP12. NLRP12 was immunoprecipitated and clearly caspase-1 protein was bound to NLRP12 protein in both control and allergen treated cells.

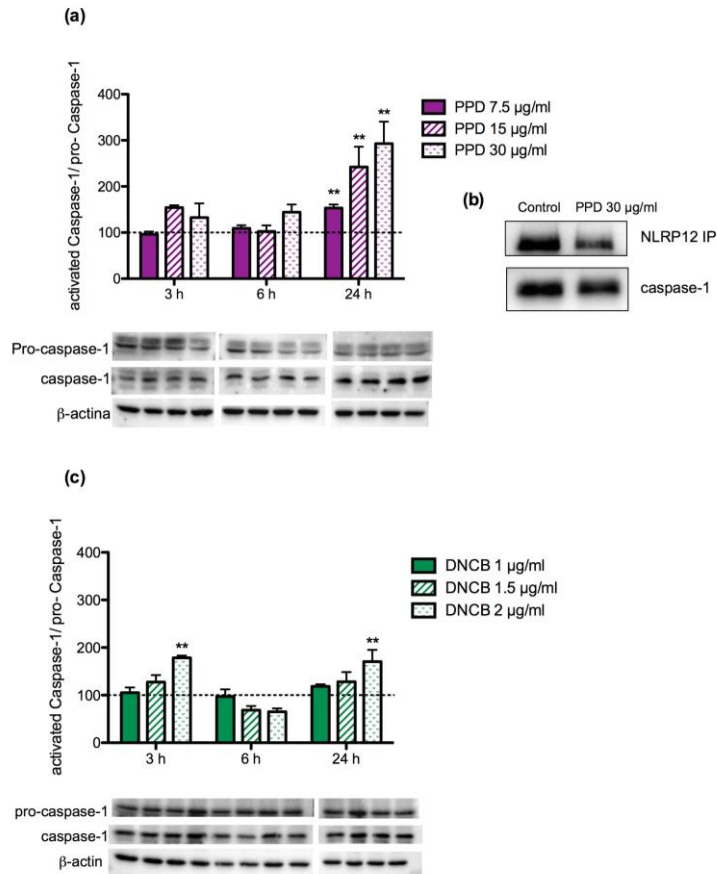


**Fig. 30 Effects of contact allergens on caspase-1 activation and analysis of interaction between NLRP12 and caspase-1 by co-immunoprecipitation [29].**

NCTC 2544 cells were treated for different times with PPD 7.5, 15 and 30 µg/ml (a) and DNCB 1, 1.5 and 2 µg/ml (c) or DMSO as vehicle control. After treatment, caspase-1 activation was assessed by WB analysis. Representative blots are reported at the bottom of each graph. The results are expressed as a ratio between activated caspase-1/pro-caspase-1 and as mean ± SEM of n=3 independent experiments. Statistical analysis was performed by Dunnett's test, with \*\*p<0,01 versus vehicle-treated cells at different point.

NCTC 2544 cells were treated for 24 h with 30 µg/ml or DMSO as vehicle control and immunoprecipitated by anti-NLRP12 specific antibody, caspase-1 protein was then visualized by WB in NLRP12 immunoprecipitated samples (b).

**DISCUSSION of “NLRP12 protein and the NLRP3 inflammasome complex in the induction of IL-18 in human keratinocytes: further developments”.**

The second part of my thesis aimed to understand the modulation of NLRP3 inflammasome by contact allergen of different potency in human KCs. NCTC 2544 were treated with the strong allergen PPD and the extreme allergen DNCB. In addition, the localization of NLRP12 was clarified in NLRP3 inflammasome complex by co-immunoprecipitation experiments. NLRP3 is a multiproteic complex composed by three proteins: a cytosolic receptor, NLRP3, an adopter protein, ASC and the effector protein, caspase-1 (Schroder and Tschopp, 2010). The working hypothesis was that allergens of different potency may differently activate the NLRP3 inflammasome depending on their potency. Indeed different kinetics were observed, with the extreme allergen DNCB induces more rapid activation of all of them, compared to the strong allergen PPD.

I then wanted to link NLR12 with NLRP3 inflammasome by investigating its localization by immunoprecipitation. Co-immunoprecipitation is a technique that is used to confirm protein-protein interactions. In order to understand the link of NLRP12 and the NLRP3 inflammasome proteins, co-immunoprecipitation experiments were performed by immunoprecipitating NLRP12 and assessing the co-precipitation of NLRP3, ASC and pro-caspase-1 by Western blot analysis. While in control cells, NLRP3, ASC and pro-caspase-1 co-immunoprecipitated with NLRP12, in allergen treated cells a decrease in ASC associated NLRP12 was observed, which could shift ASC to a better bond with NLRP3 and pro-caspase-1 so as to favor its activation and release.

Similar experiments will be conducted with DNCB.

**RESULTS of “Development of an *in vitro* method to estimate the sensitization induction level of contact allergens”.**

The other objective of my thesis was to optimize an *in vitro* system for the estimation of the No Estimation Sensitization Induction Level (NESIL) necessary for risk assessment and full replacement of experimental animals for the characterization of skin sensitizers. The RhE IL-18 assay previously developed in our laboratory in collaboration with S.Gibbs at the VU Medical Centre in Amsterdam was used as experimental model.

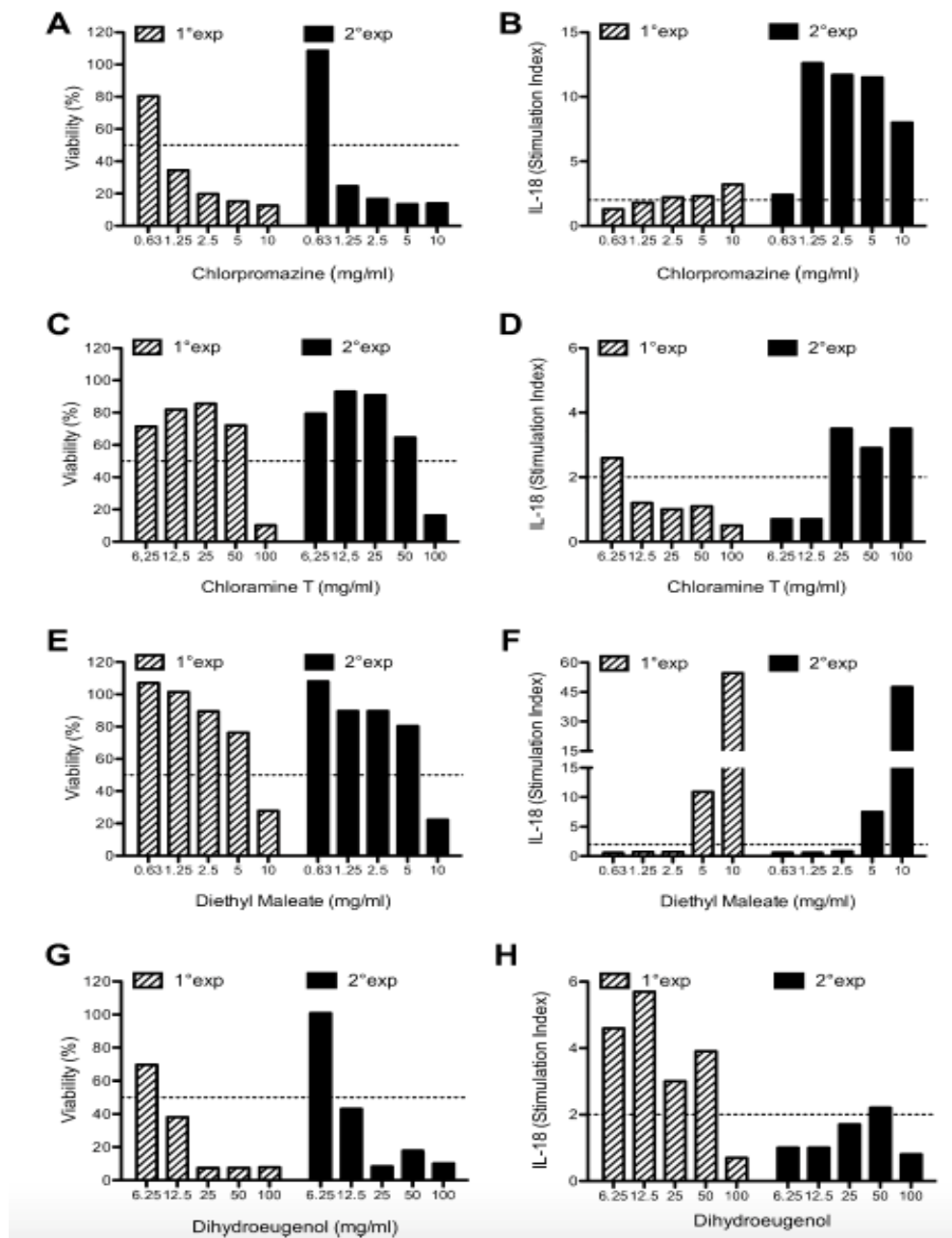
Additional 14 chemicals using commercially available EpiDerm™ model (Galbiati et al., 2017). Chemicals were selected from the ICCVAM database. Allergens of different potency (1 extreme, 2 strong, 3 moderate and 4 weak) were investigated together with chemicals misclassified at the LLNA, namely benzyl salicylate and benzyl cinnamate for which no sensitization was observed in human predictive studies, and benzyl alcohol for which positive responses were reported in humans. In Table 7, the LLNA EC3 and the human NOEL or LOEL values are reported.

Chemical name	CAS #	LLNA EC3 (%) <sup>a</sup>	LLNA potency category	Human NOEL (µg/cm <sup>2</sup> )
Benzoquinone	106-51-4	0.01	Extreme	N.A.
Chlorpromazine	69-09-0	0.14	Strong	1150 <sup>†</sup>
Chloramine T	127-65-1	0.4	Strong	N.A.
Benzyl salicylate <sup>b</sup>	118-58-1	2.9	Moderate	17,717 <sup>**</sup>
Diethyl maleate	141-05-9	2.1	Moderate	1600 <sup>†</sup>
Dihydroeugenol	2785-87-7	6.8	Moderate	N.A.
Benzyl cinnamate <sup>b</sup>	103-41-3	18.4	Weak	4720 <sup>**</sup>
2,4-Dichloronitrobenzene	611-06-3	20	Weak	N.A.
Imidazolidinyl urea	39236-46-9	24	Weak	5000
Limonene	5989-27-5	69	Weak	5517
Benzyl alcohol <sup>c</sup>	100-51-6		N.C.	5900
Isopropanol	67-63-0		N.C.	N.A.
Dimethyl isophthalate <sup>e</sup>	1459-93-4		N.C.	N.A.
4-Aminobenzoic acid	150-13-0		N.C.	N.A.

**Table 7. Chemical tested and *in vivo* LLNA potency classification [30]**



Experiments were run accordingly with the SOP developed for the EE IL-18 assay (Gibbs et al., 2013; Teunis et al., 2013, 2014), which foresees two independent runs for each chemical to be tested. RhE was exposed to the selected chemicals for 24 h as described in materials and methods section. Cell viability was assessed by the MTT assay and IL-18 release by ELISA. Of the selected chemicals, only benzoquinone had to be excluded due to its interference with both MTT assay and the ELISA. The results obtained in two independent experiments are shown in Fig. 31 for each compound five increasing concentrations were tested. Graphics on the left show cell viability, while IL-18 release is shown on the right (stimulation index). Dotted lines were set at 50% viability and IL-18 SI-2, cut off for positivity.



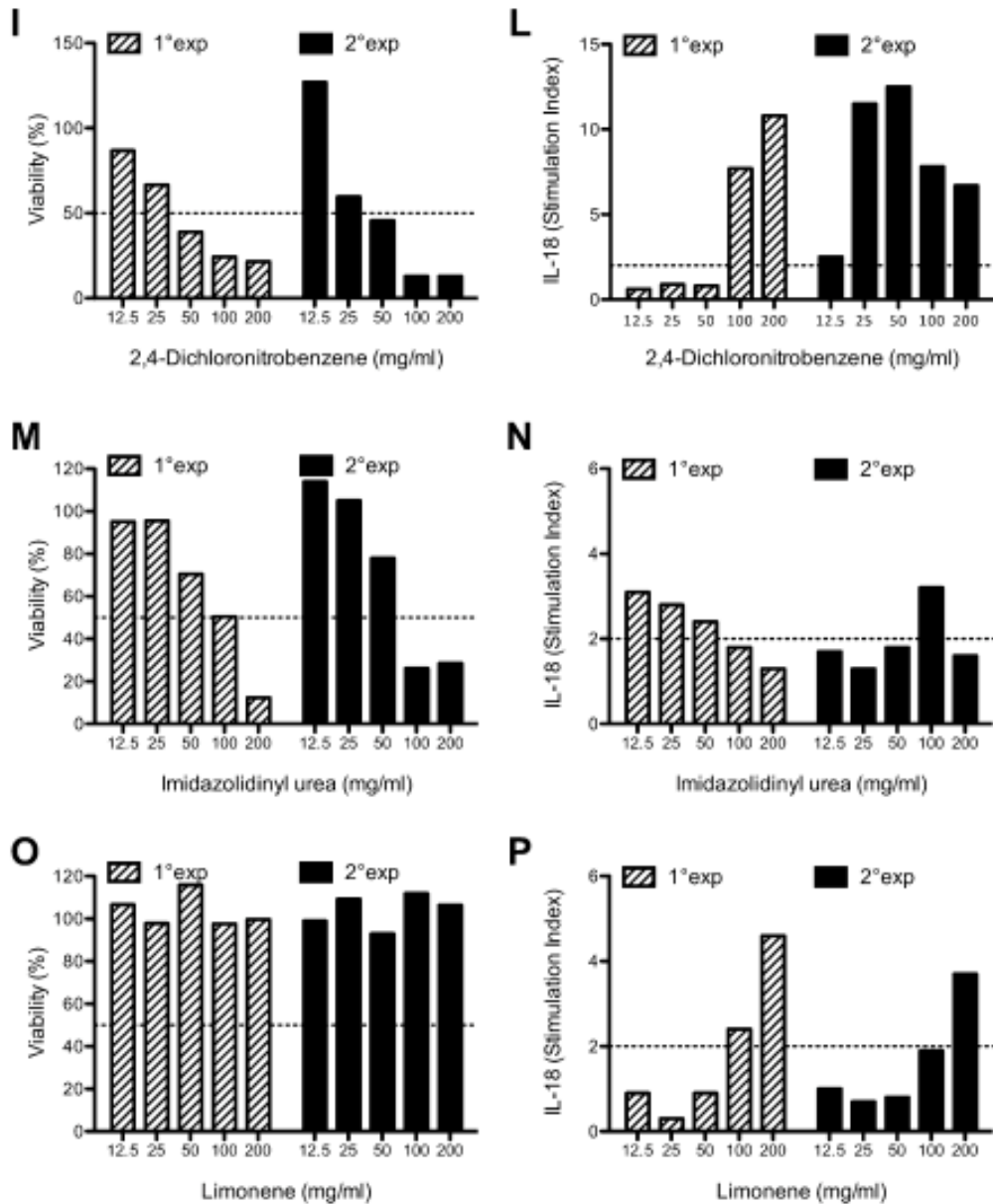


**Fig. 31 Dose-response effects of the selected compounds on cell viability and IL-18 release [30].** Data obtained from two independent experiments are represented (1° and 2° exp). RhE was exposed to increasing concentrations of the selected chemicals for 24 h. Viability was assessed by MTT while IL-18 by ELISA. Viability (A, C, E, G, I, M, O) is expressed as % vs vehicle treated RhE (100%), and IL-18 as stimulation index (SI) compared to vehicle treated RhE (B, D, F, H, L, N, P). The dotted lines are set at 50% viability and IL-18 SI=2.

The contact allergens chlorpromazine, chloramine T, diethyl maleate, dihydroeugenol, 2,4-dichloronitrobenzene, imidazolidinyl urea and limonene were able to a different extent to induce a IL-18 SI  $\geq$  2.0, while the non-sensitizers isopropanol and 4-aminobenzoic acid (Fig. 32) failed to induce IL-18 release.

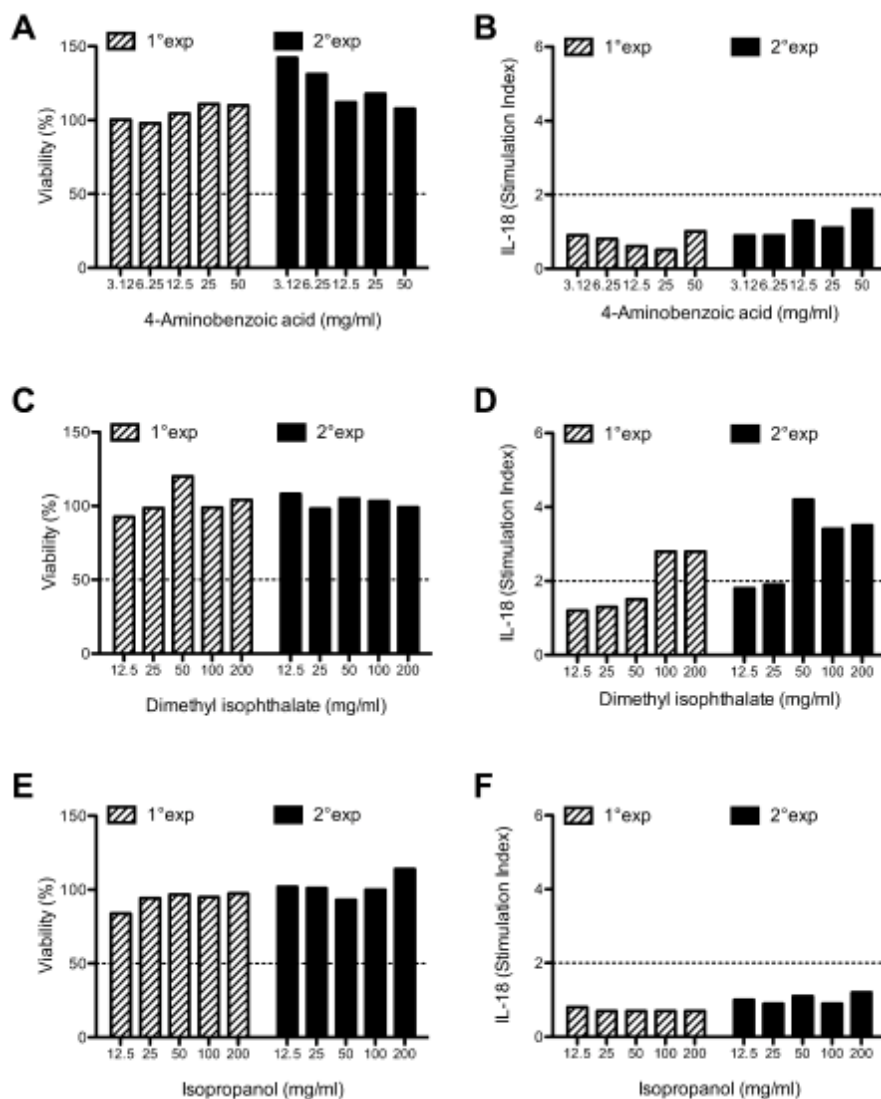


**Fig. 32 Dose-response effects of the selected non-sensitizers on cell viability and IL-18 release [30].** Data obtained from two independent experiments are represented (1° and 2° exp). RhE was exposed to increasing concentrations of the selected chemicals for 24 h. Viability was assessed by MTT while IL-18 by ELISA. Viability (A, C, E) is expressed as % vs vehicle treated RhE (100%), and IL-18 as stimulation index (SI) compared to vehicle treated RhE (B, D, F). The dotted lines are set at 50% viability and IL-18 SI=2.

Comparing the two experiments, cytotoxicity data are less variable compared to the release of IL-18, which may reflect a different degree of KCs activation between different RhE batches. This greater variability is also seen in the data obtained with the positive control DNCB 2 mg/ml: IL18 SI  $15.4 \pm 4.9$  (min 8.0, max 24.4), viability  $11.6 \pm 3.6\%$  (min 6.9, max 16.2), data is mean SD, n= 11 independent experiments. Despite this, the positive/negative classification is not affected as for the prediction model the fold increase in intracellular IL-18 is  $\geq 2.0$  in at

least one of the concentrations tested in two independent experiments the chemical is classified chemical as contact sensitizer. The correlation between cytotoxicity and the strength of IL-18 release is not always straightforward. For some allergens, the decrease in cell viability is associated with the increase in IL-18 release. In other cases, increased IL-18 release can be observed at not cytotoxic concentrations, as in the case of limonene where a dose related release of IL-18 was observed in the absence of cytotoxicity.

An unexpected dose-related IL-18 release was observed with dimethyl isophthalate (Fig. 32 D). While no EC50 values were obtained, IL-18 SI-2 could be calculated: 69.2 mg/ml in the 1 exp and 26.1 mg/ml in the 2 exp. This compound is classified as a not sensitizer in the LLNA. In spite of phthalates being widely used additives in plastics, there are few reports of skin problems caused by them (Johansen et al., 2011), and two cases of contact allergy to dimethyl phthalate has been reported (Capon et al., 1996), which may support the positive result observed. In Fig. 33 data obtained with the misclassified compound are reported. Benzyl cinnamate (Fig. 33 A, B) and benzyl salicylate (Fig. 33 C, D) are classified in the LLNA as contact sensitizers (moderate and weak, respectively), and in the RhE IL-18 assay as non-sensitizers since they failed to induce IL-18 release. Benzyl salicylate is classified as a not relevant human allergen (Lapczynski et al., 2007; Schnuch et al., 2007; Urbisch et al., 2015) and there are no human data for benzyl cinnamate that support its classification as contact sensitizer (Bhatia et al., 2007; Ohkawara et al., 2010; Api et al., 2008). These two compounds are considered as false positives in the LLNA, both of which were properly classified by the RhE IL-18 assay. Otherwise, benzyl alcohol (Fig. 33 E, F), classified as a non-sensitizer based on the LLNA data, scored as a contact sensitizer with IL-18 RhE assay as it was able to reach an IL-18 stimulation index 2.0. Literature research showed that benzyl alcohol is sensitizer in humans (Api et al.,

2007; Belsito et al., 2012; Scognamiglio et al., 2012). Thus, these three chemicals were correctly classified in the IL-18 RhE assay.

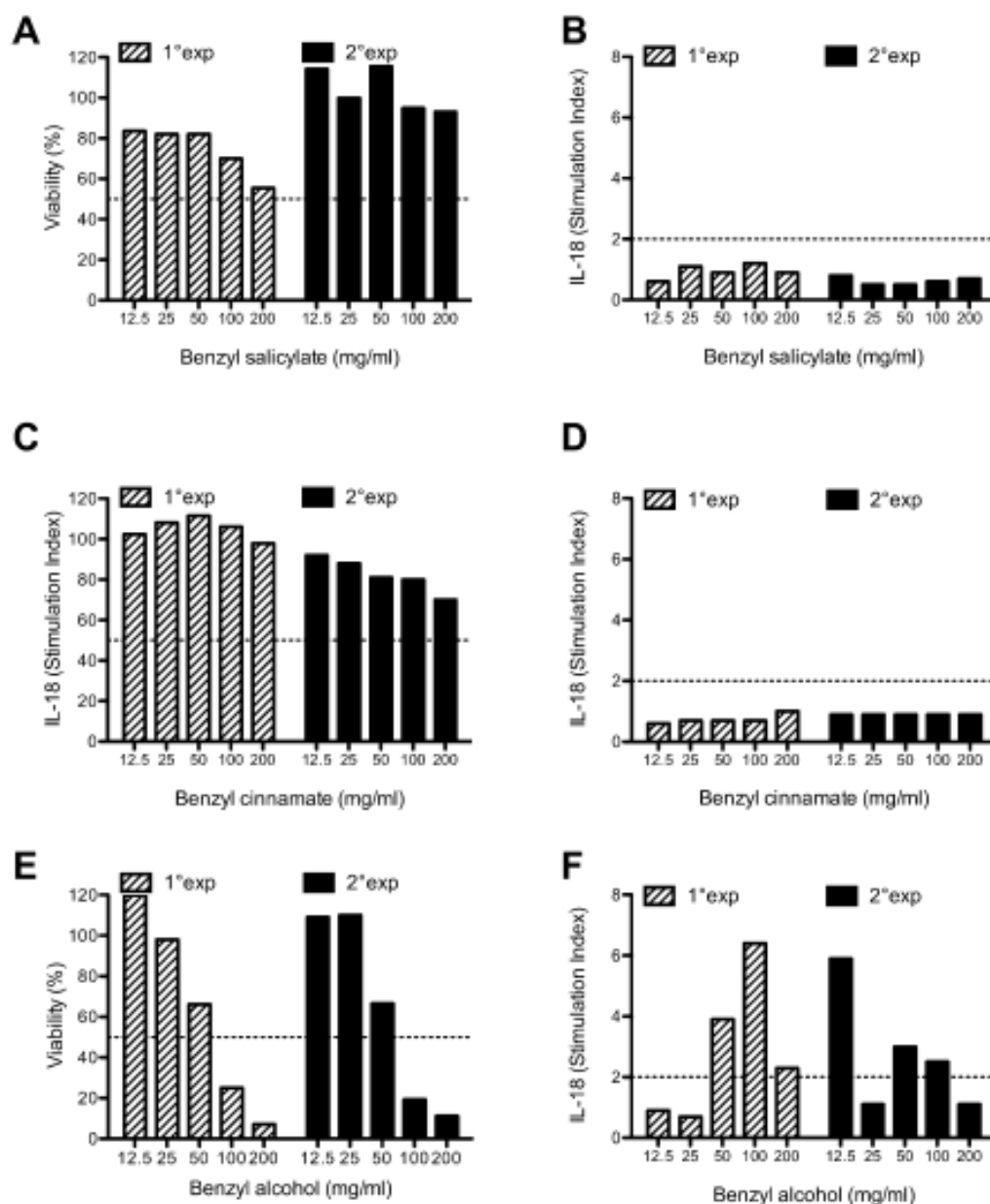


**Fig. 33. Effects on cell viability and IL-18 release of chemicals misclassified in the LLNA [30].** RhE was treated for 24 h with increasing concentrations benzyl salicylate (A, B), benzyl cinnamate (C, D), and benzyl alcohol (E, F). Viability was assessed by MTT while IL-18 by ELISA. Viability (A, C, E) is expressed as % vs vehicle treated RhE (100%), and IL-18 as stimulation index (SI) compared to vehicle treated RhE (B, D, F). The dotted lines are set at 50% viability and IL-18 SI-2.

As it is emerging in many other *in vitro* studies, data obtained using human cells seem to correlate better with *in vivo* human data. Nevertheless, additional weak allergens should be

tested to define whether the RhE IL-18 assay can correctly identify weak allergens and false negative compounds at the LLNA.

*In vitro* EC50 and IL-18 SI2 showed a good correlation with *in vivo* LLNA EC3 and human DSA05 (Gibbs et al., 2013). The next step was to investigate the possibility to use a simple approach to estimate the *in vivo* induction sensitization level, based on these two values. Curves were created, using reference skin sensitizers of different potency, namely DNCB, isoeugenol, cinnamal and benzocaine *in vitro* and *in vivo* data. In Table 8, the *in vivo* and *in vitro* values for the reference contact allergens are reported.

Reference contact sensitizers used to create the regression curves for the estimation of the *in vivo* EC3 and human NOEL

Chemical	CAS #	LLNA EC3 (%)	Human NOEL ( $\mu\text{g}/\text{cm}^2$ )	<i>In vitro</i> EC50 (% and $\mu\text{g}/\text{cm}^2$ )		<i>In vitro</i> IL-18 SI-2 (% and $\mu\text{g}/\text{cm}^2$ )	
DNCB	97-00-7	0.08	8.8	0.05	25	0.03	15
Isoeugenol	97-54-1	1.2	250	0.88	440	0.21	105
Cinnamal	104-55-2	3	591	1.1	550	0.5	250
Benzocaine	94-09-7	22	2000	4.81	2405	3.12	1560

**Table 8. Reference contact sensitizers used to create the regression curves for the estimation of the *in vivo* EC3 and human NOEL [30].** *In vivo* values were obtained from ICCVAM database (NIH Publication No. 11-7709), Research Institute for Fragrance Materials (RIFM) database, Griem et al. (2003), Api et al. (2008), Natsch et al. (2013), Basketter et al. (2014), Urbisch et al. (2015). *In vitro* EC50 and IL-18 SI2 values are the arithmetic means obtained in two independent experiments, and were calculated from RhE exposed to the selected compounds as described in materials and methods.

Linear regression curves were created by plotting *in vivo* LLNA EC3 or human NOEL values against *in vitro* EC50 or IL-18 SI2 arithmetic mean values (Fig. 34). A  $R^2 > 0.90$  with a  $p < 0.05$  was obtained for all combinations (Fig. 34 insets). The predicted LLNA EC3 (%) and human NOEL ( $\text{mg}/\text{cm}^2$ ) values for the tested chemicals were then calculated based on the arithmetic means of *in vitro* EC50 or IL-18 SI2 values obtained in two independent experiments. Despite different dose response profiles obtained for same chemicals in IL-18 release, comparing the *in vitro* predicted values with *in vivo* available data reported in Table 9, with the exception of chloramine T for which the LLNA EC3 was underestimated (and no human data is available), an excellent correspondence was observed. The predicted LLNA EC3 values were very close to the actual values, and each compound remained within the same LLNA class. The predicted

human data are more difficult to interpret because of the limited human NOEL data available for the tested compounds (de facto available only for imidazolidinyl urea and limonene). For the latter two compounds, however, the values were comparable, suggesting that the proposed approach can be indeed a valid strategy to estimate the *in vivo* LLNA EC3 and human NOEL starting from *in vitro* data.

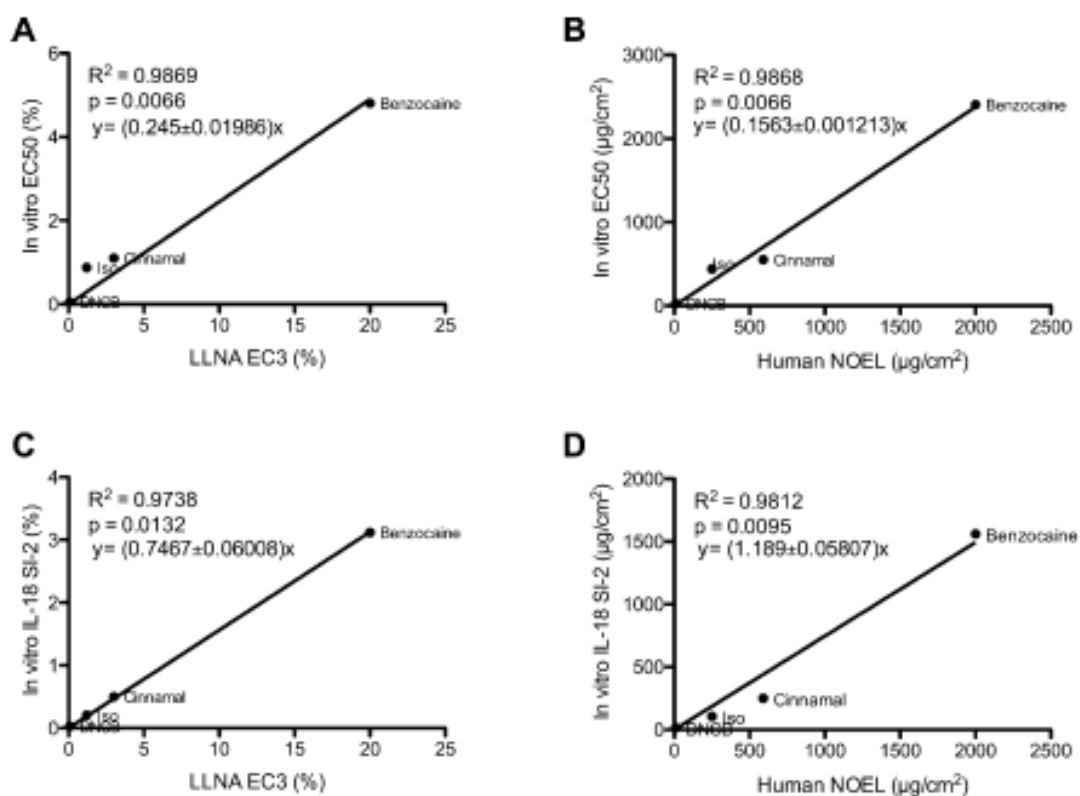


**Fig. 34 Linear regression curves of RhE assay with LLNA EC3 and human NOEL [30].** (A, B) Regression analysis of RhE-EC50 data with LLNA EC3 (A) and human NOEL (B). (B, D) Regression analysis of RhE-IL-18 SI2 data with LLNA EC3 (C) and human NOEL (D). Curves were created using data reported in Table 8. R2, p values, relative equations and slope errors are reported in each panel, and were calculated using GraphPad Prism (GraphPad Software, San Diego, CA, USA).



**DISCUSSION of “Development of an *in vitro* method to estimate the sensitization induction level of contact allergens”.**

While incredible progress has been made in the development of alternative *in vitro* tests to assess contact hypersensitivity, currently it is not possible to estimate sensitizing potency, necessary for quantitative risk assessment and full replacement of animals. The third objective of my thesis was to provide a simple, mechanistic based *in vitro* method to classify chemicals according to their sensitization potential and to estimate their induction sensitization level. Results obtained support the possibility of using the RhE IL-18 assay for the identification and potency estimation of contact sensitizers.

The use of reconstituted epidermis overcomes the limitation of chemical solubility and stability in water solution, which are the major limitations of many *in vitro* methods based on the used of submerged cultures. Topical application in relevant vehicles is only possible in RhE models, which mimic *in vivo* chemical bio-availability more closely, and therefore may lead to improved assessment of sensitizer potency (Van der Veen et al., 2014; Corsini et al., 2016). The predicted potency values we estimated were very close to the actual values, suggesting that the proposed approach can indeed be a valid strategy to estimate the *in vivo* LLNA EC3 and human NOEL starting from *in vitro* data. Overall, the arithmetic means of EC50 and IL-18 SI-2 values obtained in two independent experiments predicted similar *in vivo* values. The advantage of IL-18 SI-2 is evident in cases of non-cytotoxic compounds for which it is not possible to calculate an EC50, e.g. limonene.

Chemical	Predicted LLNA EC3 (%) based on EC50	Predicted LLNA EC3 (%) based on IL-18 SI2	Predicted human NOEL ( $\mu\text{g}/\text{cm}^2$ ) based on EC50	Predicted human NOEL ( $\mu\text{g}/\text{cm}^2$ ) based on IL-18 SI2	<i>In vitro</i> EC50 (% and $\mu\text{g}/\text{cm}^2$ )	<i>In vitro</i> IL-18 SI-2 (% and $\mu\text{g}/\text{cm}^2$ )
Benzoquinone	-	-	-	-	-	-
Chlorpromazine	0.45	0.77	46	80	0.11 55	0.12 60
Chloramine T	27.14	8.70	2797	911	6.65 3325	1.36 680
Benzyl salicylate	-	-	-	-	-	-
Diethyl maleate	3.14	1.86	321	194	0.76 382	0.29 145
Dihydroeugenol	3.51	6.72	360	703	0.86 428	1.05 525
Benzyl cinnamate	-	-	-	-	-	-
2,4-Dichloronitrobenzene	16.82	22.78	1733	2384	4.12 2060	3.56 1780
Imidazolidinyl urea	40.57	48.94	4176	5122	9.93 4965	7.65 3825
Limonene	-	61.55	-	6442	-	9.62 4810
Benzyl alcohol	28.00	23.03	2952	2410	6.86 3430	3.60 1800
Isopropanol	-	-	-	-	-	-
Dimethyl isophthalate	-	30.45	-	3188	-	4.76 2380
4-Aminobenzoic acid	-	-	-	-	-	-

**Table 9. Calculated *in vivo* LLNA EC3 and human NOEL for the tested chemicals based on *in vitro* EC50 and IL-18 SI-2 values [30].** *In vivo* values were obtained from ICCVAM database (NIH Publication No. 11-7709), Research Institute for Fragrance Materials (RIFM) database, Basketter et al. (1996), Griem et al. (2003), Api et al. (2008), Natsch et al. (2013), Basketter et al. (2014), Urbisch et al. (2015). *In vitro* EC50 and IL-18 SI2 were calculated by interpolation from linear regression analysis of data reported in Figures 31-33 from RhE exposed to the selected compounds as described in the Materials and Methods section. mg/ml values were converted to % and mg/cm<sup>2</sup> for an easier comparison with *in vivo* data. *In vitro* values are the mean of two independent experiments. –, value not estimated.

Generally, a good relationship between LLNA EC3 values and human repeated insult patch test (HRIPT) thresholds was historically shown (Griem et al., 2003; Schneider and Akkan, 2004; Basketter et al., 2005) but it is important to mention the limitations associated with the human data: a lot of data comes from older studies; human maximization test (HMT) and HRIPT have differences in sensitivity; there is not a well standardized protocol; the intrinsic potency of chemical skin sensitizers in humans requires experimental studies of dubious ethics; and the intraspecies variability of human susceptibility to skin sensitization may confound the results (Gerberick et al., 2001; Griem et al., 2003; Schneider and Akkan, 2004; Basketter et al., 2005; ICCVAM, 2011). More potent contact allergens are expected to evoke at lower concentrations a stronger innate inflammatory reaction than less potent allergens, which will in turn influence the migration of skin dendritic cells, their degree of activation and, therefore, the quality of immune responses elicited (Kimber et al., 2012). Results obtained confirmed the previous ones (Gibbs et al., 2013; Teunis et al., 2014) that showed how there

is a general trend for IL-18 induction/cytotoxicity at lower concentrations for extreme/strong sensitizers, whereas higher concentrations are required in the case of weak sensitizers.

The only compound apparently underestimated was chloramine T: an LLNA EC<sub>3</sub> value of 27.14% based on EC<sub>50</sub> or of 8.70% based on IL-18 SI-2 were predicted versus a value of 0.14% in the animal studies. It is important to mention that in the LLNA positive responses are obtained by both contact and respiratory sensitizers, while the RhE IL-18 assay identify only contact allergens. It is thus possible that chloramine T would be mainly a type I sensitizer, and a weak contact sensitizer. This is likely to be the case in humans, where IgE-mediated allergic asthma caused by chloramine T is well known (Wass et al.,1989; Kramps et al.,1981), while skin symptoms, mainly allergic contact urticaria, have only seldom been reported (Dooms-Goossens et al., 1983; Lombardi et al., 1989; Kanerva et al., 1997), perfectly fitting our findings.

Regarding the yes/no classification, based on animal data benzyl salicylate and benzyl cinnamate were incorrectly classified as not sensitizers, and 2 non-sensitizers (benzyl alcohol, dimethyl isophthalate) were incorrectly classified as sensitizers. However, based on human data all chemicals, except dimethyl isophthalate, were correctly classified by the RhE IL-18 assay. Benzyl salicylate and benzyl cinnamate are fragrance ingredient compounds that can be found in cosmetics, shampoos, and toilets soaps as in household cleaners and detergents. It has emerged that both compounds, that share a similar chemical structure, are classified as not relevant human allergens (Lapczynski et al., 2007; Schnuch et al., 2007; Bhatia et al., 2007; Ohkawara et al., 2010). Benzyl alcohol is a fragrance used like benzyl salicylate and benzyl cinnamate with a different chemical structure. Due to the presence of electronegative substituent and a side chain on the aromatic ring able to generate H bonds, benzyl alcohol acts as a sensitizer in human (Api et al., 2007; Belsito et al., 2012; Scognamiglio et al., 2012).

Dimethyl isophthalate, considered as a not sensitizer in the LLNA, was classified as positive in the RhE IL-18 assay, inducing a dose-related release of IL-18. Only few cases of contact allergy to dimethyl phthalate has been reported (Capon et al., 1996), which may support our findings of dimethyl phthalate being a weak sensitizer.

A comment should be made regarding 2,4-dichloronitrobenzene, mostly present in agrochemical products, which is often used as non-sensitizer structural analog to DNCB in animal studies. Even if the weak sensitizing potential of DNCB (LLNA EC3 of 20%) has been demonstrated in the LLNA by Basketter et al. (1996), there are evidences in literature that this compound is a human contact sensitizer, supporting our results (Basketter et al., 1996; Aleksic et al., 2007; Cruz et al., 2007; Roberts and Aptula, 2014).

To achieve a complete replacement of animals in skin sensitization assessment, dose-response information and evaluation of relative skin sensitizing potency to support effective risk assessment is necessary. Here, a very simple and straightforward approach to estimate the LLNA EC3 or human NOEL of a chemical sensitizer has been described. In all biological responses, there are of course unavoidable variabilities, which also apply to *in vitro* and *in vivo* values used in this study. However, when it comes to risk assessment we still tend to use one value and apply a safety factor to take care of variability. This is also the case of quantitative risk assessment for skin sensitization where to calculate the acceptable exposure level, the NESIL is divided by a Sensitization Assessment Factor, which takes care of inter-individual variability, vehicle and matrix effects, and use considerations (Api et al., 2008).

In conclusion, even if further compounds must be tested to better define the applicability and limitation of the RhE IL-18 potency test, using reference contact allergens, standard curves can be created to estimate *in vivo* sensitization induction level, which can be useful in risk assessment. A consortium of academic and industrial partners has now established a generic

SOP for the method applicable to several RhE models, and the validation of RhE IL-18 potency test is ongoing, results are expected in 2018.

---

**CHAPTER SEVEN**  
FUTURE PERSPECTIVES

---

As future perspectives the following experiments can be foreseen:

- To better understanding of the molecular mechanisms of allergen-induced IL-18 production, the use of antioxidants could be a choice to better explain the role contact allergen-induced oxidative stress NLRP12 and Blimp-1 modulation.
- To further study the signal transduction pathways involved in allergen-induced IL-18 production, the role played by other proteins, should be investigated and may offer the possibility to discriminate between weak, strong, extreme sensitizers.
- Finally, a better understanding of the molecular mechanisms underlying potency using dendritic cells as experimental model is mandatory to achieve a full replacement of animal's models in contact hypersensitivity.

---

## **ANNEX**

Equivalent Epidermis  
VUmc, Amsterdam

---



During my PhD, the Derma Lab of VUmc (Amsterdam) hosted me for three months to learn how to make RhE. This experience was done to reproduce RhE at Toxicology Lab (Milan), to perform new experiments and to compare the new results with the results previously obtained with the NCTC 2544 cell line.

Below the protocol adopted (all pictures were taken by me).

For the preparation of an **equivalent epidermis** of the skin on a dermal matrix or a filter matrix, the epidermis can be recreated without the use of fibroblasts. This model gives to researcher the opportunity to investigate the role of the keratinocytes by itself in the skin. Skin can be stored in 1X Hanks media with 1% pen/strep, at 4°C for maximum 72 h (Fig. 35).

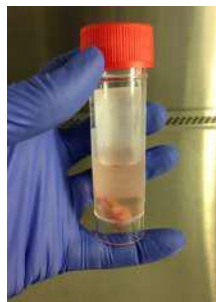


**Fig. 35**

#### **DAY 1 - SKIN PREPARATION (to make foreskin)**

Skin from donors (in my case, the Islamic people's foreskin) was placed in PBS 1X to be washed (Fig. 36 left side) and subsequently to be cut (Fig. 36 right side).



**Fig. 36**

It was necessary to remove the fat part of the skin. In new small Petri's dish, 4 ml of Dispase II (Roche, 295825) were added and the gauze was cut (Fig. 37). The enzyme Dispase II was able to promote the epidermal detachment from the dermis.

After that, small pieces of skin were cut and put on gauze, with epidermal side up and dermal side on the gauze, as shown in Fig. 37:

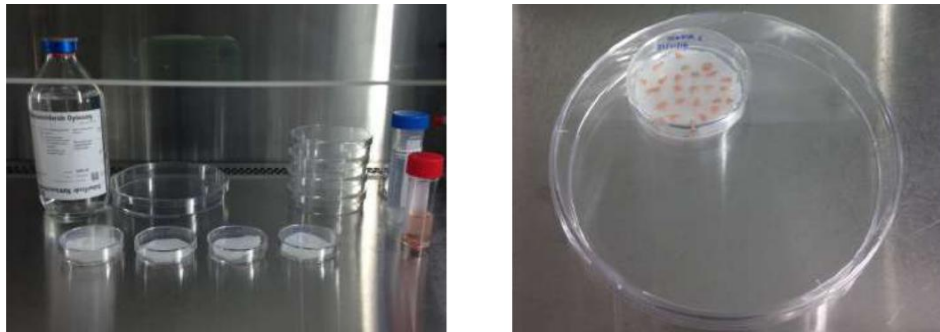


**Fig. 37**

The small Petri's dish was closed with cap and inserted in a special Petri's dish (150 mm of diameter) to prevent contaminations (Fig. 37 right side) at 4°C, overnight (o.v.).

The day after, the cells were isolated and counted, and a new Petri's dishes was coated with the collagen-IV (Fig. 38). Type IV collagen is a constituent of basement membrane and is located especially in the lamina densa.

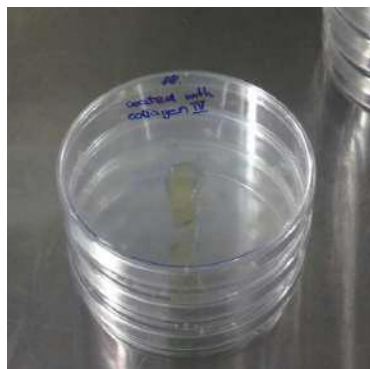


**Fig. 38**

By scraper or by swap, collagen-IV solution was spread. Petri's dishes were incubated at 37°C, 5% CO<sub>2</sub> o.n. The described step could be made also the day after, but in this case it's necessary to wait at least 2 hours (in my case, 4 h).

## **DAY 2 - KERATINOCYTES ISOLATION**

If the Petri's dishes were coated with collagen VI, it's possible to start directly.

Transfer the special huge Petri's dish from fridge to incubator for 10-15 min. KC1 media and 0,05% of trypsin solution were used to count the cells:

- KC1 media: 375 mL of DMEM Dulbecco's modification of Eagle's Media (Lonza company)
  - 125 mL of F-12 NutMix (Ham) (Gibco company, 21765-029)
  - 5 mL of penicillin/streptomycin (Gibco, 15070-063)
  - 2 mL of hydrocortisone (Sigma, H-0888)
  - 500  $\mu$ L of isoproterenol (Sigma, I-6504)
  - 50  $\mu$ L of Insulin (Sigma, I-5500)
  - 5 mL of UltrosorG (GibcoBRL, 091-2950H)
- 0,05% of trypsin solution: 20 mL of GNK buffer pH 7.3
  - 500  $\mu$ L of 1% of EDTA
  - 500  $\mu$ L of 2.5% Trypsin (GibcoBRL, 25090-028)

It was necessary to detach the epidermis from dermis, a crucial step to prevent epidermis contaminations (Fig. 39).



**Fig. 39**

The epidermis was washed 4 times in steril PBS (Fig. 40).

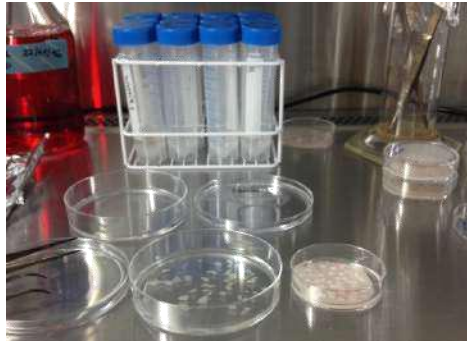


**Fig. 40**

The epidermis was placed in the tube with 5 ml of 0.05% trypsin and was incubated at 37°C in the water-bath for 15 min. During this time, a rack with two tubes per donor was prepared. On top of the tube 100  $\mu$ M and 40  $\mu$ M cell strainer were placed (Fig. 41).



**Fig. 41**

The tube with epidermis and trypsin was shaken and 7 ml of media KC1 were added. The substance was poured out of the tube on the tube with 100  $\mu$ M cell strainer. 5 ml of KC1 were pipetted on top of the cell strainer to wash it. The 100  $\mu$ M filter was taken off and was discarded it and the cellular solution was poured on to the 40  $\mu$ M filter tube. Again, 5 ml of KC1 were pipetted on top of the cell strainer to wash it. 300-500  $\mu$ L in a new eppendorf tube were kept to count the cells. The filter was discarded, and the tube was centrifuged for 5 min at 300 rpm. At the end, the cells are counted by a Burker-turk chamber (Fig. 42):

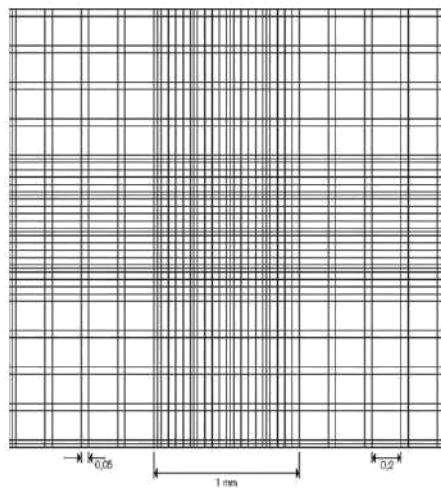


**Fig. 42**

The cells are counted in 25 squares on the left and 25 on the right, it's possible to take the average. Cells between the double lines were not considered.

*Example:* on the left I count 35 cells and on the right 29 cells. Then the average is 32 cells

$$32 \text{ cells} \times 10^4 \times 20 \text{ mL (the volume in the tube)}$$

$$6,40 \text{ cells} \times 10^6 \text{ cells}$$

the cells were diluted with medium 1 to  $4 \times 10^5$  cells/ml and 10 ml of cellular suspension were put in pre-coated Petri's dish.

### **DAY 3 - REFRESH MEDIUM**

The media was aspirated carefully and 10 ml + KGF 1 ng/ml were added slowly (for each Petri's dish). If the foreskin was refreshed the day before with KGF, it's possible to take a look on cells and to leave them in the incubator.

### **DAY 4 - REFRESH MEDIUM**

The media was aspirated carefully and 10 ml + KGF 1 ng/ml were added slowly (for each Petri's dish).

### **DAY 5 - REFRESH MEDIUM**

If the media was not refreshed on day 4, do it on day 5.

IMPORTANT: in the Fig. 43 Fibroblasts and KCs morphology is shown on left. When the foreskin has a lot of fibroblasts are around the clones of KCs (Fig. 43, on right), they have to be removed, as following: the media is removed and is washed twice with 10 ml of steril PBS. 2 ml of trypsin solution are added. After 1 minute to promote the detach of fibloblasts, the solution is removed with vacuum, the cells are washed again with 10 ml of steril PBS slowly (to remove trypsin solution) and 10 ml of KC1 and KGF 1 ng/ml are added for each petri's dish. The cells are incubated at 37°C, 1.5% CO<sub>2</sub> and 50% humidity.

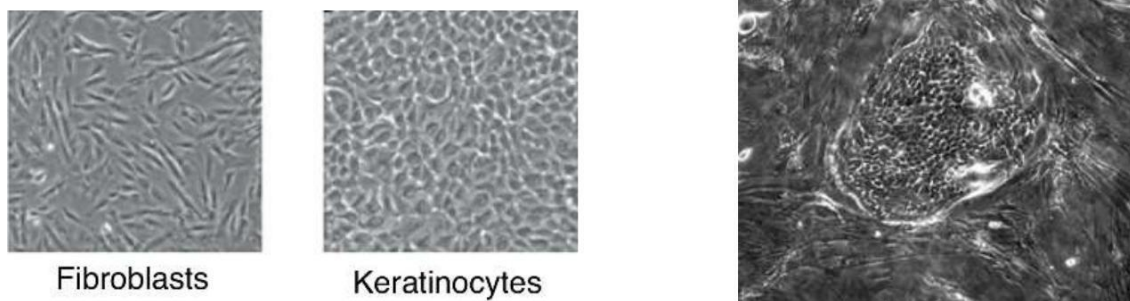


Fig. 43 Fibroblasts and KCs morfology on left [31]; Fibroblasts around KCs clone on right[ 32]

#### DAY 8 - PUT KERATINOCYTES ON FILTER

From the incubator, KCs were checked under microscope. When confluent, they were counted. If the clones of KCs are surrounded of fibroblasts, it is necessary to remove them, as described.

KCs were placed on transwell filters a 12 wells filter plate (Fig. 44):



Fig. 44

3 ml of KC1 were added outside the traswell; 1 ml of  $0,25 \times 10^6$  cells was added inside.

### **DAY 10 - REFRESH MEDIUM**

6-8 mL of KC1 + KGF 1ng/mL in each transwell (in and out) were used to refresh cells.

### **DAY 14 (Monday) - AIR EXPOSURE**

From incubator, the transwell was taken and the media was removed. A special huge Petri's dish (corning, 430597) and a round stainless steel ring with 18 holes was used, 80 mL of KC2+1 ng/ml of KGF were filled in. Each transwell was checked, and taking care, inserted in each ring (Fig. 45, left side). Remind to leave just one hole empty if you have a full Petri's dish to allow the gas exchange (Fig. 45, right side). Take care of air bubbles.

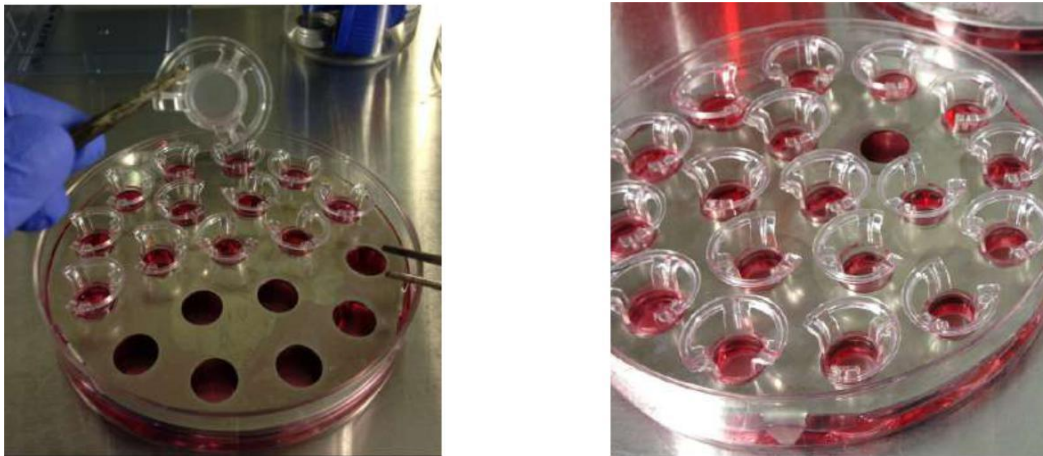


**Fig. 45**

The equivalent epidermis was incubated.

### **DAY 17.**

80 ml of KC2 + KGF 1ng/ml were used to refresh the equivalent epidermis (EE). EE was incubated.

### **DAY 21.**

80 ml of KC2 + KGF 1ng/ml were used to refresh the EE. EE was incubated.

### **DAY 24.**

80 ml of KC2 + KGF 1ng/ml were used to refresh the EE. EE was incubated.

### **DAY 27 - CHEMICAL COMPOUND EXPOSURE.**

## PUBLICATIONS:

**Papale A**, Viscardi V, Lossani C, Galbiati V, Corsini E. NLRP12 protein and the inflammasome complex in the induction of IL-18 in human keratinocytes: further developments  
(*manuscript in preparation*)

Galbiati V, **Papale A**, Marinovich M, Gibbs S, Roggen E, Corsini E. Development of an *in vitro* method to estimate the sensitization induction level of contact allergens. *Toxicol Lett.* 271:1-11. 2017.

**Papale A**, Kummer E, Galbiati V, Marinovich M, Galli CL, Corsini E. Understanding chemical allergen potency: role of NLRP12 and Blimp-1 in the induction of IL-18 in human keratinocytes. *Arch Toxicol.* 91(4):1783-1794. 2017.

Buoso E, Galasso M, Ronfani M, **Papale A**, Galbiati V, Eberini I, Marinovich M, Racchi M, Corsini E. The scaffold protein RACK1 is a target of endocrine disrupting chemicals (EDCs) with important implication in immunity. *Toxicol Appl Pharmacol.* 325:37-47. 2017.

Corsini E, Vecchi R, Marabini L, Fermo P, Becagli S, Bernardoni V, Caruso D, Corbella L, Dell'Acqua M, Galli CL, Lonati G, Ozgen S, **Papale A**, Signorini S, Tardivo R, Valli G, Marinovich M. The chemical composition of ultrafine particles and associated biological effects at an alpine town impacted by wood burning. *Sci Total Environ.* 587-588:223-231. 2017.

Corsini E, Ozgen S, **Papale A**, Galbiati V, Lonati G, Fermo P, Corbella L, Valli G, Bernardoni V, Dell'Acqua M, Becagli S, Caruso D, Vecchi R, Galli CL, Marinovich M. Insights on wood combustion generated proinflammatory ultrafine particles (UFP). *Toxicol Lett.* 266:74-84. 2017.

Galbiati V, **Papale A**, Kummer E, Corsini E. In vitro Models to Evaluate Drug-Induced Hypersensitivity: Potential Test Based on Activation of Dendritic Cells. *Front Pharmacol.* 7:204. 2016.



Corsini E, Galbiati V, **Papale A**, Kummer E, Pinto A, Guaita A, Racchi M. The role of HSP27 in RACK1-mediated PKC activation in THP-1 cells. *Immunol Res.* 64(4):940-50. 2016.

Corsini E, Galbiati V, **Papale A**, Kummer E, Pinto A, Serafini MM, Guaita A, Spezzano R, Caruso D, Marinovich M, Racchi M. Role of androgens in dheaa-induced rack1 expression and cytokine modulation in monocytes. *Immun Ageing.* 13:20. 2016.

Nikitovic D, Berdiaki A, Galbiati V, Kavasi RM, **Papale A**, Tsatsakis A, Tzanakakis GN, Corsini E. Hyaluronan regulates chemical allergen-induced IL-18 production in human keratinocytes. *Toxicol Lett.* 232(1):89-97. 2015.

Lourenço AC, Galbiati V, Corti D, **Papale A**, Martino-Andrade AJ, Corsini E. The plasticizer dibutyl phthalate (DBP) potentiates chemical allergen-induced THP-1 activation. *Toxicol In Vitro* 29(8):2001-8. 2015.

Galbiati V, **Papale A**, Galli CL, Marinovich M, Corsini E. Role of ROS and HMGB1 in Contact Allergen-Induced IL-18 Production in Human Keratinocytes. *J Invest Dermatol.* 2014.

## **ACTIVITIES:**

### **Internship abroad:**

November 2016-february 2017. VU Medical Centre, Dermatology Laboratory, directed by Prof. Sue Gibbs, Amsterdam, The Netherlands.

### **Oral communications:**

- "Role of inflammasome proteins in the induction of IL-18 in the human keratinocytes cell line NCTC 2544", ERGECD 2017, Zurig, Switzerland.
- "Understanding chemical allergen potency: role of NLRP12 and Blimp-1 in Keratinocytes", ERGECD 2015, Milan, Italy.
- "Sviluppo di un metodo *in vitro* per stimare il livello di induzione della sensibilizzazione da parte di allergeni da contatto a basso peso molecolare", SITOX 2015, Milan, Italy.

### **Poster presentations:**

- "NLRP12 protein and the inflammasome complex in the induction of IL-18 in the human keratinocytes: further developments", EUROTOX 2017, Bratislava, Slovak.
- "Molecular mechanisms involved in allergen-induced IL-18 production in the human keratinocytes cell line", ESTIV 2015, Egmond Aan Zee, The Netherlands.

### **Correlator of experimental thesis:**

- "Ruolo delle proteine dell'inflammasoma NLRP3 nell'induzione di IL-18 nella linea di cheratinociti umani NCTC 2544". Student: Veronica Viscardi. Anno accademico 2016/2017.
- "Espressione delle proteine dell'inflammasoma NLRP3 e link con la proteina NLRP12 nell'induzione di IL-18 nella linea di cheratinociti umani NCTC 2544". Student: Chiara Lossani. Anno accademico 2017/2018.

## REFERENCES:

Aiba S, Terunuma A, Manome H et al. Dendritic cells differently respond to haptens and irritants by their production of cytokines and expression of co-stimulatory molecules. *Eur J Immunol.* 27(11):3031-8. 1997.

Akiba H, Kehren J, Ducluzeau MT et al. Skin inflammation during contact hypersensitivity is mediated by early recruitment of CD8+ T cytotoxic 1 cells inducing keratinocyte apoptosis. *J Immunol.* 168(6):3079-87. 2002.

Aleksic M, Pease CK, Basketter DA et al. Investigating protein haptentation mechanisms of skin sensitizers using human serum albumin as a model protein. *Toxicol In Vitro.* 21(4):723-33. 2007.

Amer A, Franchi L, Kanneganti TD et al. Regulation of Legionella phagosome maturation and infection through flagellin and host Ipaf. *J Biol Chem.* 281(46):35217-23. 2006.

Antonopoulos C, Cumberbatch M, Mee JB et al. IL-18 is a key proximal mediator of contact hypersensitivity and allergen-induced Langerhans cell migration in murine epidermis. *J. Leukoc. Biol.* 83, 361-367. 2008.

Api AM, Basketter DA, Cadby PA et al. Dermal sensitization quantitative risk assessment (QRA) for fragrance ingredients. *Regul Toxicol Pharmacol.* 52(1):3-23. 2008.

Arlehamn CS, Pétrilli V, Gross O et al. The role of potassium in inflammasome activation by bacteria. *J Biol Chem.* 285(14):10508-18. 2010.

Arrighi JF, Rebsamen M, Rousset F et al. A critical role for p38 mitogen-activated protein kinase in the maturation of human blood-derived dendritic cells induced by lipopolysaccharide, TNF-alpha, and contact sensitizers. *J Immunol.* 166(6):3837-45. 2001.

Arthur JC, Lich JD, Ye Z et al. Cutting edge: NLRP12 controls dendritic and myeloid cell migration to affect contact hypersensitivity. *J Immunol.* 185(8):4515-9. 2010.

Basketter DA, Alépée N, Ashikaga T et al. Categorization of chemicals according to their relative human skin sensitizing potency. *Dermatitis.* 25(1):11-21. 2014.

Basketter DA, Clapp C, Jefferies D et al. Predictive identification of human skin sensitization thresholds. *Contact Dermatitis.* 53(5):260-7. 2005.

Basketter DA, Balikie L, Dearman RJ et al. Use of the local lymph node assay for the estimation of relative contact allergenic potency. *Contact Dermatitis.* 42(6):344-8. 2000.

Basketter DA, Scholes EW, Fielding I et al. Dichloronitrobenzene: a reappraisal of its skin sensitization potential. *Contact Dermatitis.* 34(1):55-8. 1996.

- Basketter D, Dooms-Goossens A, Karlberg AT et al. The chemistry of contact allergy: why is a molecule allergenic? *Contact Dermatitis*. 32(2):65-73. 1995.
- Belsito D, Bickers D, Bruze M et al. A toxicological and dermatological assessment of aryl alkyl alcohols when used as fragrance ingredients. *Food Chem Toxicol*. 50 Suppl 2: S52-99. 2012.
- Berg DJ, Leach MW, Kühn R et al. Interleukin 10 but not interleukin 4 is a natural suppressant of cutaneous inflammatory responses. *J Exp Med*. 182(1):99-108. 1995.
- Bhatia SP, Wellington GA, Cocchiara J et al. Fragrance material review on benzyl cinnamate. *Food Chem Toxicol*. 45 Suppl 1: S40-8. 2007.
- Boehme KW, Compton T. Innate sensing of viruses by toll-like receptors. *J Virol*. 78(15):7867-73. 2004.
- Boyden ED, Dietrich WF. Nalp1b controls mouse macrophage susceptibility to anthrax lethal toxin. *Nat Genet*. 38(2):240-4. 2006.
- Bradford, MM. A rapid and sensitive method for the quantitation of microgram quantities of protein utilizing the principle of protein-dye binding. *Analyt. Biochem*. 72, 248–254. 1976.
- Bürckstümmer T, Baumann C, Blüml S et al. An orthogonal proteomic-genomic screen identifies AIM2 as a cytoplasmic DNA sensor for the inflammasome. *Nat Immunol*. 10(3):266-72. 2009.
- Capon F, Cambie MP, Clinard F et al. Occupational contact dermatitis caused by computer mice. *Contact Dermatitis*. 35(1):57-8. 1996.
- Cavani A, Nasorri F, Prezzi C et al. Human CD4+ T lymphocytes with remarkable regulatory functions on dendritic cells and nickel-specific Th1 immune responses. *J Invest Dermatol*. 114(2):295-302. 2000.
- Chang DH, Angelin-Duclos C, Calame K. BLIMP-1: trigger for differentiation of myeloid lineage. *Nat Immunol*. 1(2):169-76. 2000.
- Collo G, Neidhart S, Kawashima E et al. Tissue distribution of the P2X7 receptor. *Neuropharmacology*. 36(9):1277-83. 1997.
- Corsini E, Roggen EL, Galbiati V et al. Alternative Approach for Potency Assessment: *In Vitro* Methods. *Cosmetics*. 3(1), 7. 2016.
- Corsini E, Papale A., Galbiati V. et al. Safety Evaluation of Cosmetic Ingredients: *In Vitro* Opportunities for the Identification of Contact Allergens *Cosmetics*. 1(1), 61-74. 2014.
- Corsini E, Galbiati V, Mitjans et al. NCTC 2544 and IL-18 production: a tool for the identification of contact allergens. *Toxicol In Vitro*. 27(3):1127-34. 2013.

Corsini E, Mitjans M, Galbiati V et al. Use of IL-18 production in a human keratinocyte cell line to discriminate contact sensitizers from irritants and low molecular weight respiratory allergens. *Toxicol In Vitro*. 23(5):789-96. 2009.

Corsini, E, Roggen, EL. Immunotoxicology: opportunities for non-animal test development. *Altern. Lab. Anim.* 37, 387–397. 2009.

Corsini, E, Limioli, E, Marinovich, M, et al. Selective induction of interleukin-12 by chemical allergens in reconstituted human epidermis. *ATLA*. 27, 261-269. 1999.

Corsini, E, Primavera, A, Marinovich, M, et al. Selective induction of interleukin-1  $\alpha$  in murine keratinocyte by chemical allergens. *Toxicology*. 129, 193-200. 1998.

Coutant, KD, de Fraissinette, AB, Cordier, A, et al. Modulation of the activity of human monocyte-derived dendritic cells by chemical haptens, a metal allergen, and a staphylococcal superantigen. *Toxicol. Sci.* 52:189–98. 1999.

Craven RR, Gao X, Allen IC et al. Staphylococcus aureus alpha-hemolysin activates the NLRP3-inflammasome in human and mouse monocytic cells. *PLoS One*. 4(10): e7446. 2009.

Cruz MT, Neves BM, Gonçalo M et al. Effect of skin sensitizers on inducible nitric oxide synthase expression and nitric oxide production in skin dendritic cells: role of different immunosuppressive drugs. *Immunopharmacol Immunotoxicol*. 29(2):225-41. 2007.

Cumberbatch M, Dearman RJ, Antonopoulos C et al. Interleukine-18 induces Langerhans cell migration by a tumor necrosis factor  $\alpha$  and IL-1 $\beta$  dependent mechanism. *Immunology*. 102, 323-330. 2001.

De Nardo D, Latz E. NLRP3 inflammasomes link inflammation and metabolic disease. *Trends Immunol*. 32(8):373-9. 2011.

Di Virgilio F. The P2Z purinoceptor: an intriguing role in immunity, inflammation and cell death. *Immunol Today*. 16(11):524-8. 1995.

Divkovic M, Pease CK, Gerberick GF et al. Hapten-protein binding: from theory to practical application in the *in vitro* prediction of skin sensitization. *Contact Dermatitis*. 53(4):189-200. 2005.

Dooms-Goossens A, Gevers D, Mertens A et al. Allergic contact urticaria due to chloramine. *Contact Dermatitis*. 9(4):319-20. 1983.

dos Santos GG, Reinders J, Ouwehand K et al. Progress on the development of human *in vitro* dendritic cell based assays for assessment of the sensitizing potential of a compound. *Toxicol Appl Pharmacol*. 236(3):372-82. 2009.

Dostert C, Pétrilli V, Van Bruggen R et al. Innate immune activation through Nalp3 inflammasome sensing of asbestos and silica. *Science*. 320(5876):674-7. 2008.

Duewell P, Kono H, Rayner KJ et al. NLRP3 inflammasomes are required for atherogenesis and activated by cholesterol crystals. *Nature*. 464(7293):1357-61. 2010.

Duncan JA, Bergstralh DT, Wang Y et al. Cryopyrin/NALP3 binds ATP/dATP, is an ATPase, and requires ATP binding to mediate inflammatory signaling. *Proc Natl Acad Sci U S A*. 104(19):8041-6. 2007.

Ebert LM, Schaerli P, Moser B. Chemokine-mediated control of T cell traffic in lymphoid and peripheral tissues. *Mol Immunol*. 42(7):799-809. 2005.

Emter R, Ellis G, Natsch A. Performance of a novel keratinocyte-based reporter cell line to screen skin sensitizers *in vitro*. *Toxicol Appl Pharmacol*. 245(3):281-90. 2010.

Enk AH, Katz SI. Early molecular events in the induction phase of contact sensitivity. *Proc. Natl. Acad. Sci. USA* 89, 1398–1402. 1992.

Falzone S, Munerati M, Ferrari D et al. The purinergic P2Z receptor of human macrophage cells. Characterization and possible physiological role. *J Clin Invest*. 95(3):1207-16. 1995.

Faulkner L, Meng X, Park BK et al. The importance of hapten-protein complex formation in the development of drug allergy. *Curr Opin Allergy Clin Immunol*. 14(4):293-300. 2014.

Faustin B, Lartigue L, Bruey JM et al. Reconstituted NALP1 inflammasome reveals two-step mechanism of caspase-1 activation. *Mol Cell*. 25(5):713-24. 2007.

Fazekas de St Groth S, Webster RG, Dartyner A. Two new staining procedures for quantitative estimation of proteins on electrophoretic strips, *Biochim Biophys Acta*. 71, 377–391. 1963.

Feldmeyer L, Werner S, French LE et al. Interleukin-1, inflammasomes and the skin. *Eur J Cell Biol*. 89(9):638-44. 2010.

Fernandes-Alnemri T, Yu JW, Datta et al. AIM2 activates the inflammasome and cell death in response to cytoplasmic DNA. *Nature*. 458(7237):509-13. 2009.

Ferrari D, Pizzirani C, Adinolfi E et al. The P2X7 receptor: a key player in IL-1 processing and release. *J Immunol*. 2006 Apr 1;176(7):3877-83. Review. Erratum in: *J Immunol*. 179(12):8569. 2007.

Ferrari D, Chiozzi P, Falzone S et al. Extracellular ATP triggers IL-1 beta release by activating the purinergic P2Z receptor of human macrophages. *J Immunol*. 159(3):1451-8. 1997.

Finger JN, Lich JD, Dare LC et al. Autolytic proteolysis within the function to find domain (FIIND) is required for NLRP1 inflammasome activity. *J Biol Chem*. 287(30):25030-7. 2012.

Fink SL, Bergsbaken T, Cookson BT. Anthrax lethal toxin and Salmonella elicit the common cell death pathway of caspase-1-dependent pyroptosis via distinct mechanisms. *Proc Natl Acad Sci U S A*. 105(11):4312-7. 2008.

Franchi L, Muñoz-Planillo R, Núñez G. Sensing and reacting to microbes through the inflammasomes. *Nat Immunol*. 13(4):325-32. 2012.

Franchi L, Kanneganti TD, Dubyak GR et al. Differential requirement of P2X7 receptor and intracellular K<sup>+</sup> for caspase-1 activation induced by intracellular and extracellular bacteria. *J Biol Chem*. 282(26):18810-8. 2007.

Franchi L, McDonald C, Kanneganti TD et al. Nucleotide-binding oligomerization domain-like receptors: intracellular pattern recognition molecules for pathogen detection and host defense. *J Immunol*. 177(6):3507-13. 2006.

Fry DC, Vassilev LT. Targeting protein-protein interactions for cancer therapy. *J Mol Med (Berl)*. 83(12):955-63. 2005.

Fubini B, Hubbard A. Reactive oxygen species (ROS) and reactive nitrogen species (RNS) generation by silica in inflammation and fibrosis. *Free Radic Biol Med*. 34(12):1507-16. 2003.

Galbiati V, Papale A, Marinovich M et al. Development of an *in vitro* method to estimate the sensitization induction level of contact allergens. *Toxicol Lett*. 271:1-11. 2017.

Galbiati V, Corsini E. The NCTC 2544 IL-18 assay for the *in vitro* identification of contact allergens. *Curr Protoc Toxicol*. Chapter 20: Unit 20.8. 2012.

Galbiati V, Mitjans M, Lucchi L et al. Further development of the NCTC 2544 IL-18 assay to identify *in vitro* contact allergens. *Toxicol In Vitro*. 25(3):724-32. 2011.

Galbiati V, Mitjans M, Lucchi L et al. Further development of the NCTC 2544 IL-18 assay to identify *in vitro* contact allergens. *Toxicol In Vitro*. 25(3):724-32. 2011.

Galbiati, V., Mitjans, M, Corsini, E. Present and future of *in vitro* immunotoxicology in drug development. *J. Immunotoxicol*. 1–13. 2010.

Gerberick GF, Aleksis M, Basketter DA et al. Chemical reactivity measurement and the predictive identification of skin sensitizers. *ATLA*. 3, 215-242. 2008.

Gerberick GF, Vassallo JD, Foertsch LM et al. Quantification of chemical peptide reactivity for screening contact allergens: a classification tree model approach. *Toxicol Sci*. 97(2):417-27. 2007.

Gerberick GF, Ryan CA, Kern PS et al. Compilation of historical local lymph node data for evaluation of skin sensitization alternative methods. *Dermatitis*. 16(4):157-202. 2005.

Gerberick GF, Robinson MK, Ryan CA et al. Contact allergenic potency: correlation of human and local lymph node assay data. *Am J Contact Dermat*. 12(3):156-61. 2001.

Gibbs S, Corsini E, Spiekstra SW et al. An epidermal equivalent assay for identification and ranking potency of contact sensitizers. *Toxicol Appl Pharmacol*. 272(2):529-41. 2013.

Gibson UE, Heid CA, Williams PM: A novel method for real time quantitative RT-PCR. *Genome Res.* 6: 995–1001. 1996.

Glover DJ, Lipps HJ, Jans DA. Towards safe, non-viral therapeutic gene expression in humans. *Nat Rev Genet.* 6(4):299–310. 2005.

Goebeler M, Trautmann A, Voss A et al. Differential and sequential expression of multiple chemokines during elicitation of allergic contact hypersensitivity. *Am J Pathol.* 158(2):431-40. 2001.

Grabbe S, Steinert M, Mahnke K, et al. Dissection of antigenic and irritative effects of epicutaneously applied haptens in mice. Evidence that not the antigenic component but nonspecific proinflammatory effects of haptens determine the concentration-dependent elicitation of allergic contact dermatitis. *J. Clin. Invest.* 98, 1158–1164. 1996.

Grabbe S, Steinbrink K, Steinert M et al. Removal of the majority of epidermal Langerhans cells by topical or systemic steroid application enhances the effector phase of murine contact hypersensitivity. *J Immunol.* 155(9):4207-17. 1995.

Griem P, Goebel C, Scheffler H. Proposal for a risk assessment methodology for skin sensitization based on sensitization potency data. *Regul Toxicol Pharmacol.* 38(3):269-90. 2003.

Halle A, Hornung V, Petzold GC et al. The NALP3 inflammasome is involved in the innate immune response to amyloid-beta. *Nat Immunol.* 9(8):857-65. 2008.

Hartwig, C, Tschernig, T, Mazzega, M, et al. Endogenous IL-18 in experimentally induced asthma affects cytokine serum levels but is irrelevant for clinical symptoms. *Cytokine.* 42, 298–305. 2008.

He D, Wu L, Kim HK et al. CD8+ IL-17-producing T cells are important in effector functions for the elicitation of contact hypersensitivity responses. *J Immunol.* 177(10):6852-8. 2006.

Heid CA, Stevens J, Livak KJ, Williams PM: Real time quantitative PCR. *Genome Res.* 6: 986–994. 1996.

Hornung V, Ablasser A, Charrel-Dennis M et al. AIM2 recognizes cytosolic dsDNA and forms a caspase-1-activating inflammasome with ASC. *Nature.* 458(7237):514-8. 2009.

Hornung V, Bauernfeind F, Halle A et al. Silica crystals and aluminum salts activate the NALP3 inflammasome through phagosomal destabilization. *Nat Immunol.* 9(8):847-56. 2008.

ICCVAM Test Method Evaluation Report 2011: usefulness and limitations of the murine local lymph node assay for potency categorization of chemicals causing allergic contact dermatitis in humans. HIH publication No.11-7709.



Jaworska JS, Natsch A, Ryan C et al. Bayesian integrated testing strategy (ITS) for skin sensitization potency assessment: a decision support system for quantitative weight of evidence and adaptive testing strategy. *Arch Toxicol.* 89(12):2355-83. 2015.

Jéru I, Duquesnoy P, Fernandes-Alnemri T et al. Mutations in NALP12 cause hereditary periodic fever syndromes. *Proc Natl Acad Sci USA.* 105(5):1614-9. 2008.

Johansen JD, Frosch, PJ, Lepoittevin JP (Eds.) *Contact Dermatitis.* 2011 5<sup>th</sup> ed. Springer, pp.719.

Jowsey IR, Basketter DA, Westmoreland C et al. A future approach to measuring relative skin sensitising potency: a proposal. *J Appl Toxicol.* 26(4):341-50. 2006.

Juliana C, Fernandes-Alnemri T, Kang S et al. Non transcriptional priming and deubiquitination regulate NLRP3 inflammasome activation. *J Biol Chem.* 287(43):36617-22. 2012.

Kadunce DP, Krueger GG. Pathogenesis of psoriasis. *Dermatol Clin.* 13(4):723-37. 1995.

Kanerva L, Alanko K, Estlander T, Sihvonen T, Jolanki R. Occupational allergic contact urticaria from chloramine-T solution. *Contact Dermatitis.* 37(4):180-1. 1997.

Kanneganti TD, Lamkanfi M, Kim YG et al. Pannexin-1-mediated recognition of bacterial molecules activates the cryopyrin inflammasome independent of Toll-like receptor signaling. *Immunity.* 26(4):433-43. 2007.

Kaplan DH, Igyártó BZ, Gaspari AA. Early immune events in the induction of allergic contact dermatitis. *Nat Rev Immunol.* 12(2):114-24. 2012.

Kawai T, Akira S. The roles of TLRs, RLRs and NLRs in pathogen recognition. *Int Immunol.* 21(4):317-37. 2009.

Kern PS, Gerberick GF, Ryan CA et al. Local lymph node data for the evaluation of skin sensitization alternatives: a second compilation. *Dermatitis.* 21(1):8-32. 2010.

Kim H, Bernstein JA. Air pollution and allergic disease. *Curr Allergy Asthma Rep.* 9(2):128-33. 2009.

Kimber I, Maxwell G, Gilmour N et al. Allergic contact dermatitis: a commentary on the relationship between T lymphocytes and skin sensitising potency. *Toxicology.* 291(1-3):18-24. 2012.

Kimber I, Basketter DA, Gerberick GF, et al. Factors affecting thresholds in allergic contact dermatitis: safety and regulatory considerations. *Contact Dermatitis.* 47(1):1-6. 2002.

Kimber I, Hilton J, Botham PA et al. The murine local lymph node assay: results of an inter-laboratory trial. *Toxicol Lett.* 55(2):203-13. 1991.

Kimber I, Hilton J, Botham PA. Identification of contact allergens using the murine local lymph node assay: comparisons with the Buehler occluded patch test in guinea pigs. *J Appl Toxicol.* 10(3):173-80. 1990.

Kimura Y, Fujimura C, Ito Y et al. Optimization of the IL-8 Luc assay as an *in vitro* test for skin sensitization. *Toxicol In Vitro.* 29(7):1816-30. 2015.

Kligman AM. The identification of contact allergens by human assay. III. The Maximization Test: a procedure for screening and rating contact sensitizers. 1966. *J Invest Dermatol.* 92(4 Suppl):151S; discussion 152S. 1989.

Kohno K, Kataoka J, Ohtsuki T et al. IFN-gamma-inducing factor (IGIF) is a costimulatory factor on the activation of Th1 but not Th2 cells and exerts its effect independently of IL-12. *J Immunol.* 158(4):1541-50. 1997.

Kramps JA, van Toorenenbergen AW, Vooren PH et al. Occupational asthma due to inhalation of chloramine-T. II. Demonstration of specific IgE antibodies. *Int Arch Allergy Appl Immunol.* 64(4):428-38. 1981.

Krasteva M, Kehren J, Ducluzeau MT, et al. Contact dermatitis I. Pathophysiology of contact sensitivity. *Eur J Dermatol.* 9(1):65-77. 1999.

Krueger GG, Stingl G. Immunology/inflammation of the skin--a 50-year perspective. *J Invest Dermatol.* 1989;92(4 Suppl):32S-51S. 1989.

Kupper TS, Fuhlbrigge RC. Immune surveillance in the skin: mechanisms and clinical consequences. *Nat Rev Immunol.* 4(3):211-22. 2004.

Lapczynski A, McGinty D, Jones L et al. Fragrance material review on benzyl salicylate. *Food Chem Toxicol.* 45 Suppl 1: S362-80. 2007.

Latz E. The inflammasomes: mechanisms of activation and function. *Curr Opin Immunol.* 22(1):28-33. 2010.

Lich JD, Williams KL, Moore CB et al. Monarch-1 suppresses non-canonical NF-kappaB activation and p52-dependent chemokine expression in monocytes. *J Immunol.* 178(3):1256-60. 2007.

Livak KJ, Schmittgen TD. Analysis of relative gene expression data using real-time quantitative PCR and the 2<sup>-Delta Delta C(T)</sup> Method. *Methods.* 25(4):402-8. 2001.

Lombardi P, Gola M, Acciai MC et al. Unusual occupational allergic contact dermatitis in a nurse. *Contact Dermatitis.* 20(4):302-3. 1989.

Lord CA, Savitsky D, Sitcheran R et al. Blimp-1/PRDM1 mediates transcriptional suppression of the NLR gene NLRP12/Monarch-1. *J Immunol.* 182(5):2948-58. 2009.

Mariathasan S, Weiss DS, Newton K et al. Cryopyrin activates the inflammasome in response to toxins and ATP. *Nature.* 440(7081):228-32. 2006.

- Mariathasan S, Newton K, Monack DM et al. Differential activation of the inflammasome by caspase-1 adaptors ASC and Ipaf. *Nature*. 430(6996):213-8. 2004.
- Martin SF. Contact dermatitis: from pathomechanisms to immunotoxicology. *Exp Dermatol*. 21(5):382-9. 2012.
- Martin SF, Dudda JC, Bachtanian E et al. Toll-like receptor and IL-12 signaling control susceptibility to contact hypersensitivity. *J Exp Med*. 205(9):2151-62. 2008.
- Martinon F, Pétrilli V, Mayor A et al. Gout-associated uric acid crystals activate the NALP3 inflammasome. *Nature*. 440(7081):237-41. 2006.
- Martinon F, Burns K, Tschopp J. The inflammasome: a molecular platform triggering activation of inflammatory caspases and processing of pro IL-beta. *Mol Cell*. 10(2):417-26. 2002.
- Martins GA, Cimmino L, Shapiro-Shelef M et al. Transcriptional repressor Blimp-1 regulates T cell homeostasis and function. *Nat Immunol*. 7(5):457-65. 2006.
- Mc Manus MT and Sharp PA. Gene silencing in mammals by small interfering RNAs. *Nature Rev Genet* 3:737-47. 2002.
- Dillin A. The specifics of small interfering RNA specificity. *Proc Natl Acad Sci USA* 100(11):6289-6291. 2002.
- Tuschl T. Expanding small RNA interference. *Nature Biotechnol* 20: 446-448. 2002.
- Megherbi R, Kiorpelidou E, Foster B et al. Role of protein haptation in triggering maturation events in the dendritic cell surrogate cell line THP-1. *Toxicol Appl Pharmacol*. 238(2):120-32. 2009.
- Mehrotra P, Upadhyaya S, Sinkar VP et al. Differential phosphorylation of MAPK isoforms in keratinocyte cell line by contact allergens and irritant. *Toxicol Mech Methods*. 17(2):101-7. 2007.
- Meller S, Lauerma AI, Kopp FM et al. Chemokine responses distinguish chemical-induced allergic from irritant skin inflammation: memory T cells make the difference. *J Allergy Clin Immunol*. 119(6):1470-80. 2007.
- Miao EA, Alpuche-Aranda CM, Dors M et al. Cytoplasmic flagellin activates caspase-1 and secretion of interleukin 1beta via Ipaf. *Nat Immunol*. 7(6):569-75. 2006.
- Mitjans M, Galbiati V, Lucchi et al. Use of IL-8 release and p38 MAPK activation in THP-1 cells to identify allergens and to assess their potency *in vitro*. *Toxicol In Vitro*. 24(6):1803-9. 2010.
- Mizuashi M, Ohtani T, Nakagawa S et al. Redox imbalance induced by contact sensitizers triggers the maturation of dendritic cells. *J Invest Dermatol*. 124(3):579-86. 2005.

Muller, G, Saloga, J, Germann, T, et al. Identification and induction of keratinocyte-derived IL-12. *J. Clin. Invest.* 94, 1799–1805. 1994.

Muruve DA, Pétrilli V, Zaiss AK et al. The inflammasome recognizes cytosolic microbial and host DNA and triggers an innate immune response. *Nature.* 452(7183):103-7. 2008.

Naik SM, Cannon G, Burbach GJ et al. Human keratinocytes constitutively express interleukin-18 and secrete biologically active interleukin-18 after treatment with pro-inflammatory mediators and dinitrochlorobenzene. *J Invest Dermatol.* 113(5):766-72. 1999.

Naisbitt DJ. Drug hypersensitivity reactions in skin: understanding mechanisms and the development of diagnostic and predictive tests. *Toxicology.* 194(3):179-96. 2004.

Nakae S, Naruse-Nakajima C, Sudo K et al. IL-1 alpha, but not IL-1 beta, is required for contact-allergen-specific T cell activation during the sensitization phase in contact hypersensitivity. *Int Immunol.* 13(12):1471-8. 2001.

Natsch A, Emter R. Reporter cell lines for skin sensitization testing. *Arch Toxicol.* 89(10):1645-68. 2015.

Natsch A, Ryan CA, Foertsch L et al. A dataset on 145 chemicals tested in alternative assays for skin sensitization undergoing prevalidation. *J Appl Toxicol.* 33(11):1337-52. 2013.

Nestle FO, Di Meglio P, Qin JZ et al. Skin immune sentinels in health and disease. *Nat Rev Immunol.* 9(10):679-91. 2009.

OECD 2012: <http://www.oecd.org/chemicalsafety/testing/adverse-outcome-pathways-molecular-screening-and-toxicogenomics.htm>

Ohkawara S, Tanaka-Kagawa T, Furukawa Y et al. Activation of the human transient receptor potential vanilloid subtype 1 by essential oils. *Biol Pharm Bull.* 33(8):1434-7. 2010.

Okamura H, Tsutsi H, Komatsu T et al. Cloning of a new cytokine that induce IFN- $\gamma$  production by T cells. *Nature.* 378, 88-91. 1995.

Ouwehand K, Spiekstra SW, Reinders J, et al. Comparison of a novel CXCL12/CCL5 dependent migration assay with CXCL8 secretion and CD86 expression for distinguishing sensitizers from non-sensitizers using MUTZ-3 Langerhans cells. *Toxicol In Vitro.* 24(2):578-85. 2010.

Papale A, Kummer E, Galbiati V et al. Understanding chemical allergen potency: role of NLRP12 and Blimp-1 in the induction of IL-18 in human keratinocytes. *Arch Toxicol.* 91(4):1783-1794. 2017.

Park S, Juliana C, Hong S et al. The mitochondrial antiviral protein MAVS associates with NLRP3 and regulates its inflammasome activity. *J Immunol.* 191(8):4358-66. 2013.

Pawson T, Nash P. Assembly of cell regulatory systems through protein interaction domains. *Science.* 300(5618):445-52. 2003.

- Peirson SN, Butler JN. "RNA extraction from mammalian tissues". *Methods Mol. Biol. Methods in Molecular Biology*. 362: 315–27. 2007.
- Peiser M, Tralau T, Heidler J, et al. Allergic contact dermatitis: epidemiology, molecular mechanisms, *in vitro* methods and regulatory aspects. Current knowledge assembled at an international workshop at BfR, Germany. *Cell Mol Life Sci*. 69(5):763-81. 2012.
- Pelegriñ P, Surprenant A. Pannexin-1 couples to maitotoxin- and nigericin-induced interleukin-1 $\beta$  release through a dye uptake-independent pathway. *J Biol Chem*. 282(4):2386-94. 2007.
- Perregaux D, Gabel CA. Interleukin-1  $\beta$  maturation and release in response to ATP and nigericin. Evidence that potassium depletion mediated by these agents is a necessary and common feature of their activity. *J Biol Chem*. 269(21):15195-203. 1994.
- Pétrilli V, Papin S, Dostert C et al. Activation of the NALP3 inflammasome is triggered by low intracellular potassium concentration. *Cell Death Differ*. 14(9):1583-9. 2007.
- Pfaffl MW. A new mathematical model for relative quantification in real-time RT-PCR. *Nucl Acids Res*. 29: 2002–2007. 2001.
- Quaranta M, Knapp B, Garzorz N et al. Intraindividual genome expression analysis reveals a specific molecular signature of psoriasis and eczema. *Sci Transl Med*. 6(244):244ra90. 2014.
- Rajamäki K, Lappalainen J, Oörni K et al. Cholesterol crystals activate the NLRP3 inflammasome in human macrophages: a novel link between cholesterol metabolism and inflammation. *PLoS One*. 5(7): e11765. 2010.
- Rathinam VA, Jiang Z, Waggoner SN et al. The AIM2 inflammasome is essential for host defense against cytosolic bacteria and DNA viruses. *Nat Immunol*. 11(5):395-402. 2010.
- Recillas-Targa F. Multiple strategies for gene transfer, expression, knockdown, and chromatin influence in mammalian cell lines and transgenic animals. *Mol Biotechnol*. 34(3):337–354. 2006.
- Reisner AH, Nemes P and Bucholtz C. The use of Coomassie Brilliant Blue G-250 perchloric acid solution for staining in electrophoresis and isoelectric focusing on polyacrylamide gels, *Anal Biochem*. 64, 509–516. 1975.
- Roberts DW, Aptula AO. Electrophilic reactivity and skin sensitization potency of SNAr electrophiles. *Chem Res Toxicol*. 27(2):240-6. 2014.
- Robinson D, Shibuya K, Mui A et al. IGIF does not drive Th1 development but synergizes with IL-12 for interferon- $\gamma$  production and activates IRAK and NF $\kappa$ B. *Immunity*. 7(4):571-81. 1997.

Rustemeyer J, Bremerich A. Outcomes after surgical treatment of facial skin basal cell carcinomas. *Acta Chir Plast.* 48(3):89-92. 2006.

Ryan CA, Gerberick GF, Gildea LA et al. Interactions of contact allergens with dendritic cells: opportunities and challenges for the development of novel approaches to hazard assessment. *Toxicol Sci.* 88(1):4-11. 2005.

Rychlik W, Spencer WJ, Rhoads RE. Optimization of the annealing temperature for DNA amplification *in vitro*. *Nucl Acids Res.* 18 (21): 6409–6412. 1990.

Sakaguchi H, Ashikaga T, Miyazawa M, et al. The relationship between CD86/CD54 expression and THP-1 cell viability in an *in vitro* skin sensitization test--human cell line activation test (h-CLAT). *Cell Biol Toxicol.* 25(2):109-26. 2009.

Sallusto F, Lenig D, Förster R et al. Two subsets of memory T lymphocytes with distinct homing potentials and effector functions. *Nature.* 401(6754):708-12. 1999.

Schneider K, Akkan Z. Quantitative relationship between the local lymph node assay and human skin sensitization assays. *Regul Toxicol Pharmacol.* 39(3):245-55. 2004.

Schnuch A, Uter W, Geier J et al. Sensitization to 26 fragrances to be labelled according to current European regulation. Results of the IVDK and review of the literature. *Contact Dermatitis.* 57(1):1-10. 2007.

Schroder K, Tschopp J. The inflammasomes. *Cell.* 140(6):821-32. 2010.

Scognamiglio J, Jones L, Vitale D et al. Fragrance material review on benzyl alcohol. *Food Chem Toxicol.* 50 Suppl 2: S140-60. 2012.

Sedmak JJ and Grossberg SE. A rapid, sensitive and versatile assay for protein using Coomassie Brilliant Blue G-250, *Anal Biochem.* 79, 544–552. 1977.

Shami PJ, Kanai N, Wang LY et al. Identification and characterization of a novel gene that is upregulated in leukaemia cells by nitric oxide. *Br J Haematol.* 112(1):138-47. 2001.

Sharkey DJ, Scalice ER, Christy KG et al. Antibodies as Thermolabile Switches: High Temperature Triggering for the Polymerase Chain Reaction. *Bio/Technology.* 12 (5): 506–509. 1994.

Smith Pease CK, Basketter DA, Patlewicz GY. Contact allergy: the role of skin chemistry and metabolism. *Clin Exp Dermatol.* 28(2):177-83. 2003.

Srinivasula SM, Poyet JL, Razmara M et al. The PYRIN-CARD protein ASC is an activating adaptor for caspase-1. *J Biol Chem.* 277(24):21119-22. 2002.

Struwe WB, Warren CE. High-throughput RNAi screening for N-glycosylation dependent loci in *Caenorhabditis elegans*. *Methods Enzymol.* 480:477-93. 2010.

Stutz A, Golenbock DT, Latz E. Inflammasomes: too big to miss. *J Clin Invest*. 119(12):3502-11. 2009.

Surprenant A, Rassendren F, Kawashima E et al. The cytolytic P2Z receptor for extracellular ATP identified as a P2X receptor (P2X7). *Science*. 272(5262):735-8. 1996.

Suzuki T, Franchi L, Toma C et al. Differential regulation of caspase-1 activation, pyroptosis, and autophagy via Ipaf and ASC in *Shigella*-infected macrophages. *PLoS Pathog*. 3(8): e111. 2007.

Tahrin Mahmood and Ping-Chang Yang. Western Blot: Technique, Theory, and Trouble Shooting. *N Am J Med Sci*. 4(9): 429–434. 2012.

Takahashi T, Kimura Y, Saito R et al. An *in vitro* test to screen skin sensitizers using a stable THP-1-derived IL-8 reporter cell line, THP-G8. *Toxicol Sci*. 124(2):359-69. 2011.

Teunis MA, Spiekstra SW, Smits M et al. International ring trial of the epidermal equivalent sensitizer potency assay: reproducibility and predictive-capacity. *ALTEX*. 31(3):251-68. 2014.

Teunis M, Corsini E, Smits M et al. Transfer of a two-tiered keratinocyte assay: IL-18 production by NCTC2544 to determine the skin sensitizing capacity and epidermal equivalent assay to determine sensitizer potency. *Toxicol In Vitro*. 27(3):1135-50. 2013.

Thomas Rustemeyer Ingrid MW van Hoogstraten, Boudewina Mary E von Blomberg et al. Mechanisms of Irritant and Allergic Contact Dermatitis Contact Dermatitis, pp.43-90. 2011.

Torigoe K, Ushio S, Okura T et al. Purification and characterization of the human interleukin-18 receptor. *J Biol Chem*. 272(41):25737-42. 1997.

Tuncer S, Fiorillo MT, Sorrentino R. The multifaceted nature of NLRP12. *J Leukoc Biol*. 96(6):991-1000. 2014.

Urbisch D, Mehling A, Guth K et al. Assessing skin sensitization hazard in mice and men using non-animal test methods. *Regul Toxicol Pharmacol*. 71(2):337-51. 2015.

van Bruggen R, Köker MY, Jansen M et al. Human NLRP3 inflammasome activation is Nox1-4 independent. *Blood*. 115(26):5398-400. 2010.

van der Veen JW, Soeteman-Hernández LG, Ezendam J et al. Anchoring molecular mechanisms to the adverse outcome pathway for skin sensitization: Analysis of existing data. *Crit Rev Toxicol*. 44(7):590-9. 2014.

van Och FM, van Loveren H, van Wolfswinkel JC, et al. Assessment of potency of allergenic activity of low molecular weight compounds based on IL-1 $\alpha$  and IL-18 production by a murine and human keratinocyte cell line. *Toxicology*. 210, 95-109. 2005.

Vanaja SK, Rathinam VA, Fitzgerald KA. Mechanisms of inflammasome activation: recent advances and novel insights. *Trends Cell Biol.* 25(5):308-15. 2015.

Vocanson M, Rozieres A, Hennino A et al. Inducible costimulator (ICOS) is a marker for highly suppressive antigen-specific T cells sharing features of TH17/TH1 and regulatory T cells. *J Allergy Clin Immunol.* 126(2):280-9, 289.e1-7. 2010.

Vocanson M, Hennino A, Rozières A, et al. Effector and regulatory mechanisms in allergic contact dermatitis. *Allergy.* 64(12):1699-714. 2009.

Walzer T, Marçais A, Saltel F et al. Cutting edge: immediate RANTES secretion by resting memory CD8 T cells following antigenic stimulation. *J Immunol.* 170(4):1615-9. 2003.

Wang B, Feliciani C, Howell BG et al. Contribution of Langerhans cell-derived IL-18 to contact hypersensitivity. *J Immunol.* 168(7):3303-8. 2002.

Wang L, Manji GA, Grenier JM et al. PYPAF7, a novel PYRIN-containing Apaf1-like protein that regulates activation of NF-kappa B and caspase-1-dependent cytokine processing. *J Biol Chem.* 277(33):29874-80. 2002.

Wass U, Belin L, Eriksson NE. Immunological specificity of chloramine-T-induced IgE antibodies in serum from a sensitized worker. *Clin Exp Allergy.* 19(4):463-71. 1989.

Williams KL, Lich JD, Duncan JA et al. The CATERPILLER protein monarch-1 is an antagonist of toll-like receptor-, tumor necrosis factor alpha-, and Mycobacterium tuberculosis-induced pro-inflammatory signals. *J Biol Chem.* 280(48):39914-24. 2005.

Wu MF, Chen ST, Hsieh SL. Distinct regulation of dengue virus-induced inflammasome activation in human macrophage subsets. *J Biomed Sci.* 20:36. 2013.

Wurm FM. Production of recombinant protein therapeutics in cultivated mammalian cells. *Nat Biotechnol.* 22(11):1393–1398. 2004.

Xu D, Chan WL, Leung BP et al. Selective expression and functions of interleukin 18 receptor on T helper (Th) type 1 but not Th2 cells. *J Exp Med.* 188(8):1485-92. 1998.

Ye Z, Lich JD, Moore CB et al. ATP binding by monarch-1/NLRP12 is critical for its inhibitory function. *Mol Cell Biol.* 28(5):1841-50. 2008.

Yoshimoto T, Takeda K, Tanaka T et al. IL-12 up-regulates IL-18 receptor expression on T cells, Th1 cells, and B cells: synergism with IL-18 for IFN-gamma production. *J Immunol.* 161(7):3400-7. 1998.

Yusuf N, Nasti TH, Huang CM et al. Heat shock proteins HSP27 and HSP70 are present in the skin and are important mediators of allergic contact hypersensitivity. *J Immunol.* 182(1):675-83. 2009.



Zaba LC, Krueger JG, Lowes MA. Resident and "inflammatory" dendritic cells in human skin. *J Invest Dermatol.* 129(2):302-8. 2009.

Zhou R, Yazdi AS, Menu P et al. A role for mitochondria in NLRP3 inflammasome activation. *Nature.* 469(7329):221-5. 2011.

Zhou R, Tardivel A, Thorens B et al. Thioredoxin-interacting protein links oxidative stress to inflammasome activation. *Nat Immunol.* 11(2):136-40. 2010.

## FIGURES:

[1][http://hmphysiology.blogspot.it/p/blog-page\\_10.html](http://hmphysiology.blogspot.it/p/blog-page_10.html)

[2]<http://kreativestudios.com/Tooltip/05Integument/02epidermis.html>

[3]Reproduced with permission from: Gober MD, Gaspari AA. *Curr Dir Autoimmun.* 2008;10:1-26.

[4][http://www.oecd.org/officialdocuments/publicdisplaydocumentpdf/?cote=env/jm/mono\(2012\)10/part1&doclanguage=en](http://www.oecd.org/officialdocuments/publicdisplaydocumentpdf/?cote=env/jm/mono(2012)10/part1&doclanguage=en)

[5]Charles A. and Dinarello MD. IL-18: A TH1 -inducing, proinflammatory cytokine and new member of the IL-1 family. *Journal of Allergy and Clinical Immunology.* 103(1): 11-24

[6]Lamkanfi M and Dixit VM. Mechanisms and functions of inflammasomes. *Cell* 157. Review.2014

[7]Jo EK, Kim JK, Shin DM et al. Molecular mechanisms regulating NLRP3 inflammasome activation. *Cell Mol Immunol.* 13(2):148-59. 2016.

[12]Picture made by me in house Tox Lab, Milan.

[13]Hemocytometer.org

[14]<https://www.mattek.com/products/epiderm/>

[15]<https://www.lsbio.com/elisakits/mouse-agrn-agrin-elisa-kit-sandwich-elisa-ls-f16819/16819>

[16]Picture made by me in house Tox Lab, Milan

[17][https://openwetware.org/wiki/RNA\\_extraction\\_using\\_trizol/tri](https://openwetware.org/wiki/RNA_extraction_using_trizol/tri)

[19][http://www3.appliedbiosystems.com/WebTroubleshooting/AbnormalAmplificationCurves/Your\\_samples\\_contain\\_degraded\\_RNA.htm](http://www3.appliedbiosystems.com/WebTroubleshooting/AbnormalAmplificationCurves/Your_samples_contain_degraded_RNA.htm)

[20]Picture made by me in house Tox Lab, Milan

[21]<https://www.thermofisher.com/it/en/home/life-science/cloning/cloning-learning-center/invitrogen-school-of-molecular-biology/rt-education/reverse-transcription-applications.html>

[22][https://en.wikipedia.org/wiki/Polymerase\\_chain\\_reaction](https://en.wikipedia.org/wiki/Polymerase_chain_reaction)

[23]<https://www.slideshare.net/elsavonlicy/innate-immunity-2013>

[24]Koch HW. Technology platforms for pharmacogenomic diagnostic assays. *Nature Reviews Drug Discovery* 3, 749–761. Review. 2004.

[25]Yuan JS, Reed A, Chen F et al. Statistical analysis of real-time PCR data. *BMC Bioinformatics*. 22;7:85. 2006.

[26]<https://www.thermofisher.com/it/en/home/references/ambion-tech-support/rnai-sirna/tech-notes/gene-specific-silencing-by-rnai.html>

[27]<https://www.thermofisher.com/it/en/home/life-science/protein-biology/protein-biology-learning-center/protein-biology-resource-library/pierce-protein-methods/co-immunoprecipitation-co-ip.html>

[28]Papale A, Kummer E, Galbiati V et al. Understanding chemical allergen potency: role of NLRP12 and Blimp-1 in the induction of IL-18 in human keratinocytes. Arch Toxicol. 91(4):1783-1794. 2017.

[29]Manuscript in preparation

[30]Galbiati V, Papale A, Marinovich M et al. Development of an *in vitro* method to estimate the sensitization induction level of contact allergens. Toxicol Lett. 271:1-11. 2017.

[31]Martínez-Santamaría L, Guerrero-Aspizua S, Del Río M. Skin bioengineering: preclinical and clinical applications. Actas Dermosifiliogr. 103(1):5-11. 2012.

[32]Aasen T, Izpisúa Belmonte JC. Isolation and cultivation of human keratinocytes from skin or plucked hair for the generation of induced pluripotent stem cells. Nat Protoc. 5(2):371-82. 2010.

## TABLE:

[8]Kimber I, Basketter DA, Butler M et al. Classification of contact allergens according to potency: Proposals. Food and Chemical Toxicology 41(12):1799-809 2004

[9]Api AM, Parakhia R, O'Brien D et al. Fragrances Categorized According to Relative Human Skin Sensitization Potency. Dermatitis. 28(5): 299–307. 2017-11-06

[10]Picture made by me at Eurotox, 2017, Bratislava. Speaker: Silvia Casati.

[11]Galbiati V, Papale A, Marinovich M et al. Development of an *in vitro* method to estimate the sensitization induction level of contact allergens. Toxicol Lett. 271:1-11. 2017.

[18]Assessment of Nucleic Acid Purity. Thermo Scientific. Retrieved 2016-09-28.

[28]Papale A, Kummer E, Galbiati V et al. Understanding chemical allergen potency: role of NLRP12 and Blimp-1 in the induction of IL-18 in human keratinocytes. Arch Toxicol. 91(4):1783-1794. 2017.

[30]Galbiati V, Papale A, Marinovich M et al. Development of an *in vitro* method to estimate the sensitization induction level of contact allergens. Toxicol Lett. 271:1-11. 2017.